

*KINETOSTATIC DESIGN OF AN ARTICULATED
LEG-WHEEL LOCOMOTION SUBSYSTEM*

by

SEUNG KOOK JUN

JUNE 2004

A thesis submitted to the Faculty of the Graduate School of the State University
of New York at Buffalo in partial fulfillment of the requirements for the degree of

MASTER OF SCIENCE

Department of Mechanical and Aerospace Engineering
State University of New York at Buffalo
Buffalo, New York 14260

ACKNOWLEDGEMENT

My thanks go first and foremost to Professor Venkat Krovi as advisor, mentor and friend. His excellence in the field and enthusiasm to work has always been a source of inspiration. I also extend my gratitude to my committee members, Dr. Roger Mayne and Dr. John Crassidis for valuable suggestions and help.

I spent many enjoyable hours with ARM Lab and department friends, Ajay, Annapurna, Chetan, Chin-pei, Dan, Glenn, Jae-jun, Jong-woo, Jong-rae, Leng-feng, Mike, Prasanna, Pravin, Rajan, Tao, Young-suk. I would like to thank them for help and advice inside and outside the school. I miss joyful friends, Deepak, JJ, Ken, Mrs. Krovi, Lei-tang, and Ravishankar giving me unforgettable recollections in Buffalo.

Finally I would like to thank my family and ji-young who have encouraged me so much over years.

CONTENTS

1	INTRODUCTION	1
1.1	Articulated leg-wheel subsystems for vehicle systems.....	2
1.1.1	Articulated Degrees of Freedom.....	2
1.1.2	Equilibration (Structural and Actuation-based).....	4
1.2	Single Degree-of-freedom Articulated Leg-Wheel Systems.....	5
1.3	Our Research Goals.....	6
1.4	Organization of the thesis.....	7
2	BRIEF BACKGROUND ON LEG-WHEEL SYSTEMS	8
3	DESIGN APPROACH	11
3.1	Applied loads at the end-effector of a leg-wheel design.....	11
3.2	User-inputs for Problem Specification.....	12
3.2.1	Kinematic Design Factors under User-Control.....	13
3.2.2	Force-related design factors under user-control	14
3.3	Specific Test Scenario	15
3.3.1	Design of the kinematic trajectory for the test case	15
3.3.2	Design of the static trajectory for the test case	15
3.4	Overview of Kinetostatic Design Approach	16
4	DESIGN/SYNTHESIS OF SDCSC LEG-WHEEL MECHANISM	18
4.1	Coupled Serial Chain (CSC) mechanisms	19
4.2	Kinematic Synthesis.....	19
4.2.1	Planar Precision Point Synthesis of SDCSC.....	19
4.2.2	Combined Kinematic Precision-Point Synthesis and Optimization	21
4.3	Static Synthesis of SDCSC Mechanism.....	24
4.3.1	Precision Torque Synthesis.....	24
4.4	Static Precision Point Synthesis and Optimization.....	27
4.4.1	Two static precision points and no free choices.	27

4.4.2	No static precision points and using both variables as free-choices.....	30
-------	--	----

5 DESIGN/SYNTHESIS OF FOURBAR LEG-WHEEL

MECHANISM.....	33
-----------------------	-----------

5.1 Kinematic Synthesis.....	33
5.1.1 Planar Precision Point Synthesis of Fourbar.....	34
5.2 Kinematic Synthesis.....	34
5.3 Kinematic Optimization	35
5.4 Static Synthesis of Fourbar with Two Precision Points	37
5.4.1 Four static precision points and no free choices.....	40
5.4.2 No static precision points and using four variables as free-choices	42

6 STATIC EQUILIBRIUM ANALYSIS.....	45
---	-----------

6.1 Background	45
6.1.1 Structures and mechanisms.....	45
6.1.2 Equilibrium Analysis	46
6.2 Static Equilibration (in a mechanism context).....	47
6.2.1 Static Balance and Gravity Compensation	47
6.2.2 Methods for Equilibration.....	48
6.3 Case Study of One-Link Mechanism.....	49
6.3.1 Examples of perfect static equilibration (using counterweight system)	49
6.3.2 Example of perfect gravity balancing (using Linear Springs).....	50
6.3.3 Examples for selective equilibria (using Hookian torsional springs).....	50
6.4 Analysis of Equilibria	52
6.4.1 Equilibrium Analysis for Spring equilibria.....	52
6.4.2 Equilibrium Analysis for Counterweight.....	53
6.5 Quantitative Measures for Evaluation of Equilibria.....	54
6.5.1 Location of the equilibrium	54
6.5.2 Sensitivity of the equilibrium.....	55
6.5.3 Basin of Attraction – magnitude and range	56
6.6 Possible Equilibrium Configurations for a One-Link Mechanism	56
6.7 Most Useful Equilibrium Case of a One Link System.....	58
6.8 Basin of Attraction Optimization	60

6.9	Equilibrium Analysis for an SDCSC-based Articulated Leg-Wheel Design.	60
6.10	Equilibrium Analysis for a Fourbar based Articulated Leg-Wheel Design..	62
7	CONCLUSION AND FUTURE WORK.....	63
7.1	Research Contributions.....	63
7.2	Future Work.....	64
7.2.1	Immediate Extensions.....	64
7.2.2	Longer-Term Extensions	64

LIST OF FIGURES

FIGURE 1.1 ARTIST’S CONCEPTION OF AN ARTICULATED LEG-WHEEL BASED LOCOMOTION SYSTEM.....	2
FIGURE 1.2 (A) THE TWO FRAMES HAVE 2 D.O.F AND (B) MOTION D.O.F ELIMINATED BY RIGID JOINT.	3
FIGURE 1.3 (A) 1 MOTION DOF ARTICULATION USING REVOLUTE JOINT AND (B) 1 MOTION DOF ARTICULATION USING PRISMATIC JOINT.....	3
FIGURE 1.4 (A) 2 MOTION DOF ARTICULATION USING (A) 2R JOINTS (B) RP JOINTS (C) PP JOINTS	3
FIGURE 1.5 (A) EQUILIBRATION FOR A 1-LINK MECHANISM AND (B) ACTIVE EQUILIBRATION TORQUE REQUIREMENT.....	4
FIGURE 1.6 CONSTRAINED SINGLE DEGREE-OF-FREEDOM MOTIONS CAN BE ACHIEVED USING: (A) SINGLE-ARTICULATION; OR (B-C) MULTIPLE- ARTICULATIONS (BUT WITH SUITABLE HARDWARE CONSTRAINTS). ...	5
FIGURE 1.7 PROPOSED ARTICULATED LEG-WHEELED SYSTEM DESIGN WITH (A) FOURBAR-BASED AND (B) SINGLE DEGREE OF FREEDOM COUPLED SERIAL CHAIN (SDCSC) BASED CONFIGURATIONS.....	6
FIGURE 2.1 (A) MARS ROVER AND (B) SIDE VIEW OF ROCKER-BOGIE CONFIGURATION [1],[2].	8
FIGURE 2.2 (A) SHRIMP III AND (B) SECTION VIEW OF SHRIMP [3].....	8
FIGURE 2.3 (A) NOMAD AND (B) TRANSFORMING CHASSIS OF NOMAD [4]....	9
FIGURE 2.4 (A) ROLLER-WALKER AND (B) LEG MECHANISM OF ROLLER- WALKER [7].....	9
FIGURE 2.5 (A) WORKPARTNER AND (B) WORKING AREA OF A WHEELED LEG [5],[6].	10
FIGURE 2.6 (A) ALDURO AND (B) LATERAL/VERTICAL WORK SPACE [13] ...	10
FIGURE 3.1 (A) SCHEMATIC AND (B) FBD OF SDCSC SUPPORTING EXTERNAL FORCE & TORQUE	11
FIGURE 3.2 (A) FORCES AT THE END-EFFECTOR AND (B) FORCES WITH DIFFERENT MOTOR TORQUE	12
FIGURE 3.3. MOTION OF THE WHEEL WITH RESPECT TO AN INERTIAL FRAME OF REFERENCE (OXY) AS VEHICLE SURMOUNTS A FIXED HEIGHT STEP – (A) SIMPLE RISING MOTION WHEN CHASSIS DOES NOT MOVE; AND (B) RISING AND OFFSET MOTION AS CHASSIS MOVES FORWARD.....	13
FIGURE 3.4 CANDIDATE KINEMATIC TRAJECTORIES – (A) OPEN-LOOP DESIRED CURVES AND (B) CLOSED LOOP DESIRED CURVE	13
FIGURE 3.5 SHAPING THE DESIRED STATIC TORQUE CURVE, INCLUDING SPECIFICATION OF THE MAXIMUM/MINIMUM TORQUE AS WELL AS TYPE/NUMBER/POSITION OF PRECISION MATCHING OF THE TORQUE SPECIFICATION.	14
FIGURE 3.6 DESIRED TORQUE DESIGN (A) BY PRECISION TORQUE AND (B) DESIRED TORQUE CURVE.....	15

FIGURE 3.7 KINETOSTATIC DESIGN: COMBINING PRECISION POINT SYNTHESIS WITH OPTIMIZATION	17	
FIGURE 4.1 (A) TWO LINKS SDCSC- BASED LEG-WHEEL DESIGN, (B) CORRESPONDING KINEMATIC DIAGRAM FOR TWO LINKS SDCSC, (C) THREE LINKS SDCSC- BASED LEG-WHEEL DESIGN AND (D) CORRESPONDING KINEMATIC DIAGRAM FOR THREE LINKS SDCSC	18	
FIGURE 4.2 DESIRED TRAJECTORY OF END-EFFECTOR FOR (A) TWO LINK SDCSC AND (B) THREE LINK SDCSC	21	
FIGURE 4.3 OBJECTIVE FUNCTION VALUES OBTAINED BY A PARAMETER SWEEP OF R_1 AND ϕ (A) $R_1 > 0$ AND (B) $R_1 < 0$	22	
FIGURE 4.4 CANDIDATE SETS OF SDCSC CONFIGURATIONS WHEN DESIGN VARIABLES ARE (A) TWO LINKS SDCSC ($R_1 = 8.3467, \phi = 30.4178$) (B) THREE LINK SDCSC CONFIGURATION I ($R_1 = -8, R_2 = 2, \phi_2 = 20.9, \phi_3 = 36$) AND (C) THREE LINK SDCSC CONFIGURATION II ($R_1 = -5.5, R_2 = -4, \phi_2 = 30.2, \phi_3 = 44.2$)	23	
FIGURE 4.5 TORSION SPRINGS AT JOINTS WITH PRELOAD ANGLE Ω , INITIAL CONFIGURATION θ AND RELATIVE DISPLACEMENT ϕ	24	
FIGURE 4.6 (A) KINEMATIC CONFIGURATION OF TWO LINK SDCSC AND (B) TORQUE AT DRIVING JOINT WHEN $k_1 = -16.6$ $k_2 = -2.4$	28	
FIGURE 4.7 (A) KINEMATIC CONFIGURATION OF THREE LINK SDCSC CONFIGURATION I AND (B) TORQUE AT DRIVING JOINT WHEN $k_1 = 0.03, k_2 = 2.2, k_3 = -3.6$	29	
FIGURE 4.8 (A) KINEMATIC CONFIGURATION OF THREE LINK SDCSC CONFIGURATION I AND (B) TORQUE AT DRIVING JOINT WHEN $k_1 = -1.7, k_2 = -5.8, k_3 = 15.3$	29	
FIGURE 4.9 MOVING TORQUE PROFILE BY CHANGING PRECISION TORQUE	30	
FIGURE 4.10 TRAJECTORY OPTIMIZATION FOR TWO LINK SDCSC CONFIGURATION I (A) AFTER FIRST ITERATION OF OPTIMIZATION AND (B) FINAL RESULT OF OPTIMIZATION ($k_1 = 0, k_2 = 0.45$)	31	
FIGURE 4.11 TRAJECTORY OPTIMIZATION FOR THREE LINK SDCSC CONFIGURATION I (A) AFTER FIRST ITERATION OF OPTIMIZATION AND (B) FINAL RESULT OF OPTIMIZATION ($k_1 = -0.001, k_2 = -0.1, k_3 = -0.15$)	31	
FIGURE 4.12 TRAJECTORY OPTIMIZATION FOR THREE LINK SDCSC CONFIGURATION II (A) AFTER FIRST ITERATION OF OPTIMIZATION AND (B) FINAL RESULT OF OPTIMIZATION ($k_1 = 0.0067, k_2 = -0.28, k_3 = -0.041$) ...	32	
FIGURE 5.1 (A) FOURBAR AND (B) APPLICATION FOURBAR TO LEG-WHEELED SYSTEM	33	
FIGURE 5.2 FOURBAR SCHEMATIC LINKAGE MADE OF (A) TWO DYADS AND (B) THREE DYADS.....	33	
FIGURE 5.3 DESIRED END-EFFECTOR TRAJECTORY (A) OPEN STEP DESIRED CURVE & PRECISION POINTS	AND (B) CLOSED DESIRED CURVE & PRECISION POINTS	35

FIGURE 5.4 KINEMATIC OPTIMIZATION RESULTS FOR OPEN DESIRED CURVE (A) CASE1 AND (B) CASE2	36
FIGURE 5.5 KINEMATIC OPTIMIZATION RESULTS FOR CLOSED DESIRED CURVE (A) CASE3 AND (B) CASE4	37
FIGURE 5.6 FOURBAR (A) FBD OF FOURBAR AND (B) SPRING PRELOAD (Ω), INITIAL (θ) AND RELATIVE (α) ANGLES AT JOINT	37
FIGURE 5.7 (A) KINEMATIC CONFIGURATION I OF FOURBAR FOR OPEN DESIRED TRAJECTORY AND (B) TORQUE AT DRIVING JOINT	41
FIGURE 5.8 (A) KINEMATIC CONFIGURATION II OF FOURBAR FOR OPEN DESIRED TRAJECTORY AND (B) TORQUE AT DRIVING JOINT	41
FIGURE 5.9 (A) KINEMATIC CONFIGURATION I OF FOURBAR FOR CLOSED DESIRED TRAJECTORY AND (B) TORQUE AT DRIVING JOINT	42
FIGURE 5.10 (A) KINEMATIC CONFIGURATION II OF FOURBAR FOR CLOSED DESIRED TRAJECTORY AND (B) TORQUE AT DRIVING JOINT	42
FIGURE 5.11 TRAJECTORY OPTIMIZATION OF FOURBAR FOR OPEN DESIRED CURVE CONFIGURATION I (A) AT FIRST ITERATION OF OPTIMIZATION AND (B) FINAL RESULT OF OPTIMIZATION	43
FIGURE 5.12 TRAJECTORY OPTIMIZATION OF FOURBAR FOR OPEN DESIRED CURVE CONFIGURATION II (A) AT FIRST ITERATION OF OPTIMIZATION AND (B) FINAL RESULT OF OPTIMIZATION	43
FIGURE 5.13 TRAJECTORY OPTIMIZATION OF FOURBAR FOR CLOSED DESIRED CURVE CONFIGURATION I (A) AT FIRST ITERATION OF OPTIMIZATION AND (B) FINAL RESULT OF OPTIMIZATION	43
FIGURE 5.14 TRAJECTORY OPTIMIZATION OF FOURBAR FOR CLOSED DESIRED CURVE CONFIGURATION II (A) AT FIRST ITERATION OF OPTIMIZATION AND (B) FINAL RESULT OF OPTIMIZATION	44
FIGURE 6.1 (A) FOURBAR AND (B) FOURBAR WITH A CONSTRAINT	45
FIGURE 6.2 (A) EQUILIBRIUM PATHS FOR LOAD VS DEFLECTION [24] AND (B) EQUILIBRIUM PATHS FOR JOINT ANGLE VS TORQUE FOR A SINGLE-DEGREE-OF-FREEDOM SYSTEMS UNDER CONSIDERATION	46
FIGURE 6.3 (A) UNBALANCED, (B) DYNAMIC MODEL, (C) STATICALLY BALANCED LINK AND (D) ONE LINK AND TENSION SPRING [16],[23]	49
FIGURE 6.4 ONE LINK WITH REVOLUTE JOINT AND HOOKIAN TORSION SPRING	51
FIGURE 6.5 (A) SPRING/EXTERNAL/BALANCE TORQUE AT JOINT AND (B) UNSTABLE EQUILIBRIA	52
FIGURE 6.6 (A) INTERNAL/SPRING/OVERALL TORQUE AT JOINT AND (B) STABLE/UNSTABLE EQUILIBRIA	53
FIGURE 6.7 (A-B) UNBALANCED SYSTEM (C-D) PARTIALLY BALANCED AND (E-F) PERFECTLY BALANCED	54
FIGURE 6.8 (A) EXTERNAL/SPRING TORQUE (WITHOUT PRELOAD) AND (B) EXTERNAL/SPRING TORQUE (VARYING PRELOAD ANGLE)	55
FIGURE 6.9 (A) TORQUE (VARYING SPRING CONSTANT) AND (B) TORQUE (VARYING EXTERNAL FORCE)	55
FIGURE 6.10 (A) ONE STABLE EQUILIBRIUM AND (B) ONE UNSTABLE EQUILIBRIUM	57

FIGURE 6.11 (A) . UNSTABLE EQUILIBRIUM < STABLE EQUILIBRIUM AND (B) . UNSTABLE EQUILIBRIUM < STABLE EQUILIBRIUM.....	57
FIGURE 6.12 (A) TWO UNSTABLE & ONE STABLE EQUILIBRIUM AND (B) ONE UNSTABLE & TWO STABLE EQUILIBRIUM.....	58
FIGURE 6.13 (A) BASIN OF ATTRACTION FOR ONE STABLE EQUILIBRIUM CASE ($K = 5\text{LB/RAD}$, $\Omega = 40\text{ DEG}$) AND (B) TORQUE AT THE END- EFFECTOR.....	58
FIGURE 6.14 (A) BASIN OF ATTRACTION FOR ONE UNSTABLE EQUILIBRIUM CASE ($K = 20\text{LB/RAD}$, $\Omega = - 80\text{ DEG}$) AND (B) TORQUE AT THE END- EFFECTOR.....	59
FIGURE 6.15 (A) BASIN OF ATTRACTION FOR TWO UNSTABLE EQUILIBRIUM CASE ($K = - 4\text{LB/RAD}$, $\Omega = -110\text{ DEG}$) AND (B) TORQUE AT THE END- EFFECTOR.....	59
FIGURE 6.16 (A) BASIN OF ATTRACTION FOR ONE UNSTABLE EQUILIBRIUM CASE ($K = 4\text{LB/RAD}$, $\Omega = 85\text{ DEG}$) AND (B) TORQUE AT THE END- EFFECTOR.....	59
FIGURE 6.17 (A) DESIRED ZONE FOR ONE LINK SYSTEM AND (B) TWO UNSTABLE & ONE STABLE EQUILIBRIUM.....	60
FIGURE 6.18 EQUILIBRIUM POSITION AND CORRESPONDING POSITION IN THE KINEMATIC CONFIGURATION OF (A) THREE LINK SDCSC CONFIGURATION I AND (B) THREE LINK SDCSC CONFIGURATION II....	61
FIGURE 6.19 STABLE AND UNSTABLE EQUILIBRIUM OF (A) THREE LINK SDCSC CONFIGURATION I AND (B) THREE LINK SDCSC CONFIGURATION II.....	61
FIGURE 6.20 (A) EQUILIBRIUM POSITION AND (B) CORRESPONDING POSITION IN THE KINEMATIC CONFIGURATION OF FOURBAR OPEN DESIRED CURVE CONFIGURATION II.....	62
FIGURE 6.21 END-EFFECTOR TORQUE OF CLOSED DESIRED CURVE CONFIGURTION I WHICH HAS (A) TWO UNSTABLE EQUILIBRIUMS AND ONE STABLE EQUILIBRIUM AND (B) ONE STABLE EQUILIBRIUM AND ONE UNSTABLE EQUILIBRIUM.....	62

Abstract

In this thesis, we examine creation of an articulated leg-wheel subsystem for vehicle systems with enhanced locomotion capabilities on uneven terrain. The articulated leg-wheel designs under consideration consist of multiple lower pair joints (revolute/prismatic) between the wheel and the chassis. We restrict our attention solely to planar articulated leg-wheel systems operating in the sagittal plane. Our emphasis in the selection process is an articulated leg-wheel design that permit the greatest motion capability between the chassis and wheel while maintaining the smallest degree-of-freedom within the articulated system. In particular, we focus our attention on the design of the articulated leg-wheel for two goals: First, we design the overall leg-wheel system to provide adequate ground clearance using method from kinematic synthesis combined with optimization. Second, we pursue the reduction of overall actuation requirements by using the notion of structural equilibration. Results from the implementation of these design methods illustrate the features and usefulness of these approaches.

1 Introduction

In recent years, there has been considerable interest in creation of land-based locomotion systems for operation on rough unprepared surfaces. The application domains lie principally in uneven-terrain exploration in extra-terrestrial [1],[5],[6], extreme terrestrial [4],[5],[6], and man-made but non-smooth environments, such as disaster-sites [7]. While high mobility, obstacle-surmounting capability and maneuverability are the obvious major requirements, additional criteria such as robustness, reliability and efficiency are extremely desirable features for systems operating on such unprepared terrains.

Legged locomotion systems have been the preferred solution for maneuvering on such rough/unprepared terrains – see [8],[9] for a review. For example, a legged robot can climb step, cross ditches, and walk on extremely rough terrain. This typical motivating argument for legged system such that leg-wheel systems can pick and choose the footholds and the articulation in the leg can help decouple the motion of the foot from the motion of the vehicle chassis to permit some degree of acceleration and to help absorb shocks.

In contrast, wheeled systems have dominated on prepared surfaces [10],[11],[12]. From a design viewpoint, one of interesting advantage of wheel is that it provides passive support for the vehicle thus no energy is spent to support weight of the vehicle. The continuous cyclic motion of wheels simplifies the actuation/control requirement (to a single DC motor with encoder feedback). The rolling contact of the wheel with the surface reduces the overall specific resistance for the motion, as compared to sliding friction. Table 1.1 contrasts the coefficients for rolling resistance and Coulomb friction for various pairs of materials. Thus, wheels have become the de-facto design standard for most man-made land-based locomotion systems due to these many advantages.

Coefficient of Friction		
Surface	Rolling Resistance	Static Friction
Low-rolling resistance car tire on dry pavement	0.006 - 0.01	0.8
Ordinary car tire on dry pavement	0.015	0.8
Truck tire on dry pavement	0.006 – 0.01	0.8
Train wheel on steel track	0.001	0.1

Table 1.1 Rolling and Static friction according to tire and road condition

The limitation however is that these benefits can be realized only on hard and prepared surfaces where the wheels operate primarily in the rolling mode without slip [10],[11],[12]. In general, the specific resistance of such locomotion systems increases rapidly with increasing surface roughness – the highest obstacle which wheel can go over can be computed as $0.38R$, as derived in APPENDIX A. Furthermore wheels are required to trace continuous paths on the surface and thus require continuous support.

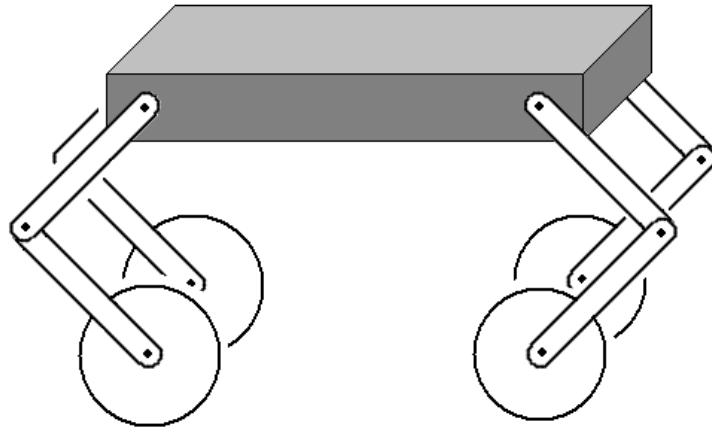


Figure 1.1 Artist's conception of an articulated leg-wheel based locomotion system.

1.1 Articulated leg-wheel subsystems for vehicle systems

Therefore, in this thesis, we will examine creation of articulated leg-wheel subsystems for vehicle systems to help provide enhanced locomotion capabilities on uneven terrain, as shown in Figure 1.1. In doing so, we wish to combine some of the benefits of legged locomotion systems with those of wheeled locomotion systems. The long-term goal of this effort is to create an uneven terrain locomotion system, having capabilities of traversing obstacles, customizing wheel axle trajectory, providing semi-active support and possessing reconfigurability.

The articulated leg-wheel designs under consideration consist of multiple lower pair joints (revolute/prismatic) between the wheel and the chassis. Numerous variants of the articulated leg-wheel system design are possible depending upon the type, number, sequencing and nature of actuation (active/passive) of the joint.

The design process must take into account important considerations such as the loss of stability, tip-over stability and ground traction for the task of locomotion on uneven terrain. However, we will specifically focus our attention on two major complementary/conflicting design criteria – workspace and suspension – in creating designs for such leg-wheel sub-systems. A *large workspace* is desirable from the viewpoint of achieving adequate ground clearance and the ability to surmount obstacles and hence the open-kinematic structure of serial-chain based systems would be preferred. However, from the viewpoint of the *suspension*, typically we need an extremely small workspace and highly stiff articulations and hence various types of closed-loop mechanical linkages have played an important role. A systematic examination of these criteria will be another underlying theme in our work. We begin this process by considering two criteria that will help us to characterize these many variants of the designs: (i) Articulated Degrees-of-Freedom and (ii) Equilibration – Actuated and Structural.

1.1.1 Articulated Degrees of Freedom

We begin by considering sagittal plane motion of the wheel with respect to the chassis within each articulated leg-wheel subsystem. We assign a frame of reference to

the chassis and another to the wheel at its axle. We will consider the wheel-axle frame as forming the end-effector of an articulated linkage and use the terminology from robotics literature to examine the workspace of such systems.

Since the orientation of the wheel (rolling about its axis) is irrelevant, we see that the wheel axle frame has 2 translation DOF, relative to chassis, as shown in Figure 1.2 (a). A variety of intermediate articulated mechanisms can now be created between the two frames. For example, Figure 1.2 (b) shows a rigid connection between the two frames which eliminates all motion degrees of freedom between the two frames.

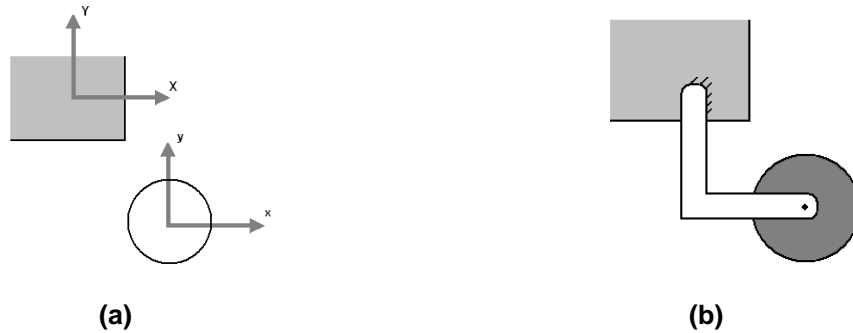


Figure 1.2 (a) The two frames have 2 D.O.F and (b) Motion D.O.F eliminated by rigid joint.



Figure 1.3 (a) 1 motion DOF articulation using revolute joint and (b) 1 motion DOF articulation using prismatic joint.

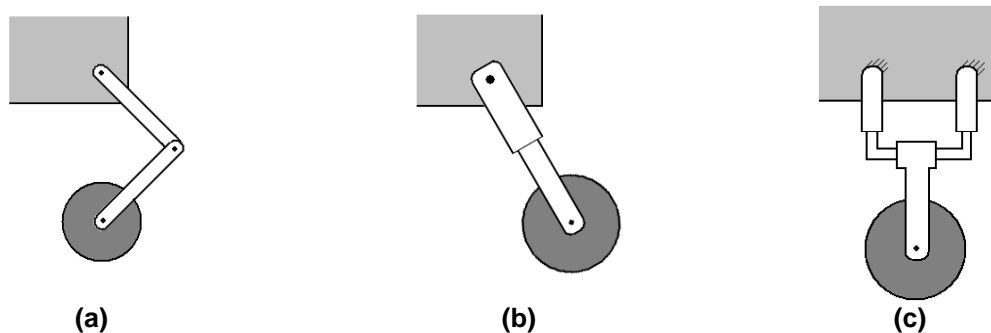


Figure 1.4 (a) 2 motion DOF articulation using (a) 2R joints (b) RP joints (c) PP joints

However, a designer can control the number of DOF that are retained/eliminated by changing types of articulations/joints (and the links) of the intermediate mechanism. We first consider the case where this articulated linkage contains a single lower-pair joint. In Figure 1.3 (a) the revolute-joint permits motion along the circle while eliminating all motion perpendicular to the circle while in (b) the prismatic joint allows all translations

along the direction of the joint while constraining all motions perpendicular to the translational axis. Adding additional articulations increases the intermediate degrees-of-freedom (DOF) with the chain resulting in a two-degree-of-freedom systems shown in Figure 1.4. In Figure 1.4 (a), we have an RR type serial-chain linkage; while in Figure 1.4 (b), we have an RP type serial-chain linkage and Figure 1.4 (c) has PP type serial-chain linkage (c) – each with 2 DOF, which does not constrain any of the wheels motion.

1.1.2 Equilibration (Structural and Actuation-based)

Adding additional articulations increases the intermediate degrees-of-freedom with the chain, such degrees-of-freedom need to be controlled/restricted either *actively* by actuation, *semi-actively* using springs and dampers or *passively* by adding some form of structural–equilibration using hardware constraints.

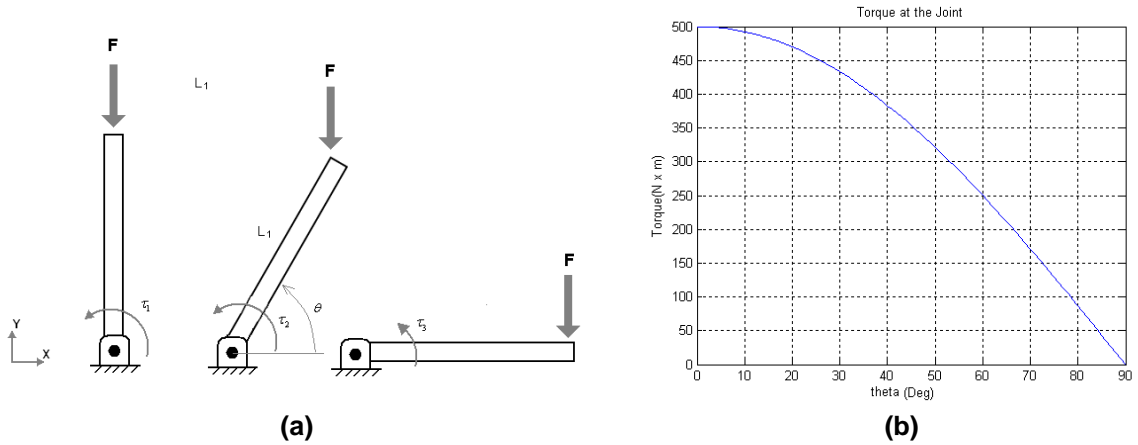


Figure 1.5 (a) Equilibration for a 1-link mechanism and (b) Active Equilibration Torque Requirement.

Since the load-bearing requirements can be significant, we will focus on the ability to use structural equilibration to bear these loads to the largest extent possible. The partitioning of the load bearing is highly configuration dependant and we will examine ways of customizing the configuration to enhance this process. This is best illustrated using the relatively simple example of a one-link mechanism required to support a constant/fixed end-effector load (shown in the Figure 1.5 (a)). By geometry of one link system, the end-effector velocity can be written as:

$$\begin{bmatrix} \dot{x} \\ \dot{y} \end{bmatrix} = \begin{bmatrix} -L_1 \sin \theta \\ L_2 \cos \theta \end{bmatrix} \dot{\theta} \quad (1.1)$$

and using the principle of virtual work one can calculate the net torque required to support a given end-effector load $\mathbf{F} = \begin{bmatrix} F_x & F_y \end{bmatrix}^T$ as:

$$-F_x \dot{x} - F_y \dot{y} + \tau \dot{\theta} = 0 \quad (1.2)$$

$$\tau = \begin{bmatrix} F_x & F_y \end{bmatrix} \begin{bmatrix} -L_1 \sin \theta \\ L_2 \cos \theta \end{bmatrix} = \begin{bmatrix} -L_1 \sin \theta & L_2 \cos \theta \end{bmatrix} \begin{bmatrix} F_x \\ F_y \end{bmatrix}$$

The torque required to support a constant load of [0, -100N] at different configuration is shown in Figure 1.5 (b). In almost all these cases the nature of constraint created now depends upon the geometry (link dimension and configuration) of the articulation. We see that when $\theta = 0^\circ$ the equilibration of the load is almost and entirely by the way of the actuation while when $\theta = 90^\circ$ corresponds to the case of pure structural equilibration.

Thus, in this example by changing configuration of legged system with low power, one can save a lot of energy consumption for supporting load and although this corresponded to a simple case, it is equally evident that the configuration selection by the designer can be a crucial design factor for designing a leg-wheel subsystem.

1.2 Single Degree-of-freedom Articulated Leg-Wheel Systems

Current trends in robotics could enable us to increase the number of articulations (and actuation) within each subsystem in an attempt to create a “general-purpose solution” to overcome the increasing surface-roughness. However, we note that this increases the overall control complexity required even for basic operation of the vehicle on flat surfaces. Instead, in our work, we will make a case for creating *passive* articulated mechanical subsystems with built-in capability for graceful system degradation to a less capable (but stable) operational mode in cases of power-failure.

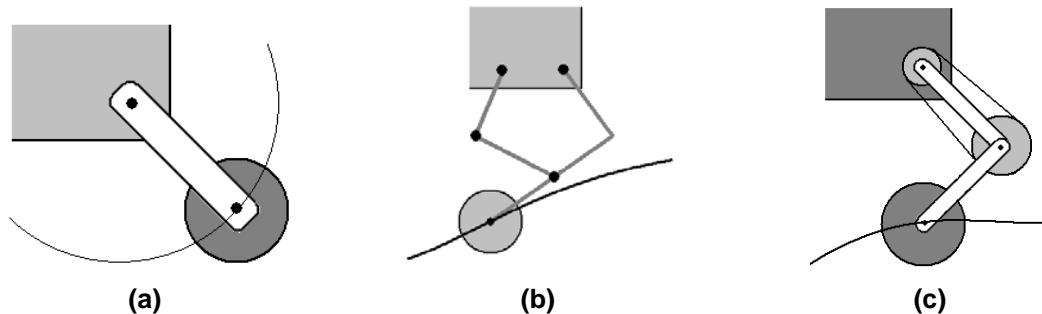


Figure 1.6 Constrained single degree-of-freedom motions can be achieved using: (a) Single-articulation; or (b-c) Multiple-articulations (but with suitable hardware constraints).

We focus our attention on various single degree-of-freedom articulated leg-wheel systems designs – the simplest form is the single revolute- or prismatic-jointed single-link articulation as discussed earlier in Section 1.1.1 which contains a simple lower-pair joint. However, simple articulations such as these have very limited geometric motion capability – for example revolute joint limits the wheel –axle to move in a circle while the prismatic joint constrains it to move in a straight line. Our emphasis in the selection process will be an articulated leg-wheel design that permits the greatest motion capability between the chassis and wheel while maintaining the smallest degree of freedom within the articulated system, i.e. we would like to permit the wheel to trace a controlled complex geometric motion trajectory relative to the chassis but keeping the relative degrees-of-freedom as small as possible.

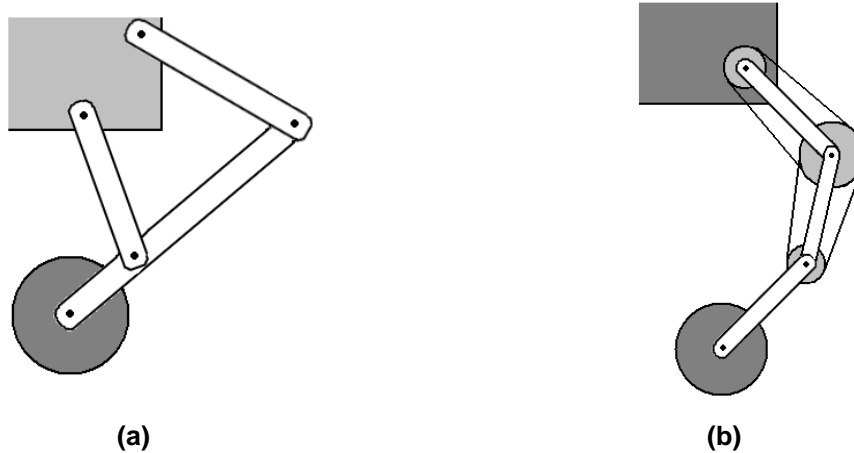


Figure 1.7 Proposed articulated leg-wheeled system design with (a) Fourbar-based and (b) Single Degree of Freedom Coupled Serial Chain (SDCSC) based configurations.

In order to permit tracing of curves of greater complexity, we need to add more joints to increase geometric motion capability. However, this also increases the number of degrees-of-freedom within the chain -- if we need to restrict the end-effector (Wheel-Axle) to a specific desired path which is 1 D.O.F curve, constraints need to be added to the overall system. As noted in Section 1.1.2, such equilibration can be achieved by imposing constraints actively or passively and in hardware or in software. We will however focus on constraint implementation in hardware with two potential designs.

- One of the proposed designs for this intermediate articulation is the well-known fourbar design. The fourbar linkage is the simplest possible pin-jointed mechanism for single degree-of-freedom motion while allowing tracing of complex motion and force-profiles and it is this versatility that is responsible for its ubiquitous use in machinery designs [19].
- *The alternate design is one that uses the Coupled Serial Chain (CSC) configuration – obtained by physically coupling the distal joint rotations of a revolute-jointed, multi-link, serial chain mechanism to the rotation of the proximal joint resulting in an Single Degree-of-freedom Coupled Serial Chain (SDCSC) mechanism. The rotation of the base link now drives all the other coupled links and increasing the number of links enables us to trace curves of increasing complexity and variety while retaining the single degree of freedom operation [15], [17].*

In this thesis, we will emphasize the design-customization and adaptation of these two single degree-of-freedom mechanisms for use on rough terrain.

1.3 Our Research Goals

The issues pertaining to creation, analysis and realization leading to the development of the full potential of these two candidate single-degree-of-freedom designs for the articulated leg-wheel system will motivate the research.

- We will examine the incorporation of greater flexibility to tackle increasing terrain roughness, achieving better chassis-terrain decoupling and reducing actuation

requirements by adapting methods from kinetostatic design optimization to design of the leg-wheel subsystems.

There are many choices of various mechanism configuration and mechanism design parameters that need to be made in order to design an articulated leg-wheel system that is capable of surmounting an obstacle using minimal actuation forces while supporting the weight of the chassis. One of the methods that we will employ to match the desired kinematic trajectories and static torque profiles is by use of methods from kinetostatic synthesis and optimization that have traditionally been used in mechanism synthesis literature. These methods offer a systematic means for selection of unknown parameters and will be discussed in some detail.

- In our work, we will examine the incorporation of flexibility to customize/tailor the passive mechanical system (preflex) responses by both the initial/offline selection of the mechanical parameters as well as online selection of the configuration/reconfiguration of select system parameters

The articulated subsystems under consideration come to equilibrium when the external forces (applied typically to the end-effector) and internal actuation forces, (applied actively due to motors or passively by springs/dampers) are balanced. These equilibrium locations depend critically upon various mechanism parameters including the physical parameters such as link-lengths and spring constants as well as the current, initial and unloaded configurations of the entire system. The designer has considerable control over selection of these parameters and one of the goals of this chapter is to explore the influence of these parameters on the system equilibria. In particular, we wish to examine not only the locations of the system equilibria but also other affiliated properties such as regions of stability and basins of attraction among others.

1.4 Organization of the thesis

The remainder of the thesis is organized as follows. Chapter 2 presents a brief survey of many of the leg-wheel designs that currently exist in the literature. Chapter 3 presents an overview of the general design process set in the framework of dimensional synthesis of mechanisms to match desired kinematic and static design specifications by a combination precision point synthesis and optimization [15], [17]. This process is then explored in detail in the specific context of design of SDCSC-based and fourbar-based articulated leg-wheel subsystems to surmount obstacles in Chapters 4 and 5. Special attention is also paid to reduce the overall actuation requirements by a combination of structural equilibrium and spring assistance. Chapter 6 is devoted to explore the influence of various mechanism parameters on passive mechanical behavior of such articulated leg-wheel systems (in terms of the locations, stability and basins of attraction on equilibrium configurations). Finally, Chapter 7 summarizes some of the contributions of this work and outlines some directions for future study.

2 Brief Background on Leg-Wheel Systems

High cross-country ability and maneuverability are the major requirements for autonomous mobile robots intended for operation on natural terrain. Many leg-wheel platforms have been developed for a variety of uneven terrain exploration in both terrestrial (arctic) and extra-terrestrial (planetary) applications. In almost all these cases, they highlight aspects of the mechanical design of the articulated leg-wheel system that endows them with their capabilities. The common thread is also that in almost all cases no systematic effort to design the articulated leg-wheel system is ever considered.

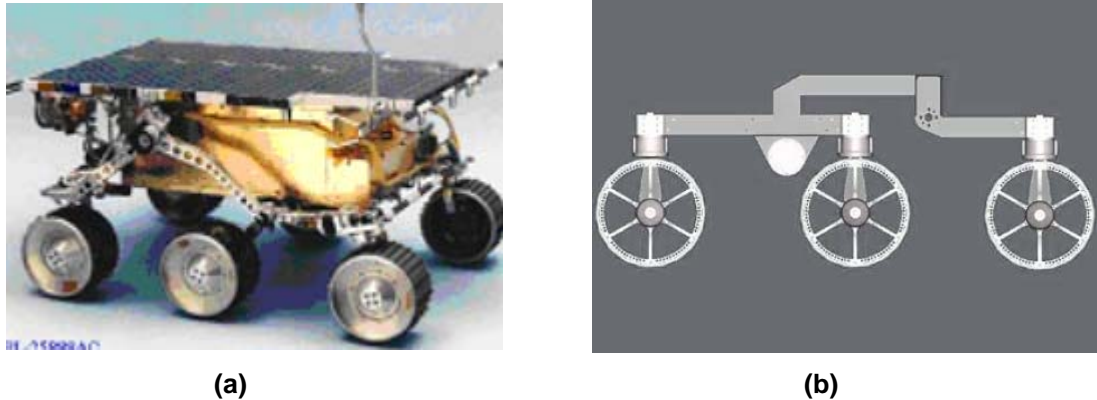


Figure 2.1 (a) Mars Rover and (b) Side View of Rocker-Bogie Configuration [1],[2].

Mars Rover [1],[2], as shown in Figure 2.1, is using a system called a rocker bogie. NASA's currently favored design, the rocker-bogie, uses a two wheeled rocker arm on a passive pivot attached to a main bogie that is connected differentially to the main bogie on the other side. The body of the rover is attached to the differential so it is suspended at an angle that is the average of the two sides. The ride is further smoothed by the rocker, which only passes on a portion of a wheel's displacement to the main bogie.

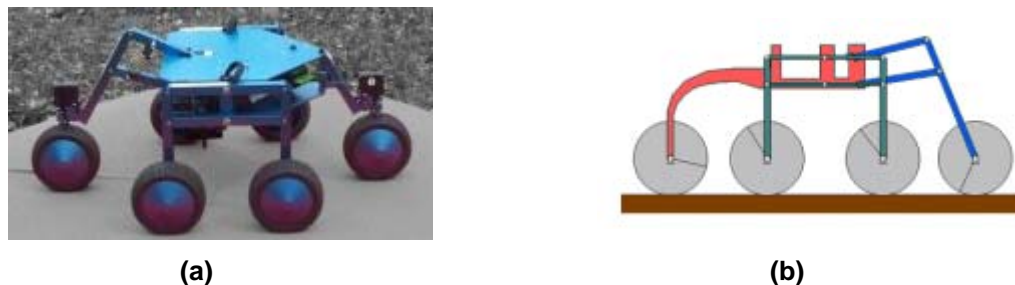
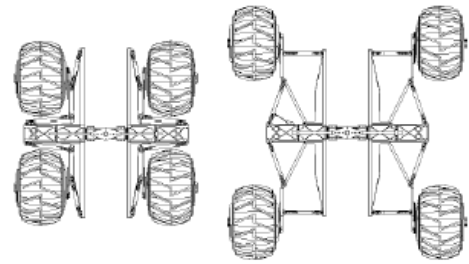


Figure 2.2 (a) SHRIMP III and (b) Section view of SHRIMP [3]

SHRIMP [3], as shown in Figure 2.2, has passive suspension including one front wheel, one trailing wheel, front wheel having a four link suspension with a spring and two middle wheels on each side connected with links. The robot can overcome the obstacle so, that the front wheel after the collision with an obstacle starts raising and stepping away. The SHRIMP's passive mobility is because of the parallel architecture of the front fork and of the bogies. The bogie design of SHRIMP ensures that the instantaneous center of rotation is always situated under the wheel axis.



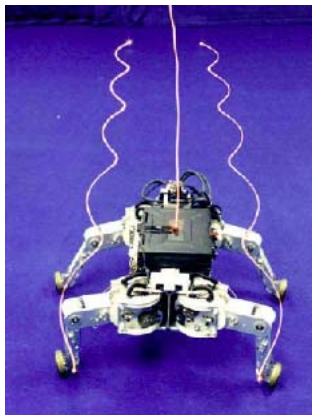
(a)



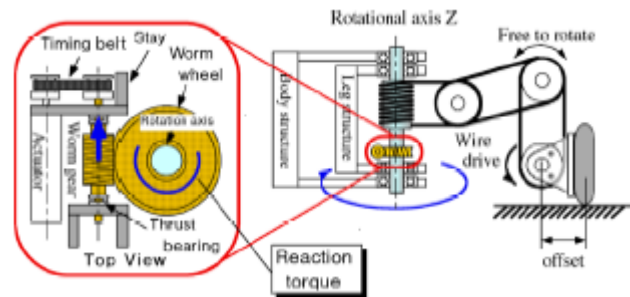
(b)

Figure 2.3 (a) NOMAD and (b) Transforming Chassis of NOMAD [4]

NOMAD [4], as shown in Figure 2.3, uses steerable 4 wheels and the steering angles of the wheels on each side are linked with a 4 bar mechanism and a lead screw. In order to distribute the normal forces on the wheels, NOMAD has two floating side frames called bogies. Each bogie is a structure that supports and deploys two wheels (left or right). By allowing the side frames to pivot on a central axle, the wheels can conform to uneven terrain and maintain even ground pressure. NOMAD features individual propulsion drive units that reside inside the wheel. This is unlike typical all-terrain vehicles, which have a central drive unit that distributes power to each of the wheels.



(a)



(b)

Figure 2.4 (a) Roller-Walker and (b) Leg Mechanism of Roller-Walker [7]

The Roller-Walker [7], as shown in Figure 2.4, realizes wheeled locomotion by roller-skating using passive wheels. Roller-Walker is hybrid robot with legs and wheels which has good efficiency by wheel running on a flat area and good ground adaptability by leg type propulsion on a irregular areas. Wheels used in this robot are passive without a driving device. They act as the foot sole in walking mode and wheels for roller-skating in wheel running mode.

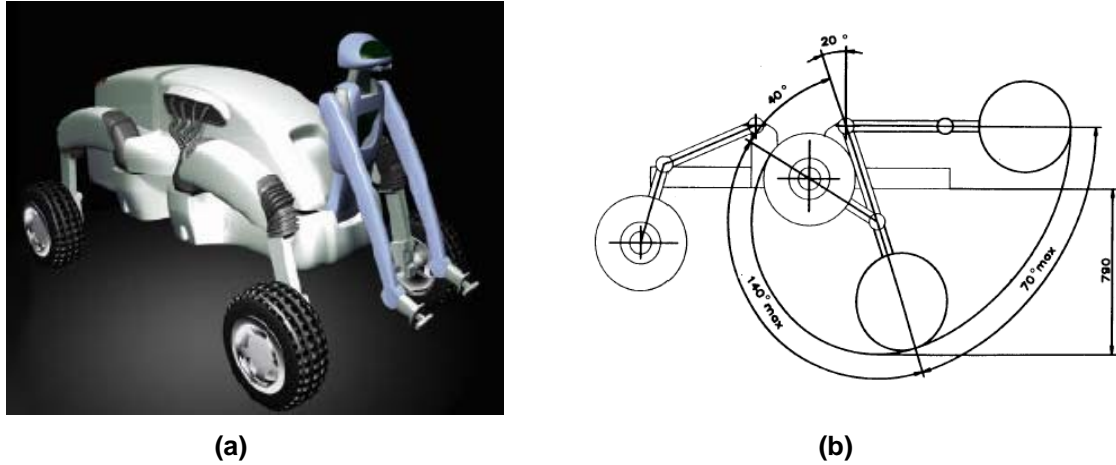


Figure 2.5 (a) WorkPartner and (b) Working Area of a Wheeled Leg [5],[6].

WorkPartner [5],[6], as shown in Figure 2.5, is using powered legs and passive wheels and active joint frame with four legs for their articulation respectively. The locomotion system allows motion with legs only, with legs and wheels powered at the same time or with wheels only. WorkPartner robot has two-arm manipulator system and its body is jointed to the platform with two joints.

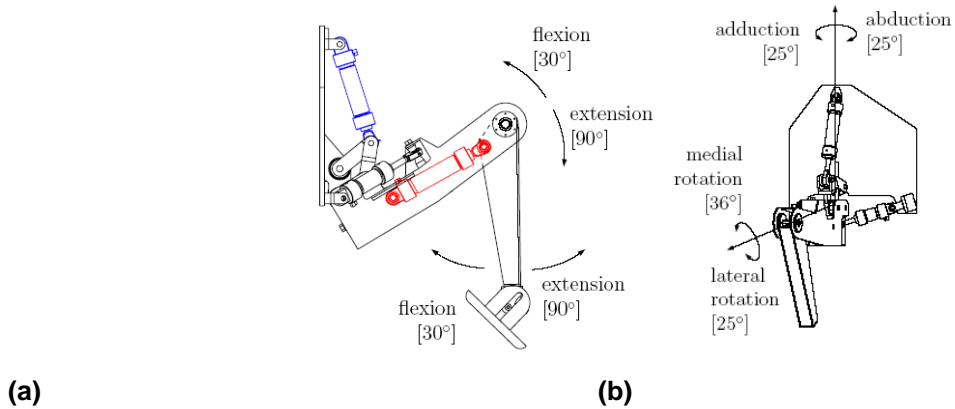


Figure 2.6 (a) ALDURO and (b) Lateral/vertical Work Space [13]

ALDURO[13], as shown in Figure 2.6, is using concept, the advantage of the maneuverability of walking machine in uneven terrain is combined with the higher speed and higher stability of a wheeled vehicle. An important feature of ALDURO is the spatial leg mechanism with anthropomorphic properties, consisting of a spherical hip-joint (with three DOF), a knee-joint (with one DOF) and a suspended foot.

3 Design Approach

We present a relatively general approach to the selection of the parameters of an articulated leg-wheel subsystem to match desired specifications. First and foremost, we develop it as a kinematic path-following problem, i.e, a problem of selecting the parameters to permit the wheel axle (which serves as the end-effector) to follow a desired pre-specified path relative to the chassis (which serves as the base). Subsequently, we use an extended kinetostatic formulation to determine parameters that also match desired force-specification (such as trying to minimize the torques necessary to equilibrate a desired end-effector load along a desired path). As evident from the above discussion, this process is dependent upon various kinematic parameters of the intermediate linkage (including the link-lengths and the selected configuration) and the static parameters (such as spring constants, etc.).

3.1 Applied loads at the end-effector of a leg-wheel design

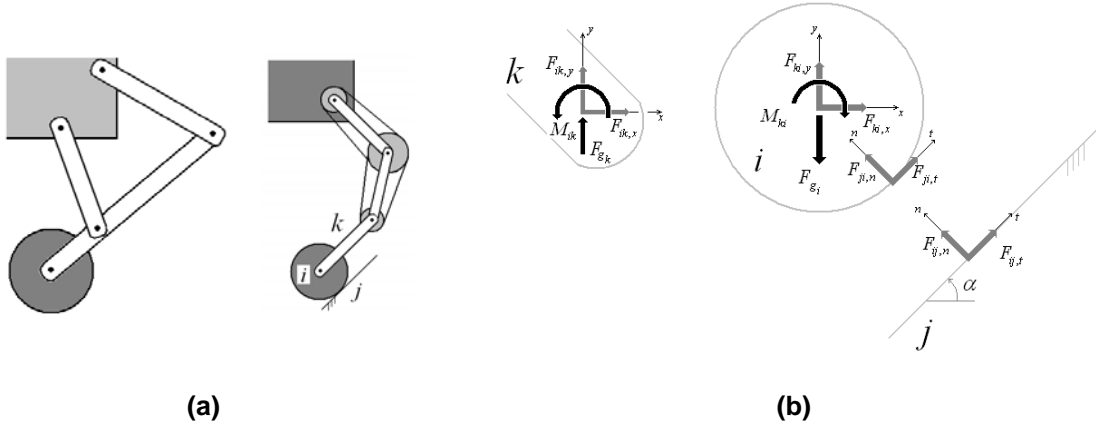


Figure 3.1 (a) Schematic and (b) FBD of SDCSC/Fourbar supporting external force & torque

Figure 3.1 depicts the schematic of an articulated subsystem (fourbar based or SDCSC based) attaching a wheel to the chassis. In order to determine the external loads that would be applied on the end-effector of this linkage, we consider the free-body-diagrams of the final link, the wheel and the ground. The overall weight of chassis (divided by number of legs) and the weight of the links in the articulation create the normal force F_g applied at the axle. We assume a ground slope of α and denote the ground, wheel and axle as bodies- j, i, k respectively. Assuming F_{ij} as force of body-i act on body-j and F_{ji} as force of body j act on body i, the force that wheel exerts on axle and force that body-j exerts on the body-k is

$$\begin{bmatrix} F_{ki,x} \\ F_{ki,y} \end{bmatrix} = \begin{bmatrix} \cos \alpha & -\sin \alpha \\ \sin \alpha & \cos \alpha \end{bmatrix} \begin{bmatrix} F_{ji,t} \\ F_{ji,n} \end{bmatrix} = \begin{bmatrix} -F_{ki,x} \\ -F_{ki,y} \end{bmatrix} \quad (3.1)$$

where the normal force of body-j is $F_{ji,n}$ and the tangent force of wheel is $F_{ji,t}$.

Given the torque exerted by the motor is M_{Motor} , the moment that wheel exerts on the axle can be computed as:

$$M_{ki} = -M_{motor} + \mu F_g R \sin \alpha = R \cdot F_{ji,t} \quad (3.2)$$

$$F_{ji,t} = \frac{M_{ki}}{R} = -\frac{M_{motor}}{R} + \mu F_g \sin \alpha \quad (3.3)$$

$$M_{ik} = -M_{ki} = M_{motor} - \mu F_g R \sin \alpha \quad (3.4)$$

Noting that the normal force of body-j $F_{ji,n}$ is $F_{ji,n} = -F_g \cos \alpha$ we get:

$$\begin{bmatrix} F_{ki,x} \\ F_{ki,y} \end{bmatrix} = \begin{bmatrix} \cos \alpha & -\sin \alpha \\ \sin \alpha & \cos \alpha \end{bmatrix} \begin{bmatrix} -\frac{M_{motor}}{R} + \mu F_g \cdot \sin \alpha \\ -F_g \cdot \cos \alpha \end{bmatrix} = \begin{bmatrix} -F_{ik,x} \\ -F_{ik,y} \end{bmatrix} \quad (3.5)$$

Equations (3.4) and (3.5) show that the moment and forces respectively, at the end-effector are intimately dependent upon the slope of the ground; but (i) more importantly moment and forces are dependent upon (ii) and can be controlled by the motor torques applied on the wheel at the axle.

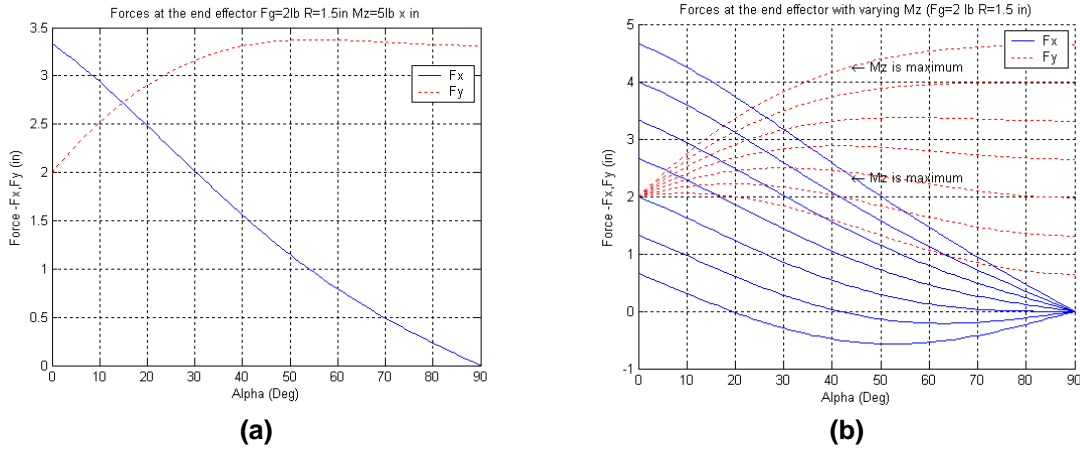


Figure 3.2 (a) Forces at the end-effector and (b) forces with different motor torque

When ground slant is zero, vertical load is same as system's weight and horizontal load is determined by reaction torque between ground and wheel driven by motor. If slant is 90 degree, x direction force comes to zero and y direction force is decided by motor torque and vertical load. As shown in Figure 3.2, by changing motor torque at the end-effector, we can control reaction forces at the end-effector. This is one of the advantages of this system, in which can control overall torque by reaction of the other motion.

3.2 User-inputs for Problem Specification

In order to achieve this, the first stage is the specification of the type of desired kinematic and static trajectories including the various magnitudes. In the next few subsections we will discuss places where we have made provision for user-inputs in our implementation. Our ultimate goal is the creation of a user-friendly tool for design of such an articulated wheeled subsystem to surmount obstacles.

3.2.1 Kinematic Design Factors under User-Control

The principal reason for introducing the articulations between chassis and wheel is to enable the robot to accommodate and overcome most obstacles by permitting the front wheel to rise up when it collides with the obstacle.

3.2.1.1 Shape of the desired kinematic motion curve

The specification of a desired kinematic motion curve would typically consist of specification of the motion of the axle with respect to a coordinate frame attached to the chassis of the moving vehicle. Additionally, a designer has freedom in selecting the type, number and locations of the precision points at which an exact matching of the desired motion trajectories would be desired. However, we note that in general the relative motions of the wheel with respect to the chassis consists of two component motions – rising and offsetting – which depend not only upon the nature of the obstacle but also upon the inherent motions of the chassis itself, as illustrated in Figure 3.3.

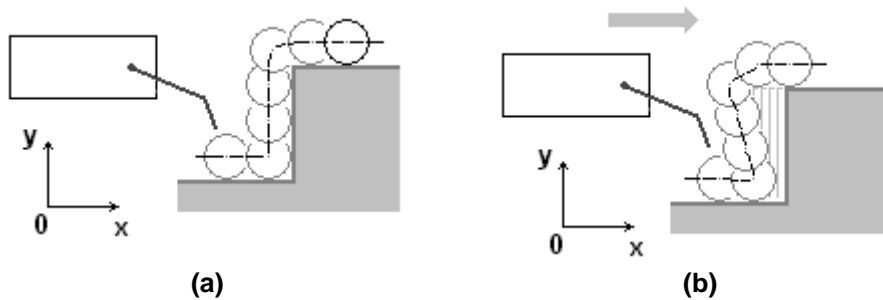


Figure 3.3. Motion of the wheel with respect to an Inertial frame of reference (OXY) as vehicle surmounts a fixed height step – (a) simple rising motion when chassis does not move; and (b) rising and offset motion as chassis moves forward.

Although the creation of the desired motion trajectory depends critically upon the selection of a chassis velocity. We nominally assume a fixed chassis for the rest of this thesis. However, we would like to note that the method can similarly be applied to treat the desired kinematic trajectories resulting from selection of wide range of chassis velocities.

3.2.1.2 Open and closed loop kinematic trajectories

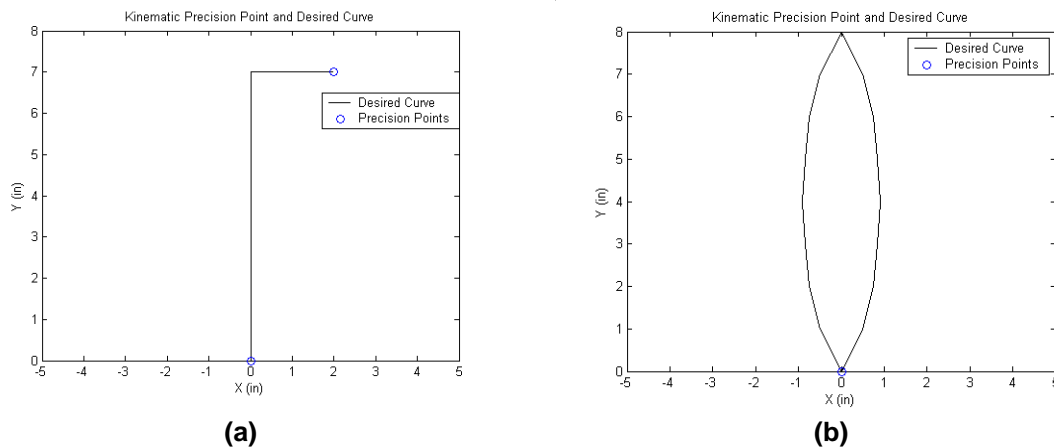


Figure 3.4 Candidate kinematic trajectories – (a) open-loop desired curves and (b) closed loop desired curve

In many cases, the wheel axle follows an open-loop curve as it surmounts an obstacle and retraces this curve in the opposite direction as the wheel moves back to its nominal/initial position. However, there are many other situations where the wheel traces a closed path with non-zero enclosed area as the axle moves over the obstacle and returns back to the nominal initial position. We will consider both such cases separately.

3.2.2 Force-related design factors under user-control

Similar to the process of specification of a kinematic trajectory, there are many choices to be made for specification of a desired static curve including:

3.2.2.1 Shape of the desired static torque curve

The final desired curve is typically specified in terms of torques required for a given relative displacement of the articulated linkage and would include specification of the maximum/minimum torque as well as number of precision points at which an exact matching of the torque specification is desired.

3.2.2.2 Position/Type/Number of Equilibria for the system

The spring reaction torques can be relatively easily determined by spring constant and initial spring deflection angle in our systems. In contrast, the external torque specification not only depends on the external load specification at the end-effector but also upon other factors such as the current system configuration, the ground slant etc. Since it is essentially the interaction of these two sets of forces that determine the location and type of equilibrium positions, the user can exert considerable influence by suitable selection of spring parameters .

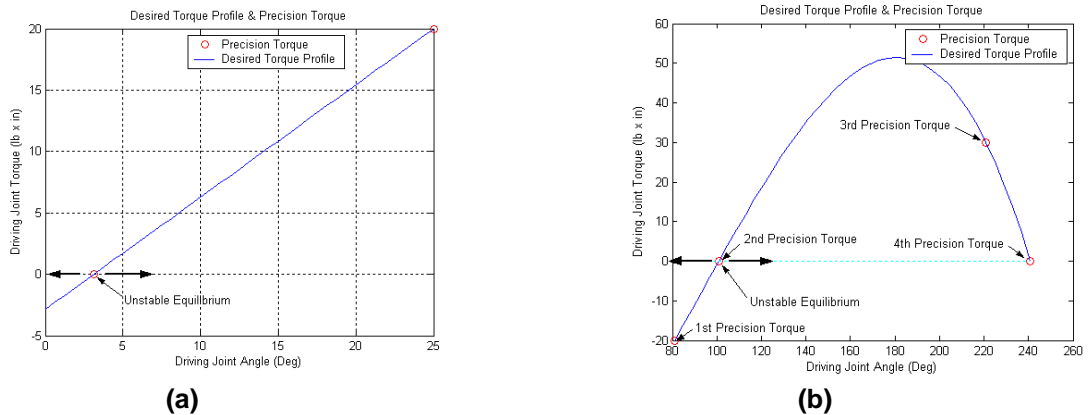


Figure 3.5 Shaping the desired static torque curve, including specification of the maximum/minimum torque as well as type/number/position of precision matching of the torque specification.

Figure 3.5 depicts examples of desired torque curve specifications that can be made by the user. For example in Figure 3.5(a) an unstable equilibrium point is placed at a certain offset angle which can help create robustness to small displacement disturbances (by way of returning torques that return the system back to the original system configuration). However beyond a certain threshold displacement, the unstable equilibrium causes the system to bifurcate to an alternative configuration. Such behaviors are extremely desirable when we wish to endow the system with sets of mechanical reflexes that can enhance its ability to traverse in uneven terrains and various aspects of

these behaviors such as transition angle, maximum and minimum torques can be controlled by design of the spring constants, preload angle etc.

3.3 Specific Test Scenario

3.3.1 Design of the kinematic trajectory for the test case

According to Uniform Building Codes(UBC), stair tread have a minimum of 7 1/2", 12" out from the narrow edge of the tread and the rise will not be more than 9 1/2". But stairs with no vertical riser or with a lip can present real problems to robot going up and down. Even worse, when stair is at angle in example spiral staircase it requires more complex adaptability and mobility to the robot. Thus in this thesis we will consider only ideal profile of step.

3.3.2 Design of the static trajectory for the test case

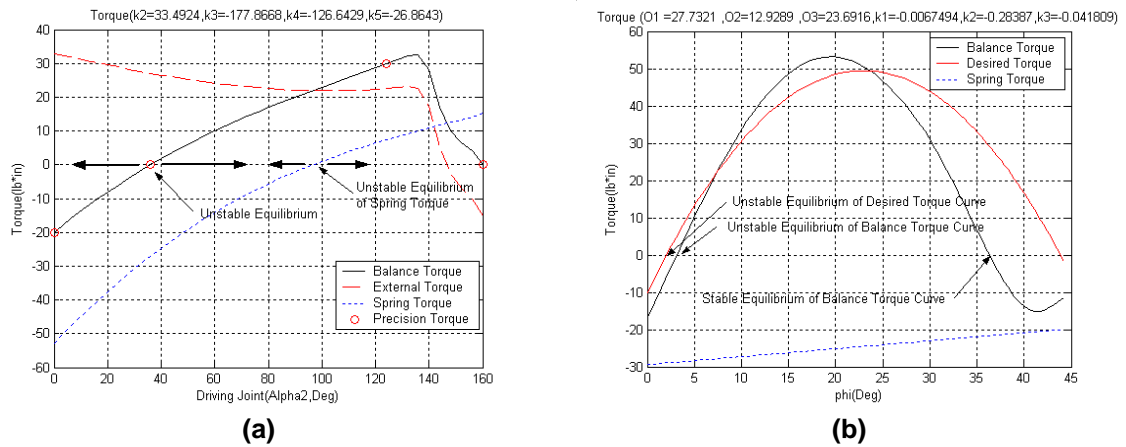


Figure 3.6 Desired Torque Design (a) by Precision torque and (b) Desired Torque Curve

Using precision torques allows for considerable freedom in determining equilibrium positions and simplicity in design of the “desired static torque” profiles. In all the designs to follow we will consider the nominal rest configuration to be one end of the range of motion. One potential disadvantage of a leg-wheel system is that poor designs may lead to significant power-consumption at the nominal rest configuration. For this reason, one would normally emphasize perfect static balancing of overall system when set on a flat surface which can be realized by requiring zero desired precision torque at the rest position. (However, from the viewpoint of robustness, we in fact select the first precision torque to nominally be a small negative number, forcing the system to come to rest against the end of the range). We note that when the end-effector is in between initial configuration and the second precision position, system torque will try to move system back to the initial configuration. Hence, the location of the second precision torque can be selected to enhance stiffness of system from the disturbance on ground. Once end-effector passes by first precision position then system torque will turn system to the final configuration determined by the other-end of the range. We note that loss of wheel contact with ground causes the external torque to drop to zero. In such a case, the current kinematic configuration relative to the location of the unstable equilibrium will try to move the system to either ends of the range as shown in Figure 3.6.

3.4 Overview of Kinetostatic Design Approach

There are many choices of various mechanism configuration and mechanism design parameters that need to be made in order to design an articulated leg-wheel system that is capable of surmounting an obstacle using minimal actuation forces while supporting the weight of the chassis. The general design problem will be solved here in the framework of dimensional synthesis of mechanisms [18], the process of determination of the dimensions of this mechanism to match desired specifications which offer a systematic means for selection of unknown parameters.

Given a set of task specifications and the type of mechanism, an optimization problem relating the parameters of the device to the set of desired specifications can be formulated and solved. Specifically, we match the desired specifications on end-effector positions and forces. Other types of design specifications can now also be explored. However, the resulting solution mechanism satisfies all these desired specifications only in the least squares sense without guaranteeing exact satisfaction of any specification.

Greater structure is added to this problem by employing Precision Point Synthesis (PPS). The requirement to match specifications exactly at precision points creates constraints between the various parameters of the mechanism which aids the final selection of the parameters of the designed device. The design constraint equations, themselves, are created from the equations of loop-closure for end-effector position specifications or by application of the principle of virtual work for end-effector force specifications as explored in the thesis [15],[16],[17].

The requirement for exact matching of more specifications at precision points creates more constraints. A limit on the number of specifications/points is finally reached and a simultaneous solution of the constraint system yields a unique mechanism. While exact matching at the greatest number of precision positions is desirable, the gains in terms of precise specification matching at many points may be offset by the disadvantage of having to solve a set of nonlinear equations. Hence, in what follows, we consider: the specification of less than maximum feasible number of precision points; a suitable partitioning of all the variables into dependent and independent variables; a suitable specification of the independent variables; leading upto the formation of a linear system of equations in terms of the dependent variables.

Desired mechanism specifications are typically presented in the form of a discrete set (of positions, orientations and forces) to be achieved or approximated as closely as possible by the manipulatory device. In optimization based schemes, we are required to match the design specifications over the range of travel of the mechanism. Hence, some method of interpolating in between the discrete specifications is required to obtain a continuous “desired curve”. The “generated curve” (or alternatively “mechanism curve”) refers to the curve generated by the mechanism whose parameters were determined earlier with the aid of the precision point equations. In general, there is no correspondence between the generated curve and the desired curve except at the precision points due to the different parameterizations. We consider different approaches for the identification of two sets of points that have a one-to-one correspondence to each other based on certain criteria. A point based measure of discrepancy is now required to enable the definition of a cumulative measure of discrepancy over the finite number of

correspondence points which now forms the objective function for the optimization. In the case of uniform specification matching, a summed squares of the discrepancy between the correspondence points is used. For mixed design specification matching requirements, a scale dependent left invariant metric reflecting engineering considerations is used.

The specification of values for the independent variables coupled with the solution of the linear system of equations for the dependent variables creates candidate mechanisms. An optimization scheme over the different candidate mechanisms yields the parameters of the optimal mechanism which satisfies the design specifications exactly at the selected precision points and in the least-squares sense elsewhere. The principal advantage of this approach is the ability to add structure to the problem while offering adequate flexibility/choices to the designer.

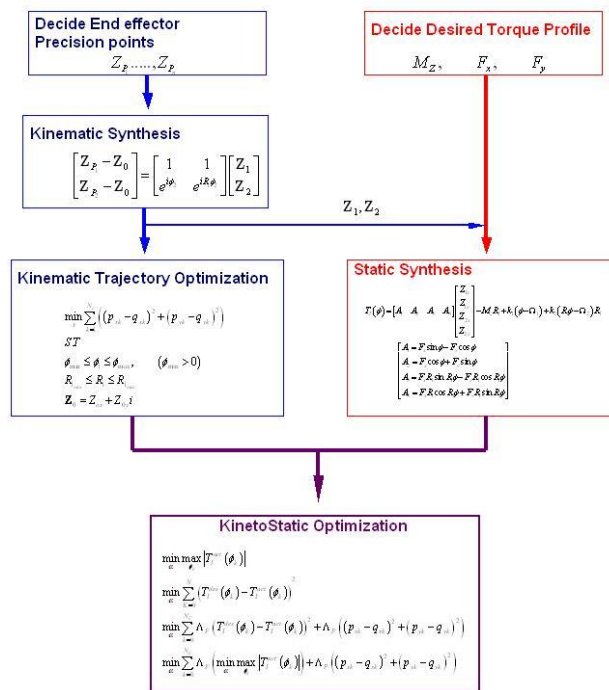


Figure 3.7 Kinetostatic Design: Combining Precision Point Synthesis with Optimization

The key steps to this process are: creation of precision point synthesis design constraints and solution to obtain feasible mechanism candidates; a method of interpolation between desired specifications; a method of obtaining correspondence between the desired specifications and obtained performance; and a measure of error to minimize between the two are summarized in Figure 3.7. These processes are going to be implemented to the design of SDCSC and Fourbar mechanism in the next two chapters.

4 Design/Synthesis of SDCSC Leg-wheel Mechanism

In this chapter, we examine the process of design of an articulated leg-wheel subsystem based on the Coupled Serial Chain (CSC) configuration originally proposed by [15],[16],[17].

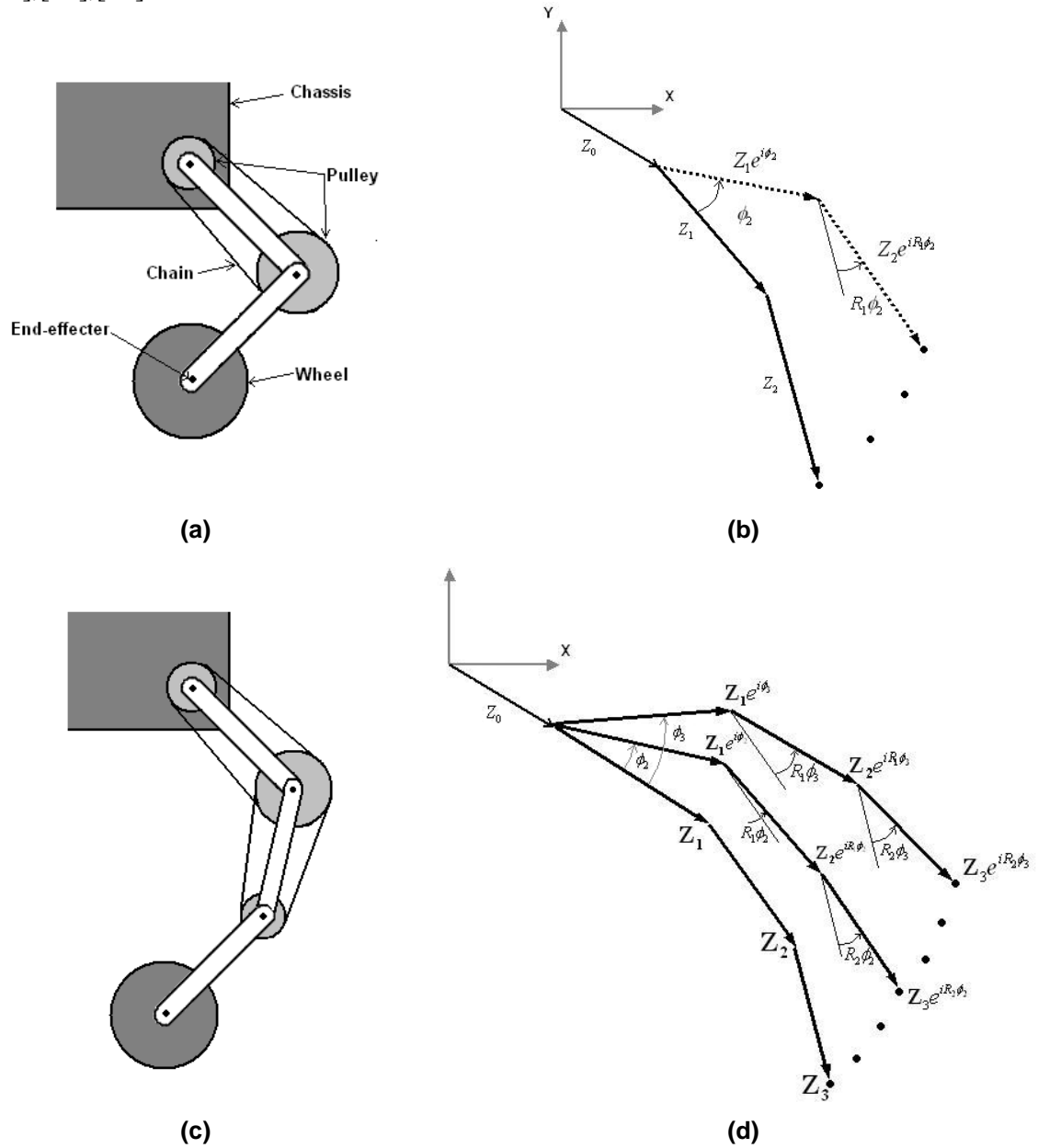


Figure 4.1 (a) Two links SDCSC- based leg-wheel design, (b) corresponding kinematic diagram for two links SDCSC, (c) Three links SDCSC- based leg-wheel design and (d) corresponding kinematic diagram for three links SDCSC

4.1 Coupled Serial Chain (CSC) mechanisms

Coupled Serial Chain (CSC) mechanisms are a novel class of mechanisms that can be physically realized by coupling of the distal joint rotations of a revolute-jointed, multi-link, serial chain mechanism to the rotation of the proximal joint. Each physical coupling between joint rotations reduces a degree of freedom. Repeated couplings between distal proximal pairs of joints can progressively reduce the overall degrees of freedom to one, resulting in a *Single Degree-of-freedom Coupled Serial Chain (SDCSC)* mechanism. The rotation of the base link now drives all the other coupled links. Increase the number of links enables us to trace curves of increasing complexity and variety while retaining the single degree of freedom operation. On one hand, like closed-loop linkages, SDCSC mechanisms have the advantage of simplicity of single DOF design and control. On the other hand, such SDCSC mechanisms resemble robotic serial chains in terms of their workspace and their anthropomorphic geometry but now require fewer actuators. Thus SDCSC mechanisms can combine the reduced-degree-of-freedom control of closed loop linkages with the modularity and compactness of serial chains and it was to combine both sets of advantages that we proposed a design for an articulated leg-wheel subsystem design based on this SDCSC configuration.

Dimensional synthesis methods, developed traditionally in the mechanism design literature, can now be applied to *design* planar and spatial SDCSC mechanisms to match desired end-effector position and force specifications and will be the focus of the rest of this chapter.

4.2 Kinematic Synthesis

The kinematic design of these SDCSC mechanisms for Rigid Body Guidance and Path Following applications was presented in [15],[16],[17]. Building on this work, we examine the use of such a kinematic design process for design of the articulated leg-wheel subsystem to surmount an obstacle. In some cases, matching of the desired specifications is beyond the geometric capability of a specific SDCSC configuration (e.g. a 2-link configuration) and in such cases, we will study the effects of increasing the number of links. Spatial counterparts of planar linkages extend the range and variety of motion due to both the increased number/types of kinematic joints as well as the richer variety of linkages formed but will not be considered here.

In the design process, we consider a two-stage process consisting of: (i) precision point synthesis for small number of precision points resulting in an adequately large number of free-choices and (ii) subsequently performing optimization over the free-choices. The desired trajectory is specified to be a standard step as discussed in Section 3.3.1.

4.2.1 Planar Precision Point Synthesis of SDCSC

The constraint equations used for kinematic precision point synthesis(PPS) approach are derived from the forward kinematics equations. The kinematic equation for the motion of the end-effector of an n-link SDCSC can be written as a function of ϕ_i , the input link rotation angle at the i^{th} position (relative to the first position) as:

$$\mathbf{Z}_{P_i} = \mathbf{Z}(\phi_i) = \mathbf{Z}_0 + \mathbf{Z}_1 e^{i\phi_1} + \mathbf{Z}_2 e^{iR_1\phi_1} + \dots + \mathbf{Z}_n e^{iR_{n-1}\phi_1} \quad \forall i = 1, \dots, m \quad (4.1)$$

Where m is number of precision point and \mathbf{Z}_i is vector of each link.

Two-Link SDCSC Kinematic Synthesis

For a two-link SDCSC and path following (PF) with two precision points, the Precision Point Constraints can be expressed as:

$$\begin{aligned} \mathbf{Z}_{P_1} &= \mathbf{Z}_0 + \mathbf{Z}_1 + \mathbf{Z}_2 \\ \mathbf{Z}_{P_2} &= \mathbf{Z}_0 + \mathbf{Z}_1 e^{i\phi_2} + \mathbf{Z}_2 e^{iR_1\phi_2} \end{aligned} \quad (4.2)$$

or in matrix form,

$$\begin{bmatrix} \mathbf{Z}_{P_1} \\ \mathbf{Z}_{P_2} \end{bmatrix} = \begin{bmatrix} 1 \\ 1 \end{bmatrix} \mathbf{Z}_0 + \begin{bmatrix} 1 & 1 \\ e^{i\phi_2} & e^{iR_1\phi_2} \end{bmatrix} \begin{bmatrix} \mathbf{Z}_1 \\ \mathbf{Z}_2 \end{bmatrix} \quad (4.3)$$

where \mathbf{Z}_{P_1} and \mathbf{Z}_{P_2} are precision points of end-effectors, and $\mathbf{Z}_0, \mathbf{Z}_1, \mathbf{Z}_2$ are the vectors of each link and R_1 is ratio between first and second pulley. The end-effector is now guaranteed to pass through each of the selected precision points on the trajectory. Equation (4.3) contains a total of four scalar constraints obtained from the two scalar loop-closure equations per precision point in the path-following problem and 8 scalar unknowns $z_{0,x}, z_{0,y}, z_{1,x}, z_{1,y}, z_{2,x}, z_{2,y}, R_1, \phi_2$. By selecting $\mathbf{Z}_0 (z_{0,x}, z_{0,y}), R_1, \phi_2$ as the four free choices, a linear solution of the equation can be obtained as:

$$\begin{bmatrix} \mathbf{Z}_1 \\ \mathbf{Z}_2 \end{bmatrix} = \begin{bmatrix} 1 & 1 \\ e^{i\phi_2} & e^{iR_1\phi_2} \end{bmatrix}^{-1} \begin{bmatrix} \mathbf{Z}_{P_1} - \mathbf{Z}_0 \\ \mathbf{Z}_{P_2} - \mathbf{Z}_0 \end{bmatrix} \quad (4.4)$$

Three-Link SDCSC Kinematic Synthesis

For a three-link SDCSC mechanism of a path following (PF) task with three precision points, the Precision Point Synthesis (PPS) constraints can be expressed as:

$$\begin{aligned} \mathbf{Z}_{P_1} &= \mathbf{Z}_0 + \mathbf{Z}_1 + \mathbf{Z}_2 + \mathbf{Z}_3 \\ \mathbf{Z}_{P_2} &= \mathbf{Z}_0 + \mathbf{Z}_1 e^{i\phi_2} + \mathbf{Z}_2 e^{iR_1\phi_2} + \mathbf{Z}_3 e^{iR_2\phi_2} \\ \mathbf{Z}_{P_3} &= \mathbf{Z}_0 + \mathbf{Z}_1 e^{i\phi_3} + \mathbf{Z}_2 e^{iR_1\phi_3} + \mathbf{Z}_3 e^{iR_2\phi_3} \end{aligned} \quad (4.5)$$

or in matrix form:

$$\begin{bmatrix} \mathbf{Z}_{P_1} - \mathbf{Z}_0 \\ \mathbf{Z}_{P_2} - \mathbf{Z}_0 \\ \mathbf{Z}_{P_3} - \mathbf{Z}_0 \end{bmatrix} = \begin{bmatrix} 1 & 1 & 1 \\ e^{i\phi_2} & e^{iR_1\phi_2} & e^{iR_2\phi_2} \\ e^{i\phi_3} & e^{iR_1\phi_3} & e^{iR_2\phi_3} \end{bmatrix} \begin{bmatrix} \mathbf{Z}_1 \\ \mathbf{Z}_2 \\ \mathbf{Z}_3 \end{bmatrix} \quad (4.6)$$

where $\mathbf{Z}_{P_1}, \mathbf{Z}_{P_2}$ and \mathbf{Z}_{P_3} are precision points of end-effectors and $\mathbf{Z}_0, \mathbf{Z}_1, \mathbf{Z}_2, \mathbf{Z}_3$ are the vectors of each link and R_1 is ratio between first and second joints and R_2 is ratio between first and third joints. The end-effector is now guaranteed to pass through each of the

selected precision points on the trajectory. Equation (4.6) contains a total of six scalar constraints obtained from the two scalar loop-closure equations per precision point in the path-following problem with 12 scalar unknowns they are $Z_{0,x}, Z_{0,y}, Z_{1,x}, Z_{1,y}, Z_{2,x}, Z_{2,y}, Z_{3,x}, Z_{3,y}, R_1, R_2, \phi_2, \phi_3$. By selecting $\mathbf{Z}_0 (Z_{0,x}, Z_{0,y})$, and R_1, R_2, ϕ_2, ϕ_3 as the six free choices, a linear solution of the equation can be obtained as:

$$\begin{bmatrix} \mathbf{Z}_1 \\ \mathbf{Z}_2 \\ \mathbf{Z}_3 \end{bmatrix} = \begin{bmatrix} 1 & 1 & 1 \\ e^{i\phi_2} & e^{iR_1\phi_2} & e^{iR_2\phi_2} \\ e^{i\phi_3} & e^{iR_1\phi_3} & e^{iR_2\phi_3} \end{bmatrix}^{-1} \begin{bmatrix} \mathbf{Z}_{P_1} - \mathbf{Z}_0 \\ \mathbf{Z}_{P_2} - \mathbf{Z}_0 \\ \mathbf{Z}_{P_3} - \mathbf{Z}_0 \end{bmatrix} \quad (4.7)$$

4.2.2 Combined Kinematic Precision-Point Synthesis and Optimization

We set desired trajectory of wheel-axle to be the standard step described in section 3.3.1. We use two precision-point synthesis for the 2-link SDCSC case and three precision points synthesis for the three link SDCSC case. As shown in Figure 4.2, we set $0+i0$ as first precision point, $2+i7$ as second and put one more precision point at $0+i7$ for three link PPS.

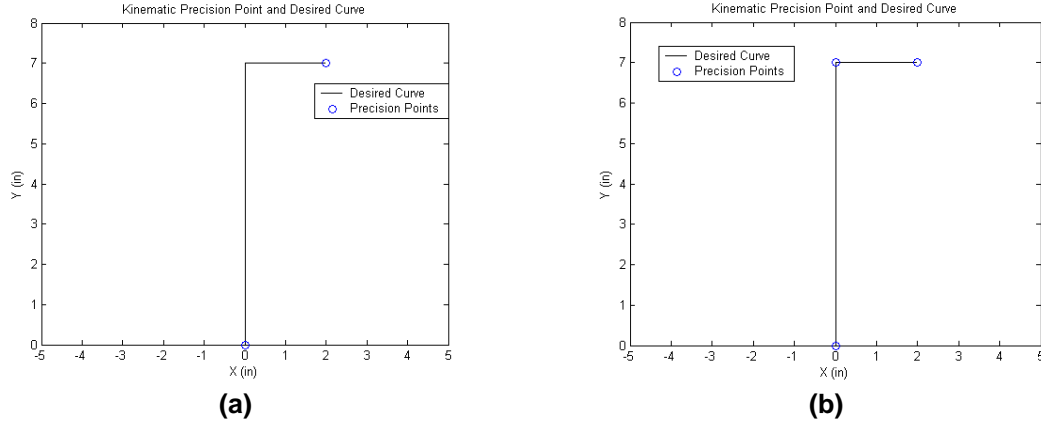


Figure 4.2 Desired trajectory of end-effector for (a) Two link SDCSC and (b) Three link SDCSC

2-link Design Synthesis

The overall design selection problem may be expressed in the form of a constrained optimization problem as:

$$\min_{\bar{x}} \sum_{k=1}^{N_c} \left((p_{xk} - q_{xk})^2 + (p_{yk} - q_{yk})^2 \right) \quad (4.8)$$

subject to

$$\phi_{\min} \leq \phi_1 \leq \phi_{\max}, \quad (\phi_{\min} > 0)$$

$$R_{1_{\min}} \leq R_1 \leq R_{1_{\max}}$$

$$\begin{bmatrix} \mathbf{Z}_1 \\ \mathbf{Z}_2 \end{bmatrix} = \begin{bmatrix} 1 & 1 \\ e^{i\phi_2} & e^{iR_1\phi_2} \end{bmatrix}^{-1} \begin{bmatrix} \mathbf{Z}_{P_1} - \mathbf{Z}_0 \\ \mathbf{Z}_{P_2} - \mathbf{Z}_0 \end{bmatrix} \quad (4.9)$$

$\mathbf{Z}_0 = Z_{0,x} + Z_{0,y}i$, $Z_{0,x}$ and $Z_{0,y}$ are constant.

We limit the ranges of ϕ and the pulley ratio R_1 to match the requirements imposed by the constraints of physical realization. Furthermore, the position of first joint of link, Z_0 , is fixed with respect to the mechanical parameters of the system i.e., the location on the chassis, and length of the first link are also limited to satisfy the feasibility constraints.

For this problem, multiple minima exist and for a systematic exploration of the process, we perform a parameter sweep over all possible combination of free choices. This problem is classified into in the case of positive value of R_1 and negative value of R_1 . The relationship between design variables and objective function can be shown by plotting all data on the same plot.

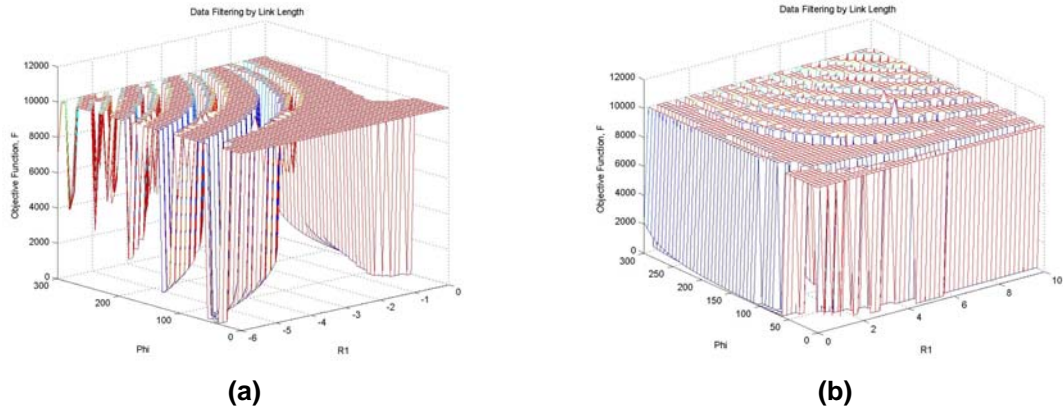


Figure 4.3 Objective function values obtained by a parameter sweep of R_1 and ϕ (a) $R_1 > 0$ and (b) $R_1 < 0$

Figure 4.3 (a) and (b) depict the computed objective functions for parameter sweep of the various values of the free choice/design variables in the two link SDCSC after filtering out results when the first link is not in the range of $L_{\min} \leq L \leq L_{\max}$. As can be clearly seen there are many choices for the minimum and we plot one candidate result of an optimization. By increasing the number of links to 3, we can get a better match of desired curves including sharp corners and while satisfying more numbers of precision points

3-link Design Synthesis

The overall design selection problem may be expressed in the form of a constrained optimization problem as:

$$\min_{\vec{x}} \sum_{k=1}^{N_c} \left((p_{xk} - q_{xk})^2 + (p_{yk} - q_{yk})^2 \right) \quad (4.10)$$

subject to

$$\begin{aligned} \phi_{\min} &\leq \phi_2 \leq \phi_{\max}, & (\phi_{\min} > 0) \\ \phi_{\min} &\leq \phi_3 \leq \phi_{\max}, & (\phi_{\min} > 0) \\ R_{1_{\min}} &\leq R_1 \leq R_{1_{\max}} \\ R_{2_{\min}} &\leq R_2 \leq R_{2_{\max}} \end{aligned} \quad (4.11)$$

$$\begin{bmatrix} \mathbf{Z}_1 \\ \mathbf{Z}_2 \\ \mathbf{Z}_3 \end{bmatrix} = \begin{bmatrix} 1 & 1 & 1 \\ e^{i\phi_2} & e^{iR_1\phi_2} & e^{iR_2\phi_2} \\ e^{i\phi_3} & e^{iR_1\phi_3} & e^{iR_2\phi_3} \end{bmatrix}^{-1} \begin{bmatrix} \mathbf{Z}_{P_1} - \mathbf{Z}_0 \\ \mathbf{Z}_{P_2} - \mathbf{Z}_0 \\ \mathbf{Z}_{P_2} - \mathbf{Z}_0 \end{bmatrix}$$

$\mathbf{Z}_0 = Z_{ox} + Z_{0y}i$, Z_{ox} and Z_{0y} are constant.

We limit the ranges of ϕ and the pulley ratio R_1, R_2 to match the requirements imposed by the constraints of physical realization. Furthermore, the position of first joint of link, Z_0 , is fixed with respect to the mechanical parameters of the system i.e., the location on the chassis, and length of the first link are also limited to satisfy the feasibility constraints.

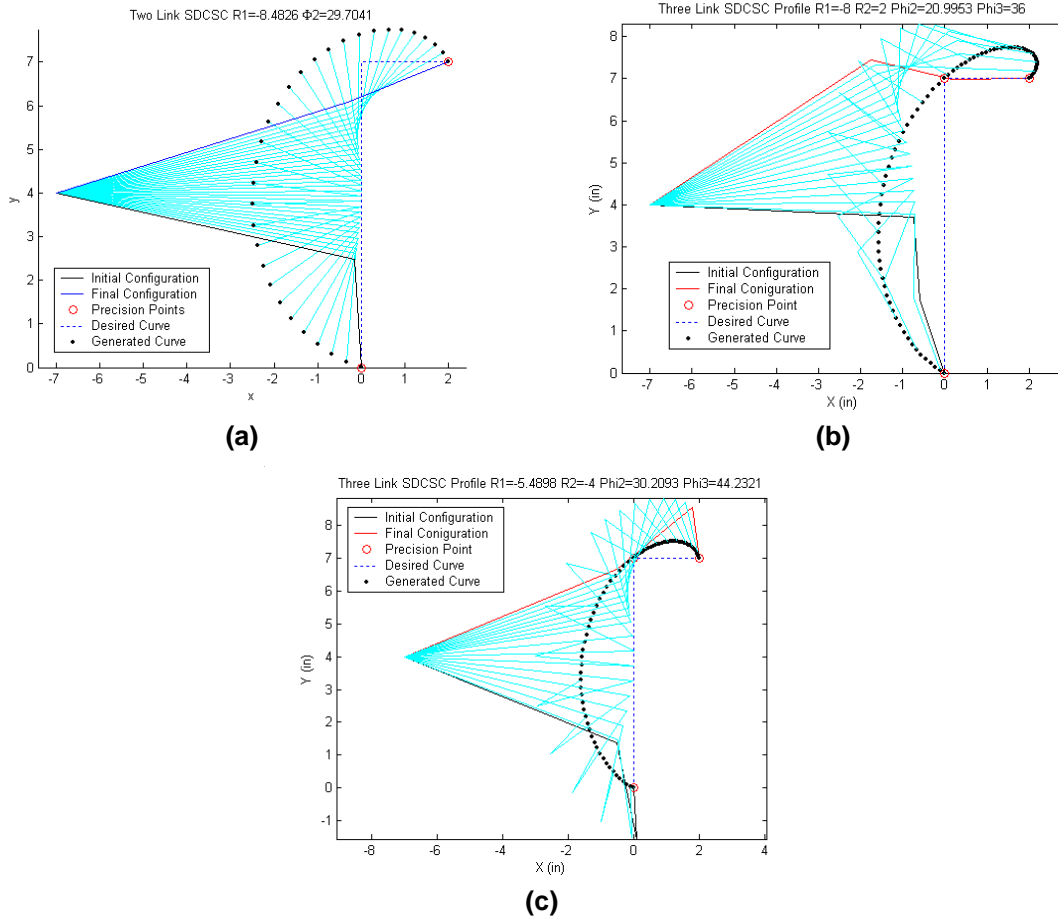


Figure 4.4 Candidate sets of SDCSC Configurations when Design Variables are (a) Two links SDCSC ($R_1 = 8.3467, \phi = 30.4178$) (b) Three link SDCSC configuration I ($R_1 = -8, R_2 = 2, \phi_2 = 20.9, \phi_3 = 36$) and (c) Three link SDCSC configuration II ($R_1 = -5.5, R_2 = -4, \phi_2 = 30.2, \phi_3 = 44.2$)

Figure 4.4 depicts the results of the optimization for both the two-link and three-link cases -- Figure 4.4 (a) shows the candidate optimal 2-link SDCSC mechanism that can sweep out the desired curve while Figure 4.4 (b-c) show two alternatives for a 3-link SDCSC mechanism that can trace the desired curve .



4.3 Static Synthesis of SDCSC Mechanism

However, in most cases, the force interaction between a linkage and its environment is very critical to the performance as in the case of our leg-wheel design. In this case, the goal of the articulation is to guide the attached wheel through several positions while supporting *a set of specified external loads*. The kinetostatic synthesis process developed in [15],[16],[17] is used to aid the selection of the optimal configuration (and determine the minimum torques required) to support these external loads by *structural equilibration*. We will also consider the addition of torsional springs at each joint to minimize/optimize the peak actuator torques by a judicious combination of *structural equilibration design* and *spring assists* was considered. The formulation and simultaneous solution of the loop-closure and static equilibrium equations at the precision points aids the process of simultaneous determination of optimal mechanism and spring parameters.

4.3.1 Precision Torque Synthesis

The constraints on the static torque are derived by using the principle of virtual work for every precision position.

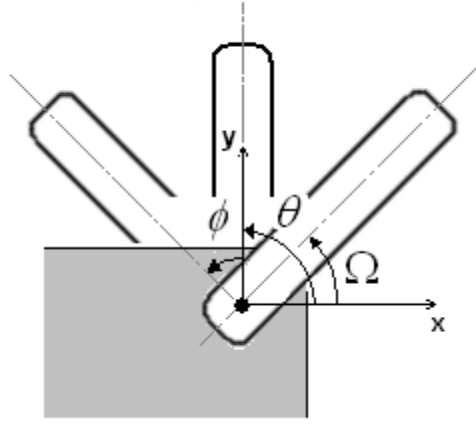


Figure 4.5 Torsion springs at joints with Preload Angle Ω , Initial Configuration θ and Relative displacement ϕ .

We also use springs to reduce the required torque (T_r) on the base joint. Figure 4.5 shows configuration of the SDCSC-based system with attached linear torsional spring at each joint. Let θ_i be the absolute initial configuration of each joint, Ω_i is the absolute configuration of each joint at which each spring is assembled and ϕ corresponds to the relative displacement of the first link from its initial configuration to the current configuration. Then β_i , the angular extension of each spring, can be written as:

$$\begin{aligned}\beta_1 &= \theta_1 + \phi - \Omega_1 \\ \beta_2 &= ((\theta_2 + R_1\phi - \Omega_2) - (\theta_1 + \phi - \Omega_1)) \\ &= ((R_1 - 1)\phi + (\theta_2 - \theta_1) + (\Omega_1 - \Omega_2))\end{aligned}\tag{4.12}$$

The virtual angular displacements, $\delta\beta_1$ and $\delta\beta_2$, can be expressed in terms of the independent virtual displacement, $\delta\phi$ as:

$$\begin{bmatrix} \delta\beta_1 \\ \delta\beta_2 \end{bmatrix} = \begin{bmatrix} \frac{\partial\beta_1}{\partial\phi} \\ \frac{\partial\beta_2}{\partial\phi} \end{bmatrix} \delta\phi = \begin{bmatrix} 1 \\ (R_1 - 1) \end{bmatrix} \delta\phi \quad (4.13)$$

Since this is a single degree-of-freedom mechanism, the feasible virtual displacements δZ_{P_x} , δZ_{P_y} and $\delta\Theta$ are function of $\delta\phi$.

$$\begin{bmatrix} \delta Z_{P_x} \\ \delta Z_{P_y} \\ \delta\Theta \end{bmatrix} = \begin{bmatrix} \frac{\partial Z_{P_x}}{\partial\phi} \\ \frac{\partial Z_{P_y}}{\partial\phi} \\ \frac{\partial\Theta}{\partial\phi} \end{bmatrix} \delta\phi \quad (4.14)$$

2-link SDCSC Mechanism

The partial derivatives in the above equation can be obtained by differentiating the forward kinematic equations (see Equations (4.5)) for the 2-link SDCSC as:

$$\begin{bmatrix} \frac{\partial Z_{P_x}}{\partial\phi} \\ \frac{\partial Z_{P_y}}{\partial\phi} \\ \frac{\partial\Theta}{\partial\phi} \end{bmatrix} = \begin{bmatrix} -Z_{1x} \sin\phi - Z_{1y} \cos\phi - R_1 Z_{2x} \sin R_1\phi - R_1 Z_{2y} \cos R_1\phi \\ Z_{1x} \cos\phi - Z_{1y} \sin\phi + R_1 Z_{2x} \cos R_1\phi - R_1 Z_{2y} \sin R_1\phi \\ R_1 \end{bmatrix} \quad (4.15)$$

Let $T_1(\phi)$ be the torque applied at the base joint required to equilibrate all the external loads. By equating the virtual work done by all the forces to zero, we get

$$\mathbf{F}_x \delta Z_{P_x} + \mathbf{F}_y \delta Z_{P_y} + \mathbf{M}_z \delta\Theta + \mathbf{T}_{Spring} \delta\beta + \mathbf{T}_1 \delta\phi = 0 \quad (4.16)$$

Substitute all the virtual work expressions into the equilibrium equation we get:

$$\left(F_x \frac{\partial Z_{P_x}}{\partial\phi} + F_y \frac{\partial Z_{P_y}}{\partial\phi} + M_z \frac{\partial\Theta}{\partial\phi} + T_1 - k_1 \beta_1 \frac{\partial\beta_1}{\partial\phi} - k_2 \beta_2 \frac{\partial\beta_2}{\partial\phi} \right) \delta\phi = 0 \quad (4.17)$$

then the actual torque requires to equilibrate the system is computed as:

$$T_1(\phi) = [A_1 \quad A_2 \quad A_3 \quad A_4] \begin{bmatrix} Z_{1x} \\ Z_{1y} \\ Z_{2x} \\ Z_{2y} \end{bmatrix} - M_z R_1 + k_1 (\theta_1 + \phi - \Omega_1) + k_2 ((R_1 - 1)\phi + (\theta_2 - \theta_1) + (\Omega_1 - \Omega_2))(R_1 - 1) \quad (4.18)$$

where

$$\begin{bmatrix} A_1 = F_x \sin \phi - F_y \cos \phi \\ A_2 = F_x \cos \phi + F_y \sin \phi \\ A_3 = F_x R_1 \sin R_1 \phi - F_y R_1 \cos R_1 \phi \\ A_4 = F_x R_1 \cos R_1 \phi + F_y R_1 \sin R_1 \phi \end{bmatrix}$$

Further Examination of the Torque Constraint Equation

The torque at driving joint can be divided into expression for torque required to equilibrate the external load and contribution of the internal spring torques.

$$T_{Ext}(\phi) = -[A_1 \quad A_2 \quad A_3 \quad A_4] \begin{bmatrix} Z_{1x} \\ Z_{1y} \\ Z_{2x} \\ Z_{2y} \end{bmatrix} + M_z R_1 \quad (4.19)$$

$$\begin{aligned} T_{Spring}(\phi) &= k_1(\theta_1 + \phi - \Omega_1) + k_2((R_1 - 1)\phi + (\theta_2 - \theta_1) + (\Omega_1 - \Omega_2))(R_1 - 1) \\ &= (k_1 + k_2(R_1 - 1)^2)\phi + k_1(\theta_1 - \Omega_1) + k_2(R_1 - 1)((\theta_2 - \theta_1) + (\Omega_1 - \Omega_2)) \end{aligned} \quad (4.20)$$

The spring equation can also be rewritten in terms of the relative angular motion of the first joint as a linear equation as:

$$\begin{aligned} T(\phi) - T_{Ext}(\phi) &= \underbrace{(k_1 + k_2(R_1 - 1)^2)}_A \phi + \underbrace{-k_1(\theta_1 - \Omega_1) - k_2(R_1 - 1)((\theta_2 - \theta_1) + (\Omega_1 - \Omega_2))}_B \\ &= A\phi + B = A(\theta_1 + \phi + (\frac{B - A\theta_1}{A})) \end{aligned} \quad (4.21)$$

This demonstrates the fact that all linear torsional springs (attached at the various joints) of an SDCSC mechanism can in fact be replaced by a single equivalent torsional spring with spring constant $K_{eq} = A$ and an initial unloaded configuration of $\Omega_{eq} = -(\frac{B - A\theta_1}{A})$.

3-link SDCSC Mechanism

Simply in the case of three link SDCSC problem, system has three springs so we get six variables such as $k_1, k_2, k_3, \Omega_1, \Omega_2$ and Ω_3 . The external torque contributed by external load at the wheel axis and spring torque to compensate external load are

$$\mathbf{T}_{Ext} = \begin{bmatrix} A_1 & A_2 & A_3 & A_4 & A_5 & A_6 \end{bmatrix} \begin{bmatrix} z_{1,x} \\ z_{1,y} \\ z_{2,x} \\ z_{2,y} \\ z_{3,x} \\ z_{3,y} \end{bmatrix} + \mathbf{M}_Z R_2 \quad (4.22)$$

$$\begin{pmatrix} A_1 = -F_x \sin \phi + F_y \cos \phi \\ A_2 = -F_x \cos \phi - F_y \sin \phi \\ A_3 = -F_x R_1 \sin(R_1 \phi) + F_y R_1 \cos(R_1 \phi) \\ A_4 = -F_x R_1 \cos(R_1 \phi) - F_y R_1 \sin(R_1 \phi) \\ A_5 = -F_x R_2 \sin(R_2 \phi) + F_y R_2 \cos(R_2 \phi) \\ A_6 = -F_x R_2 \cos(R_2 \phi) - F_y R_2 \sin(R_2 \phi) \end{pmatrix}$$

$$\begin{aligned} T_{Spring}(\phi) &= k_1(\theta_1 + \phi - \Omega_1) + k_2((R_1 - 1)\phi + (\theta_2 - \theta_1) + (\Omega_1 - \Omega_2))(R_1 - 1) \\ &\quad + k_3((R_2 - R_1 + 1)\phi + (\theta_3 - \theta_2 + \theta_1) + (\Omega_2 - \Omega_3 - \Omega_1))(R_2 - R_1 + 1) \\ &= (k_1 + k_2(R_1 - 1)^2 + k_3(R_2 - R_1 + 1)^2)\phi + k_1(\theta_1 - \Omega_1) \\ &\quad + k_2(R_1 - 1)((\theta_2 - \theta_1) + (\Omega_1 - \Omega_2)) + k_3(R_2 - R_1 + 1)((\theta_3 - \theta_2 + \theta_1) + (\Omega_2 - \Omega_3 - \Omega_1)) \\ &= A\phi + B \end{aligned} \quad (4.23)$$

4.4 Static Precision Point Synthesis and Optimization

The desired torque curve is assumed to be given as a function of ϕ to be decided by the user. Noting from Eq. (4.21) or (4.23) that we only have two design variables for use in the static synthesis process regardless of number of links of SDCSC mechanism. These can be used in the following three ways.

- Two static precision points and no free choices (presented below in Section 4.4.1).
- One static precision point and using one of the variables as a free choice (not presented)
- No static precision points but with both variables as free-choices (in Section 4.4.2)

4.4.1 Two static precision points and no free choices.

For a two static precision position problem, the spring constants are calculated by substituting precision torques – the specified torques ($T_i(\phi_i)$) at the precision points (ϕ_i) – into equation (4.18)

$$\begin{bmatrix} A \\ B \end{bmatrix} = \begin{bmatrix} \phi_1 & 1 \\ \phi_2 & 1 \end{bmatrix}^{-1} \begin{bmatrix} T_1(\phi_1) - T_{Ext}(\phi_1) \\ T_2(\phi_2) - T_{Ext}(\phi_2) \end{bmatrix} \quad (4.24)$$

The desired k_i and corresponding Ω can be decided by solving:

$$\begin{bmatrix} k_1 \\ k_2 \end{bmatrix} = \begin{bmatrix} -1 & -(R_1 - 1)^2 \\ -(\theta_1 - \Omega_1) & -(R_1 - 1)((\theta_2 - \theta_1) + (\Omega_1 - \Omega_2)) \end{bmatrix}^{-1} \begin{bmatrix} A \\ B \end{bmatrix} \quad (4.25)$$

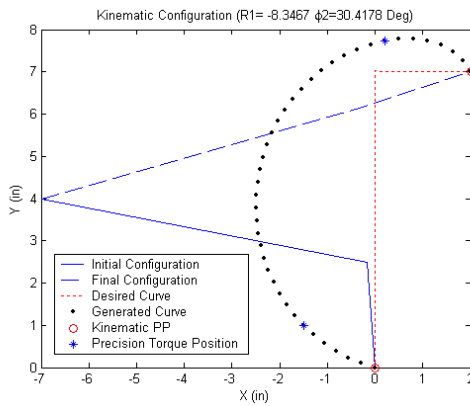
$$\begin{bmatrix} A \\ B \end{bmatrix} = \begin{bmatrix} 0 & 0 \\ (k_1 - k_2(R_1 - 1)) & k_2(R_1 - 1) \end{bmatrix} \begin{bmatrix} \Omega_1 \\ \Omega_2 \end{bmatrix} + \begin{bmatrix} -(k_1 + k_2(R_1 - 1)^2) \\ -k_1\theta_1 - k_2(R_1 - 1)(\theta_2 - \theta_1) \end{bmatrix} \quad (4.26)$$

This gives the designer considerable freedom for selection of a spring constant by varying the initial unloaded configuration (Equation (4.25)). The vice versa process of determining the best unloaded configuration for a given k_1 and k_2 (as shown in (4.26)) is not well defined. For three link SDCSC case, the relationship between the individual torsional spring parameters k_1, k_2, k_3 and the generalized lumped spring parameters A, B can be expressed as:

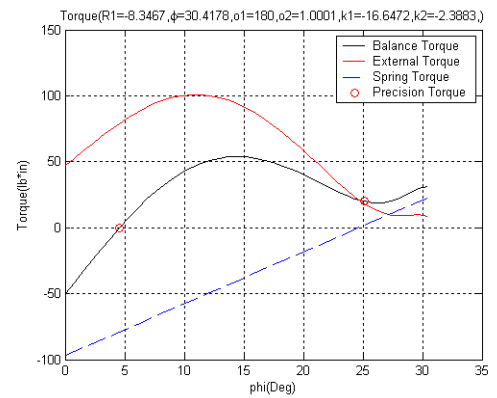
$$\begin{bmatrix} A \\ B \end{bmatrix} = \begin{bmatrix} -1 & -(R_1 - 1)^2 & -(R_2 - R_1 + 1)^2 \\ -(\theta_1 - \Omega_1) & -(R_1 - 1)((\theta_2 - \theta_1) + (\Omega_1 - \Omega_2)) & -(R_2 - R_1 + 1)((\theta_3 - \theta_2 + \theta_1) + (\Omega_2 - \Omega_3 - \Omega_1)) \end{bmatrix} \begin{bmatrix} k_1 \\ k_2 \\ k_3 \end{bmatrix} = \mathbf{S} \begin{bmatrix} k_1 \\ k_2 \\ k_3 \end{bmatrix} \quad (4.27)$$

Since, there are more unknowns than equations we note that a secondary optimization in terms of the k_i 's may be easily created. We will however solve for the unknown spring constants in the least-square sense using pseudo-inverse of \mathbf{S} matrix.

$$\begin{bmatrix} k_1 \\ k_2 \\ k_3 \end{bmatrix} = \mathbf{S}^T (\mathbf{S}\mathbf{S}^T)^{-1} \begin{bmatrix} A \\ B \end{bmatrix} \quad (4.28)$$



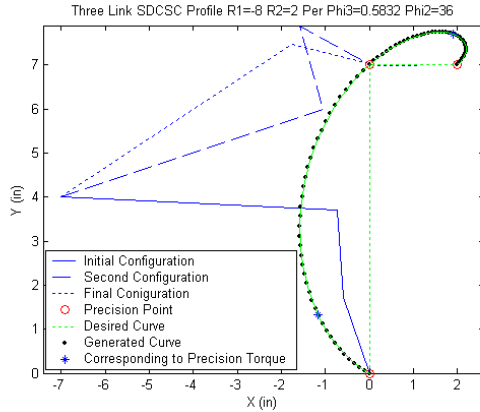
(a)



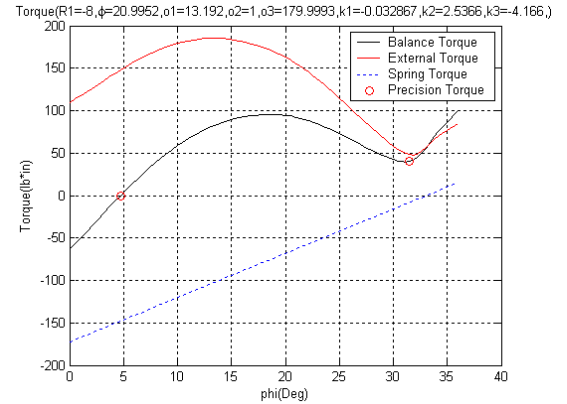
(b)

Figure 4.6 (a) Kinematic Configuration of Two Link SDCSC and (b) Torque at driving joint when $k_1 = -16.6$ $k_2 = -2.4$



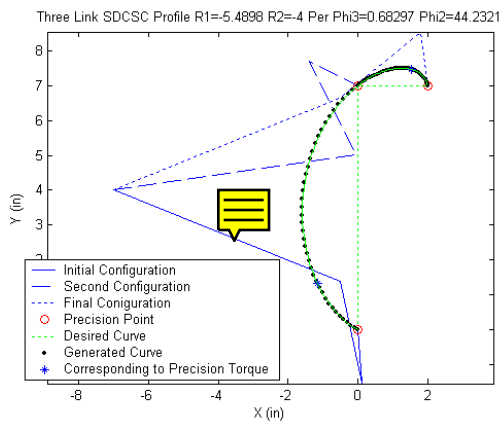


(a)

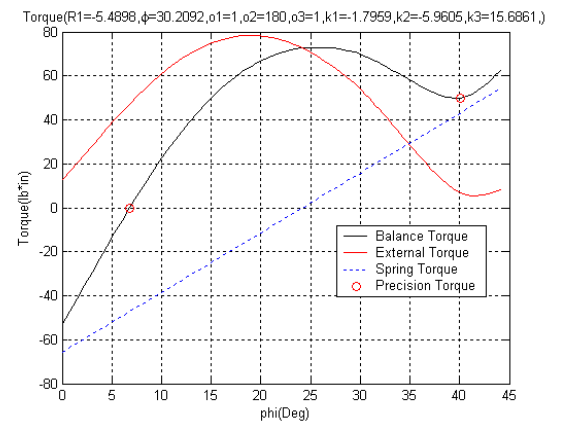


(b)

Figure 4.7 (a) Kinematic Configuration of Three Link SDCSC Configuration I and (b) Torque at driving joint when $k_1 = 0.03$, $k_2 = 2.2$, $k_3 = -3.6$



(a)



(b)

Figure 4.8 (a) Kinematic Configuration of Three Link SDCSC Configuration I and (b) Torque at driving joint when $k_1 = -1.7$, $k_2 = -5.8$, $k_3 = 15.3$

Part (a) of Figure 4.6, Figure 4.7 and Figure 4.8 show the kinematic configurations at each precision point and the position to the precision torque. To design precision torque we should consider the position on the kinematic profile (a) and torque profile (b). In part (b) of Figure 4.6, Figure 4.7 and Figure 4.8, we set first precision torque as zero to demonstrate the capability of designing stable/unstable equilibrium position. The issues of pertaining to selection of precision points and corresponding torques will be discussed further in the equilibrium analysis Chapter 6.

We note that by using two precision points in static PPS we get a unique torque profile for any kinematic configuration. Thus we can move torque profile only by changing precision torque condition as shown in Figure 4.9.

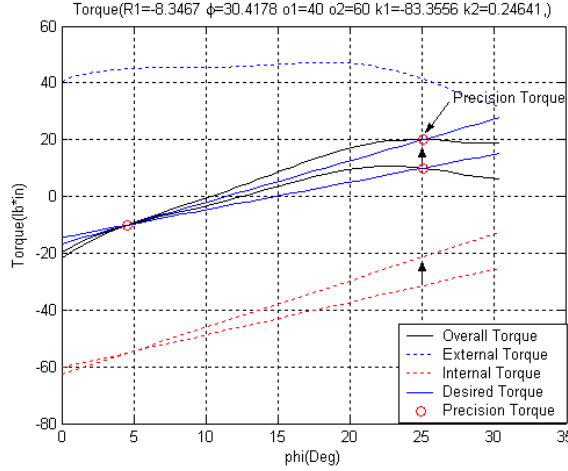


Figure 4.9 Moving Torque profile by changing Precision Torque

4.4.2 No static precision points and using both variables as free-choices

A variety of objective functions can be employed as noted below. Three possible sets of minimizations including force consideration in their objective include:

- First, minimizing the absolute value of the peak input torques evaluated at discrete values ϕ_k , over the optimization variables α .

$$\min_{\alpha} \max_{\phi_k} |T_I^{act}(\phi_k)| \quad (4.29)$$

- Second, minimizing over the optimization variables α , the summed least squares error between the obtained input torque, $T_I^{act}(\phi_k)$, and a desired input torque profile, $T_I^{des}(\phi_k)$, evaluated at discrete input crank angle values ϕ_k .

$$\min_{\alpha} \sum_{K=0}^N (T_I^{des}(\phi_k) - T_I^{act}(\phi_k))^2 \quad (4.30)$$

- Third, minimizing over the optimization variables α , a weighted sum of the end-effector discrepancy and input torque error.

$$\min_{\alpha} \sum_{k=0}^{N_c} \Lambda_F (T_I^{des}(\phi_k) - T_I^{act}(\phi_k))^2 + \Lambda_P \left((p_{xk} - q_{xk})^2 + (p_{yk} - q_{yk})^2 \right) \quad (4.31)$$

$$\min_{\alpha} \sum_{k=0}^{N_c} \Lambda_F \left(\min_{\alpha} \max_{\phi_k} |T_I^{act}(\phi_k)| \right) + \Lambda_P \left((p_{xk} - q_{xk})^2 + (p_{yk} - q_{yk})^2 \right) \quad (4.32)$$

The most satisfying solution is minimizing peak input torque and discrepancy between desired and generated curve of end-effector over the entire range of motion. The optimization is carried out over the many candidate solution to obtain best specification. By introducing, the torque at first joint, T_i as:

$$T_i = T_{Ext} - T_{Spring} = T_{Ext} + (A\phi_i + B) \quad (4.33)$$

and using A,B as the design variables

$$\min_{A,B} \sum_{K=0}^N \left(T_I^{des}(\phi_k) - T_I^{act}(\phi_k) \right)^2 \quad (4.34)$$

Figure 4.10, Figure 4.11 and Figure 4.10 show the result of performance of such a static optimization in the form of torque profiles corresponding to the three kinematic configurations represented in previous section 4.2.2. Parts (a) of each figure depicts the first iteration of optimization and parts (b) shows the final optimized torque profiles. In the SDCSC static optimization, the approximation of generated torque to the desired curve mainly depends on external torque which determined by kinematic configuration and external loads. Because internal torque of SDCSC mechanism is linear function, we cannot match complex profiles with rapid changes of curvature. This issue will be discussed in the equilibrium analysis chapter 6.

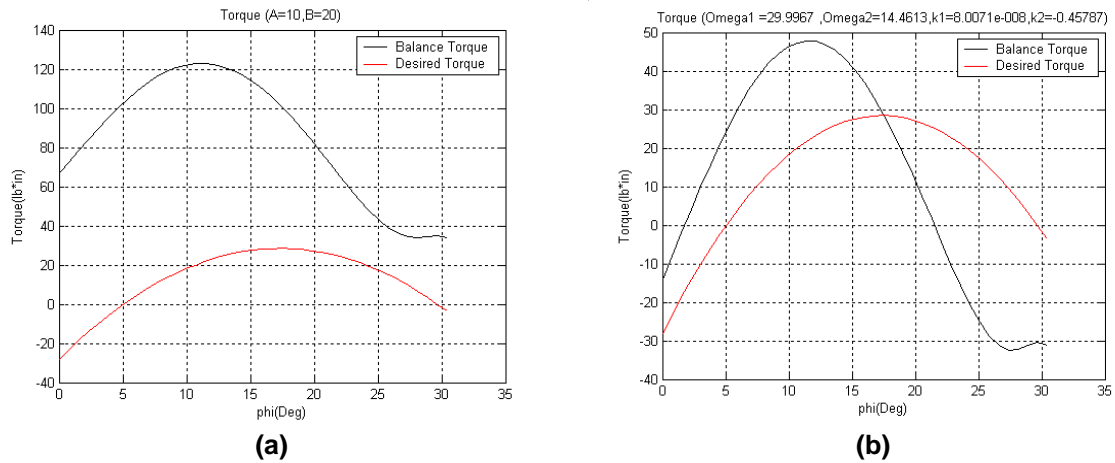


Figure 4.10 Trajectory Optimization for Two Link SDCSC Configuration I (a) After First Iteration of Optimization and (b) Final Result of Optimization ($k_1 = 0, k_2 = 0.45$)

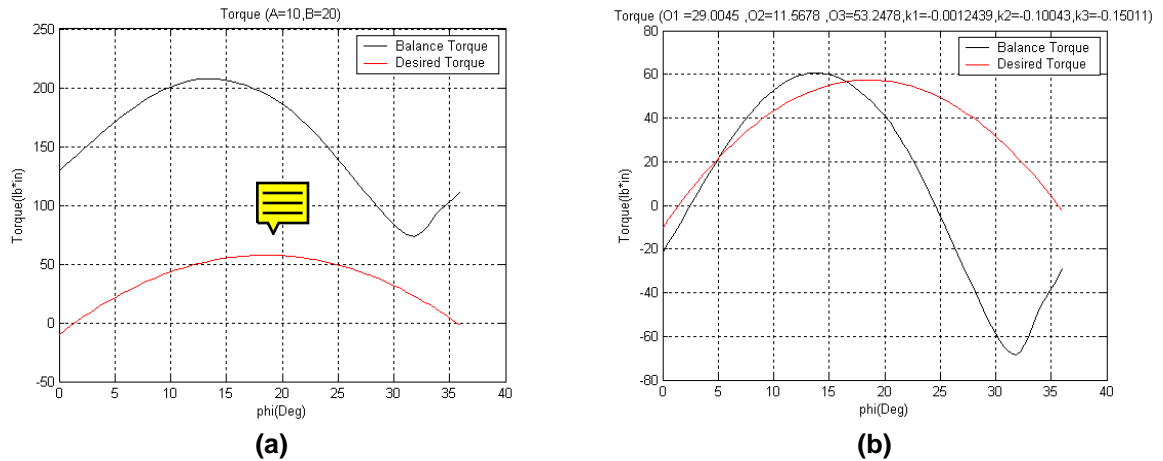
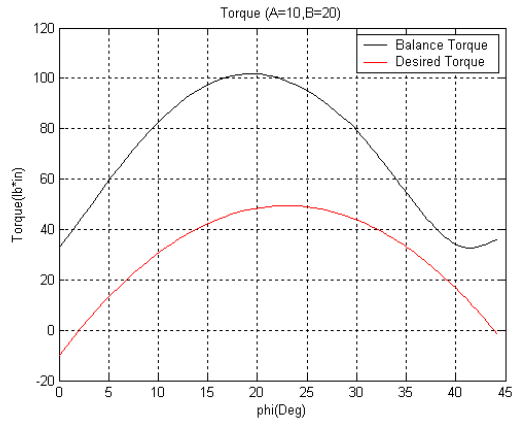
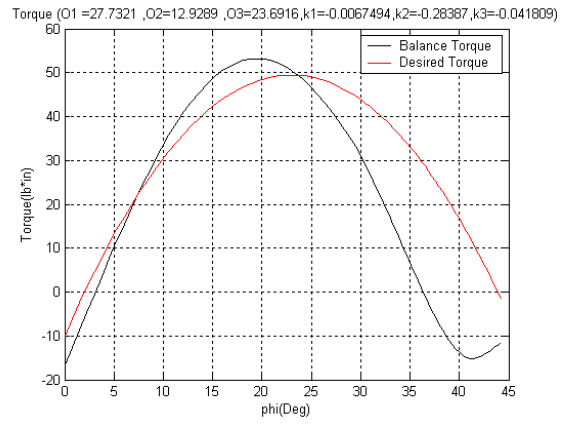


Figure 4.11 Trajectory Optimization for Three Link SDCSC Configuration I (a) After First Iteration of Optimization and (b) Final Result of Optimization ($k_1 = -0.001, k_2 = -0.1, k_3 = -0.15$)





(a)



(b)

Figure 4.12 Trajectory Optimization for Three Link SDCSC Configuration II (a) After First Iteration of Optimization and (b) Final Result of Optimization $k(k_1 = 0.0067, k_2 = -0.28, k_3 = -0.041)$



5 Design/Synthesis of Fourbar Leg-wheel Mechanism

In this chapter we examine the design process of articulate leg-wheel design based on fourbar mechanism. The fourbar linkage has the simplest possible pin-jointed mechanism for single DOF controlled motion. It is in fact the most common and ubiquitous device used in machinery. It is also extremely versatile in terms of the types of motions that can be generated [19].

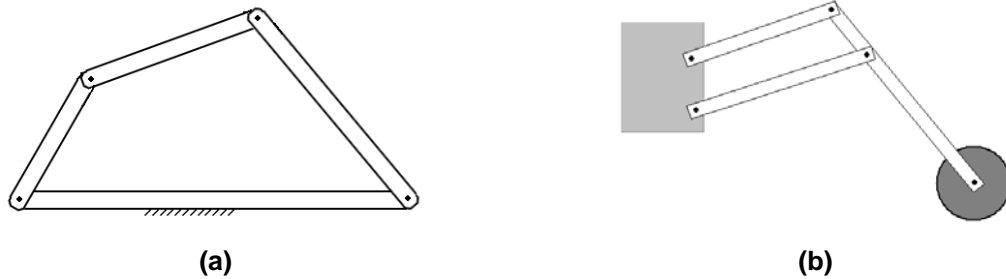


Figure 5.1 (a) Fourbar and (b) Application Fourbar to Leg-wheeled System

5.1 Kinematic Synthesis

Path following is defined as the control of a point in the plane such that it follows some prescribed path. This is typically accomplished with a fourbar crank-rocker or double-rocker, wherein a point on the coupler traces the desired output path.

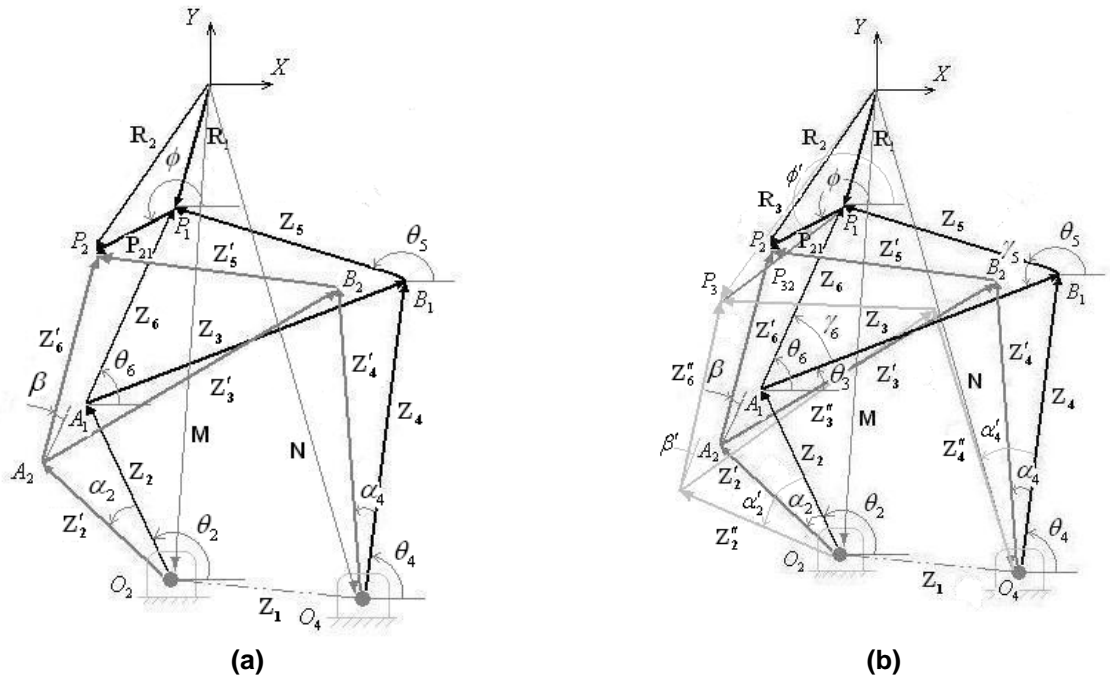


Figure 5.2 Fourbar Schematic Linkage made of (a) Two Dyads and (b) Three Dyads.

5.1.1 Planar Precision Point Synthesis of Fourbar

The points for successive location of the output link in the plane are referred to as precision points. The number of precision points which can be synthesized is limited by the number of equations available for solution. The fourbar linkage can be synthesized by closed-form methods up to five precision points for path following problem. The four or more precision points synthesis problems involve the solutions of nonlinear so we consider only two and three precision points problems [19].

5.2 Kinematic Synthesis

Two Precision Points

Total variable are $\mathbf{Z}_2(\theta_2, z_2)$, $\mathbf{Z}_4(\theta_4, z_4)$, $\mathbf{Z}_5(\theta_5, z_5)$, $\mathbf{Z}_6(\theta_6, z_6)$, \mathbf{R}_1 , \mathbf{R}_2 , α_2 , α_4 , β , ϕ , \mathbf{M} , \mathbf{N} and $\mathbf{R}_1, \mathbf{R}_2, \beta, \phi$ are determined by problem description. Let set base joint vectors \mathbf{M} and \mathbf{N} as free choices and then solve it for the other vectors. The loop-closure equations of a Fourbar mechanisms are:

$$\begin{aligned} \mathbf{M} + \mathbf{Z}_2 + \mathbf{Z}_6 &= \mathbf{R}_1 \\ \mathbf{M} + \mathbf{Z}'_2 + \mathbf{Z}'_6 &= \mathbf{R}_2 \\ \mathbf{N} + \mathbf{Z}_4 + \mathbf{Z}_5 &= \mathbf{R}_1 \\ \mathbf{N} + \mathbf{Z}'_4 + \mathbf{Z}'_5 &= \mathbf{R}_2 \end{aligned} \quad (5.1)$$

we can express \mathbf{Z}'_2 and \mathbf{Z}'_6 (\mathbf{Z}'_4 and \mathbf{Z}'_5) in terms of \mathbf{Z}_2 and \mathbf{Z}_6 (\mathbf{Z}_4 and \mathbf{Z}_5).

$$\begin{bmatrix} 1 & 1 \\ e^{i\alpha_2} & e^{i\beta} \end{bmatrix} \begin{bmatrix} \mathbf{Z}_2 \\ \mathbf{Z}_6 \end{bmatrix} = \begin{bmatrix} \mathbf{R}_1 - \mathbf{M} \\ \mathbf{R}_2 - \mathbf{M} \end{bmatrix} \quad \begin{bmatrix} 1 & 1 \\ e^{i\alpha_4} & e^{i\beta} \end{bmatrix} \begin{bmatrix} \mathbf{Z}_4 \\ \mathbf{Z}_5 \end{bmatrix} = \begin{bmatrix} \mathbf{R}_1 - \mathbf{N} \\ \mathbf{R}_2 - \mathbf{N} \end{bmatrix} \quad (5.2)$$

this can be written in the form of matrix:

$$\begin{bmatrix} \mathbf{Z}_2 \\ \mathbf{Z}_6 \\ \mathbf{Z}_4 \\ \mathbf{Z}_5 \end{bmatrix} = \begin{bmatrix} 1 & 1 & 0 & 0 \\ e^{i\alpha_2} & e^{i\beta} & 0 & 0 \\ 0 & 0 & 1 & 1 \\ 0 & 0 & e^{i\alpha_4} & e^{i\beta} \end{bmatrix}^{-1} \begin{bmatrix} \mathbf{R}_1 - \mathbf{M} \\ \mathbf{R}_2 - \mathbf{M} \\ \mathbf{R}_1 - \mathbf{N} \\ \mathbf{R}_2 - \mathbf{N} \end{bmatrix} \quad (5.3)$$

where vector \mathbf{Z}_2 , \mathbf{Z}_6 , \mathbf{Z}_4 and \mathbf{Z}_5 are position vector of Fourbar, \mathbf{M} and \mathbf{N} are position vector of first link fixed on the chassis.

Three Precision Points

Same as the two precision point case, From kinematics of fourbar and loop-closure equation,

$$\begin{aligned} \mathbf{M} + \mathbf{Z}_2 + \mathbf{Z}_6 &= \mathbf{R}_1 & \mathbf{N} + \mathbf{Z}_4 + \mathbf{Z}_5 &= \mathbf{R}_1 \\ \mathbf{M} + \mathbf{Z}'_2 + \mathbf{Z}'_6 &= \mathbf{R}_2 & \mathbf{N} + \mathbf{Z}'_4 + \mathbf{Z}'_5 &= \mathbf{R}_2 \\ \mathbf{M} + \mathbf{Z}''_2 + \mathbf{Z}''_6 &= \mathbf{R}_3 & \mathbf{N} + \mathbf{Z}''_4 + \mathbf{Z}''_5 &= \mathbf{R}_3 \end{aligned} \quad (5.4)$$

Express $\mathbf{Z}'_2, \mathbf{Z}'_6, \mathbf{Z}''_2, \mathbf{Z}''_6$ ($\mathbf{Z}'_4, \mathbf{Z}'_5, \mathbf{Z}''_4, \mathbf{Z}''_5$) with $\mathbf{Z}_2, \mathbf{Z}_6$ ($\mathbf{Z}_4, \mathbf{Z}_5$) then

$$\begin{bmatrix} 1 & 1 & 1 \\ 1 & e^{i\alpha_2} & e^{i\beta} \\ 1 & e^{i\alpha_2'} & e^{i\beta'} \end{bmatrix} \begin{bmatrix} \mathbf{M} \\ \mathbf{Z}_2 \\ \mathbf{Z}_6 \end{bmatrix} = \begin{bmatrix} \mathbf{R}_1 \\ \mathbf{R}_2 \\ \mathbf{R}_3 \end{bmatrix} \quad \begin{bmatrix} 1 & 1 & 1 \\ 1 & e^{i\alpha_2} & e^{i\beta} \\ 1 & e^{i\alpha_2'} & e^{i\beta'} \end{bmatrix} \begin{bmatrix} \mathbf{N} \\ \mathbf{Z}_4 \\ \mathbf{Z}_5 \end{bmatrix} = \begin{bmatrix} \mathbf{R}_1 \\ \mathbf{R}_2 \\ \mathbf{R}_3 \end{bmatrix} \quad (5.5)$$

and write in matrix form, we yield:

$$\begin{bmatrix} \mathbf{M} \\ \mathbf{Z}_2 \\ \mathbf{Z}_6 \\ \mathbf{N} \\ \mathbf{Z}_4 \\ \mathbf{Z}_5 \end{bmatrix} = \begin{bmatrix} 1 & 1 & 1 & 0 & 0 & 0 \\ 1 & e^{i\alpha_2} & e^{i\beta} & 0 & 0 & 0 \\ 1 & e^{i\alpha_2'} & e^{i\beta'} & 0 & 0 & 0 \\ 0 & 0 & 0 & 1 & 1 & 1 \\ 0 & 0 & 0 & 1 & e^{i\alpha_2} & e^{i\beta} \\ 0 & 0 & 0 & 1 & e^{i\alpha_2'} & e^{i\beta'} \end{bmatrix}^{-1} \begin{bmatrix} \mathbf{R}_1 \\ \mathbf{R}_2 \\ \mathbf{R}_3 \\ \mathbf{R}_1 \\ \mathbf{R}_2 \\ \mathbf{R}_3 \end{bmatrix} \quad (5.6)$$

5.3 Kinematic Optimization

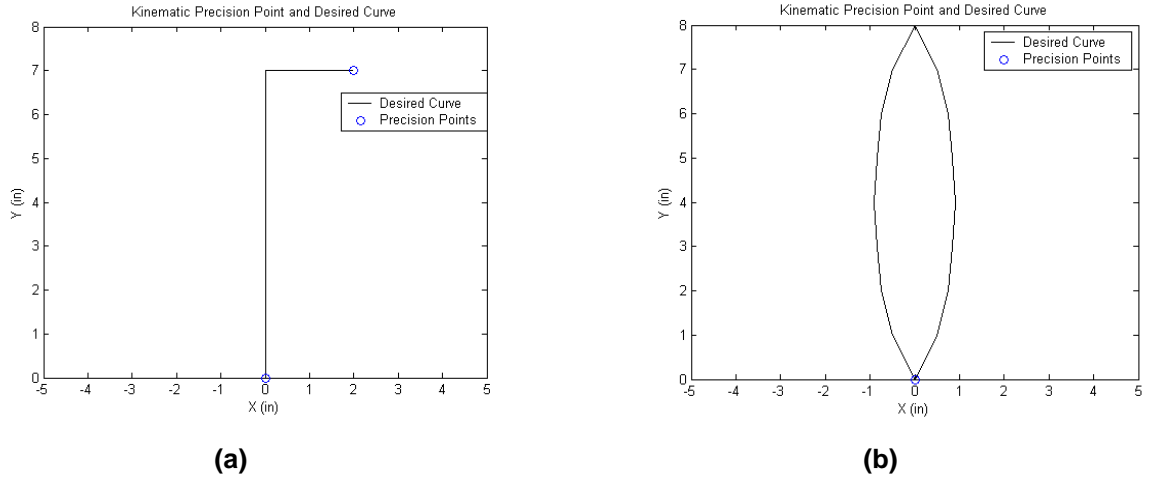


Figure 5.3 Desired End-effector Trajectory (a) Open Step Desired Curve & Precision Points and (b) Closed Desired Curve & Precision Points

To optimize the discrepancy between generated curve and desired curve, each curve should be divided into same length line segments/points and calculate their distances.

Two PPS with Optimization

We will present result of 2 PPS with optimization. The objective function is taken to be the structural error between the desired and actual path computed using arc length based correspondence points [15]. The design variables are $\alpha_2, \alpha_4, \beta$. The optimization objective function is stated as

$$\min_{\mathbf{D}} \sum_{k=1}^N \left((P_{xk} - q_{xk})^2 + (P_{yk} - q_{yk})^2 \right) \quad (5.7)$$

subject to

$$\begin{bmatrix} \mathbf{Z}_2 \\ \mathbf{Z}_6 \\ \mathbf{Z}_4 \\ \mathbf{Z}_5 \end{bmatrix} = \begin{bmatrix} 1 & 1 & 0 & 0 \\ e^{i\alpha_2} & e^{i\beta} & 0 & 0 \\ 0 & 0 & 1 & 1 \\ 0 & 0 & e^{i\alpha_4} & e^{i\beta} \end{bmatrix}^{-1} \begin{bmatrix} \mathbf{R}_1 - \mathbf{M} \\ \mathbf{R}_2 - \mathbf{M} \\ \mathbf{R}_1 - \mathbf{N} \\ \mathbf{R}_2 - \mathbf{N} \end{bmatrix}$$

$$L_{2Min} \leq L_2 \leq L_{2Max}$$

$$L_{3Min} \leq L_3 \leq L_{3Max}$$

$$\alpha_{2Min} \leq \alpha_2 \leq \alpha_{2Max} \quad \text{and} \quad \mathbf{M} \text{ and } \mathbf{N} \text{ are constant vectors.}$$

$$\alpha_{4Min} \leq \alpha_4 \leq \alpha_{4Max}$$

$$\beta_{Min} \leq \beta \leq \beta_{Max}$$

where \mathbf{D} is a vector of design variables $(\alpha_2, \alpha_4, \beta)$, L_2/L_3 are second/third link length, \mathbf{P} is generated end-effector position and \mathbf{q} is desired end-effector position. Among the possible configurations, we determine two desirable configurations as shown in Figure 5.3.

Two acceptable configurations of fourbar for open desired curve and closed desired curve each are shown in Figure 5.4 and Figure 5.5. In closed desired curve case, the trajectory of end-effector is inside of obstacle so it is not desirable. To make end-effector follow desired curve, the chassis should move back. As shown in Figure 5.5, although we can find some configuration which have similar trajectory with desired curve, two precision point synthesis is not enough for closed desired curve problem. Because we cannot set the edge of step as precision point in two precision point problem, the generated curve does not pass through the edge of step which is one of important position to climb up step.

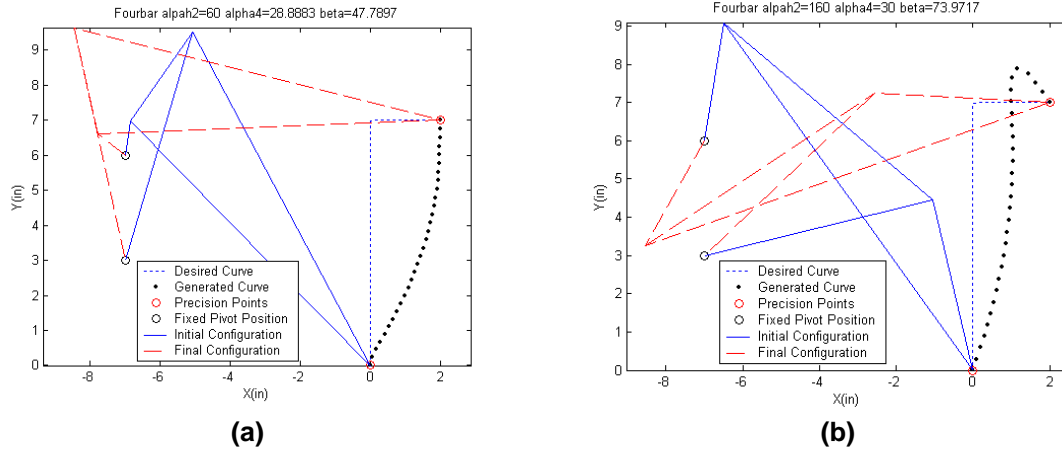


Figure 5.4 Kinematic Optimization results for Open Desired Curve (a) Case1 and (b) Case2



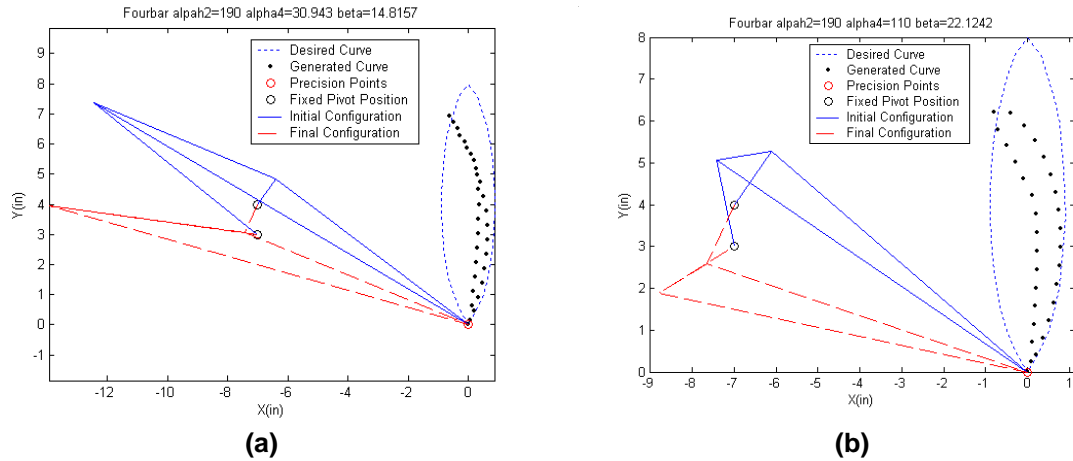


Figure 5.5 Kinematic Optimization results for Closed Desired Curve (a) Case3 and (b) Case4

5.4 Static Synthesis of Fourbar with Two Precision Points

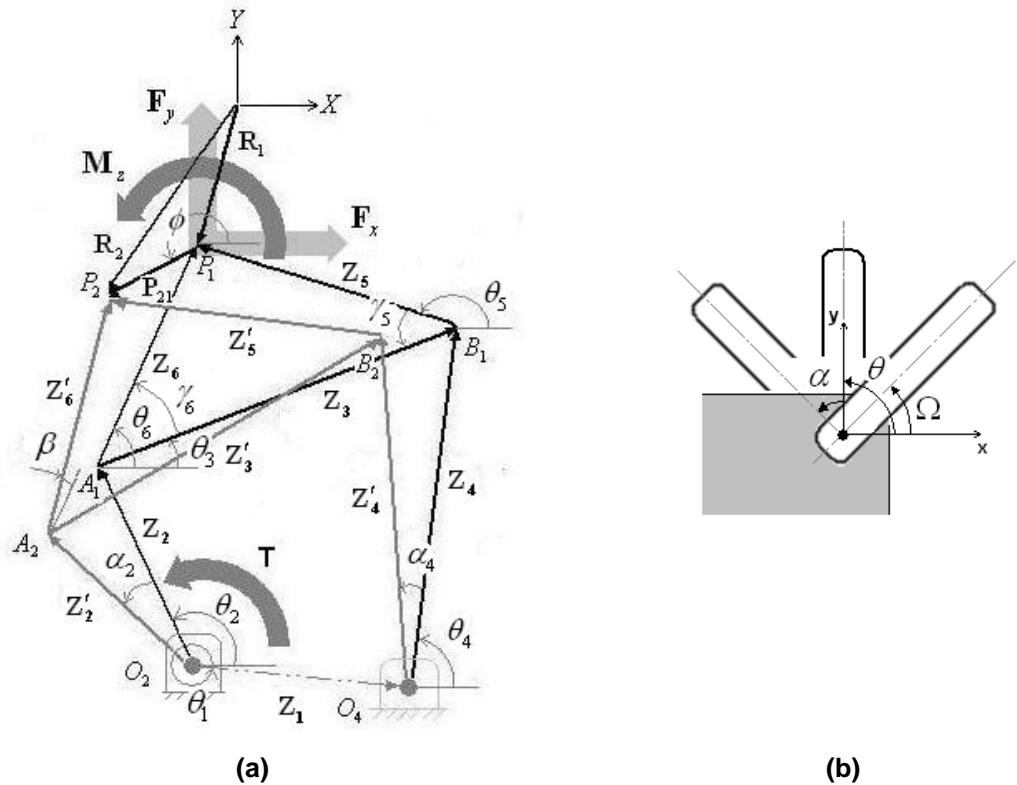


Figure 5.6 Fourbar (a) FBD of Fourbar and (b) Spring preload (Ω), initial (θ) and relative (α) angles at Joint

By the principle of virtual work [20],[21], a system to be in equilibrium, the total virtual work done by external forces during a virtual displacement must be zero. In general case, such statement can be written as:

$$\delta W = \sum \mathbf{T}_{reaction}^T \delta \alpha_2 + \sum \mathbf{F}^T \delta \mathbf{P} + \sum \mathbf{M} \delta \phi + \sum T_{Spring} \delta \beta = 0 \quad (5.8)$$

The external forces associated with the fourbar linkage are shown in Figure 5.6 (a). Let $T_{reaction}$ the reaction torque applied at the driving joint required to equilibrate the external loadings when F_x, F_y & M_z are applied at the end-effector P. The total virtual work done can be written as:

$$\delta W = T_{reaction} \delta \alpha_2 + F_x \delta P_x + F_y \delta P_y + M_z \delta \phi + T_{Spring} \delta \sigma \quad (5.9)$$

By equating the sum of virtual work done by the individual forces and torque to zero, we get,

$$T_{reaction} \delta \alpha_2 + F_x \delta P_x + F_y \delta P_y + M_z \delta \phi + T_{Spring} \delta \sigma = 0 \quad (5.10)$$

By forward kinematics equation of fourbar mechanism,

$$\begin{aligned} z_2 \cos \theta_2 + z_3 \cos \theta_3 &= z_1 \cos \theta_1 + z_4 \cos \theta_4 \\ z_2 \sin \theta_2 + z_3 \sin \theta_3 &= z_1 \sin \theta_1 + z_4 \sin \theta_4 \end{aligned} \quad (5.11)$$

From equation (5.11), we get

$$\begin{aligned} \begin{bmatrix} z_2 \sin \theta_2 \\ z_2 \cos \theta_2 \end{bmatrix} \delta \theta_2 + \begin{bmatrix} z_3 \sin \theta_3 \\ z_3 \cos \theta_3 \end{bmatrix} \delta \theta_3 &= \begin{bmatrix} z_4 \sin \theta_4 \\ z_4 \cos \theta_4 \end{bmatrix} \delta \theta_4 \\ \begin{bmatrix} \delta \theta_3 \\ \delta \theta_4 \end{bmatrix} &= \begin{bmatrix} -z_3 \sin \theta_3 & z_4 \sin \theta_4 \\ -z_3 \cos \theta_3 & z_4 \cos \theta_4 \end{bmatrix}^{-1} \begin{bmatrix} z_2 \sin \theta_2 \\ z_2 \cos \theta_2 \end{bmatrix} \delta \theta_2 \end{aligned} \quad (5.12)$$

so we can represent $\delta \theta_3$ and $\delta \theta_4$ in terms of $\delta \theta_2$,

$$\begin{aligned} \begin{bmatrix} \delta \theta_3 \\ \delta \theta_4 \end{bmatrix} &= \begin{bmatrix} \frac{z_2 (\sin \theta_4 \cos \theta_2 - \cos \theta_4 \sin \theta_2)}{z_3 (\sin \theta_3 \cos \theta_4 - \cos \theta_3 \sin \theta_4)} \\ \frac{z_2 (\sin \theta_3 \cos \theta_2 - \cos \theta_3 \sin \theta_2)}{z_4 (\sin \theta_3 \cos \theta_4 - \cos \theta_3 \sin \theta_4)} \end{bmatrix} \delta \theta_2 \\ \begin{bmatrix} \delta \theta_3 \\ \delta \theta_4 \end{bmatrix} &= \begin{bmatrix} \frac{z_2 \sin(\theta_4 - \theta_2)}{z_3 \sin(\theta_3 - \theta_4)} \\ \frac{z_2 \sin(\theta_3 - \theta_2)}{z_4 \sin(\theta_3 - \theta_4)} \end{bmatrix} \delta \theta_2 \end{aligned} \quad (5.13)$$

Since $\delta \theta_6, \delta \theta_3$ and $\delta \phi$ are angular displacement of same rigid body,

$$\delta \theta_6 = \delta \theta_3 = \delta \phi \quad (5.14)$$

And the relationship between $\alpha_2, \alpha_4, \beta$ and $\theta_2, \theta_3, \theta_4$ is

$$\begin{aligned} \theta_2 &= \theta_{2,initial} + \alpha_2 & \delta \theta_2 &= \delta \alpha_2 \\ \theta_3 &= \theta_{3,initial} + \beta & \delta \theta_3 &= \delta \beta \\ \theta_4 &= \theta_{4,initial} + \alpha_4 & \delta \theta_4 &= \delta \alpha_4 \end{aligned} \quad (5.15)$$

The feasible motion can now be written as

$$\begin{bmatrix} \delta\theta_2 \\ \delta\theta_3 \\ \delta\theta_4 \end{bmatrix} = \begin{bmatrix} 1 \\ \frac{z_2 \sin(\theta_4 - \theta_2)}{z_3 \sin(\theta_3 - \theta_4)} \\ \frac{z_2 \sin(\theta_3 - \theta_2)}{z_4 \sin(\theta_3 - \theta_4)} \end{bmatrix} \delta\theta_2 = \begin{bmatrix} 1 \\ A_1 \\ A_2 \end{bmatrix} \delta\theta_2 \text{ or } \begin{bmatrix} \delta\alpha_2 \\ \delta\beta \\ \delta\alpha_4 \end{bmatrix} = \begin{bmatrix} 1 \\ \frac{z_2 \sin(\theta_4 - \theta_2)}{z_3 \sin(\theta_3 - \theta_4)} \\ \frac{z_2 \sin(\theta_3 - \theta_2)}{z_4 \sin(\theta_3 - \theta_4)} \end{bmatrix} \delta\alpha_2 = \begin{bmatrix} 1 \\ A_1 \\ A_2 \end{bmatrix} \delta\alpha_2 \quad (5.16)$$

$$\left(A_1 = \frac{z_2 \sin(\theta_4 - \theta_2)}{z_3 \sin(\theta_3 - \theta_4)}, \quad A_2 = \frac{z_2 \sin(\theta_3 - \theta_2)}{z_4 \sin(\theta_3 - \theta_4)} \right)$$

Substituting it to virtual work equilibrium equation, δP_x and δP_y is decided by kinematics of mechanism and $\delta\phi$ is same as $\delta\theta_6$ & $\delta\theta_3$. The displacement of end-effector, δP , is

$$\mathbf{P} = \mathbf{M} + (z_2 \cos \theta_2 + z_6 \cos(\theta_3 + \gamma_6))\mathbf{i} + (z_2 \sin \theta_2 + z_6 \sin(\theta_3 + \gamma_6))\mathbf{j} \quad (5.17)$$

Differentiating it and represent $\delta\theta_3$ as in terms of $\delta\theta_2$ or $\delta\alpha_2$,

$$\begin{aligned} \delta\mathbf{P} &= (-z_2 \sin \theta_2 \delta\theta_2 - z_6 \sin(\theta_3 + \gamma_6) \delta\theta_3)\mathbf{i} + (z_2 \cos \theta_2 \delta\theta_2 + z_6 \cos(\theta_3 + \gamma_6) \delta\theta_3)\mathbf{j} \\ &= (-z_2 \sin \theta_2 \delta\theta_2 - z_6 \sin(\theta_3 + \gamma_6) A_1 \delta\theta_2)\mathbf{i} + (z_2 \cos \theta_2 \delta\theta_2 + z_6 \cos(\theta_3 + \gamma_6) A_1 \delta\theta_2)\mathbf{j} \\ &= \delta\theta_2 (-z_2 \sin \theta_2 - z_6 \sin(\theta_3 + \gamma_6) A_1)\mathbf{i} + \delta\theta_2 (z_2 \cos \theta_2 + z_6 \cos(\theta_3 + \gamma_6) A_1)\mathbf{j} \\ &= \delta\alpha_2 (-z_2 \sin \theta_2 - z_6 \sin(\theta_3 + \gamma_6) A_1)\mathbf{i} + \delta\alpha_2 (z_2 \cos \theta_2 + z_6 \cos(\theta_3 + \gamma_6) A_1)\mathbf{j} \end{aligned} \quad (5.18)$$

$$\left(A_1 = \frac{z_2 \sin(\theta_4 - \theta_2)}{z_3 \sin(\theta_3 - \theta_4)} \right)$$

where σ_i as the angular extension of each spring,

$$\begin{aligned} \sigma_2 &= \theta_{2,initial} + \alpha_2 - \Omega_2 \\ \sigma_3 &= (\theta_{3,initial} + \beta - \Omega_3) - (\theta_{2,initial} + \alpha_2 - \Omega_2) \\ \sigma_4 &= \theta_{4,initial} + \alpha_4 - \Omega_4 \\ \sigma_5 &= (\theta_{5,initial} + \beta - \Omega_5) - (\theta_{4,initial} + \alpha_4 - \Omega_4) \end{aligned} \quad (5.19)$$

The virtual angular displacements σ_2 , σ_3 , σ_4 and σ_5 can be expressed in terms of independent virtual angular displacement, α_2 , α_4 , β as:

$$\begin{aligned} \frac{\partial \sigma_2}{\partial \alpha_2} &= 1 \\ \frac{\partial \sigma_3}{\partial \alpha_2} &= \frac{\partial \beta}{\partial \alpha_2} - 1 = \frac{A_1 \partial \alpha_2}{\partial \alpha_2} - 1 = A_1 - 1 \\ \frac{\partial \sigma_4}{\partial \alpha_2} &= \frac{\partial \alpha_4}{\partial \alpha_2} = \frac{A_2 \partial \alpha_2}{\partial \theta_2} = A_2 \\ \frac{\partial \sigma_5}{\partial \alpha_2} &= \frac{\partial \beta}{\partial \alpha_2} - A_2 = \frac{A_1 \partial \alpha_2}{\partial \alpha_2} - A_2 = A_1 - A_2 \end{aligned} \quad (5.20)$$

$$\left(A_1 = \frac{z_2 \sin(\theta_4 - \theta_2)}{z_3 \sin(\theta_3 - \theta_4)}, \quad A_2 = \frac{z_2 \sin(\theta_3 - \theta_2)}{z_4 \sin(\theta_3 - \theta_4)} \right)$$

Thus equilibrium equation of virtual work is

$$\begin{aligned}
& \left(T_{reaction} + F_x \frac{\partial P}{\partial \alpha_2} + F_y \frac{\partial P}{\partial \alpha_2} + \mathbf{M} \cdot \frac{\partial \phi}{\partial \alpha_2} - k_2 \sigma_2 \frac{\partial \sigma_2}{\partial \alpha_2} - k_3 \sigma_3 \frac{\partial \sigma_3}{\partial \alpha_2} - k_4 \sigma_4 \frac{\partial \sigma_4}{\partial \alpha_2} - k_5 \sigma_5 \frac{\partial \sigma_5}{\partial \alpha_2} \right) \partial \alpha_2 = 0 \\
& \left(T_{reaction} + F_x (-z_2 \sin \theta_2 - z_6 \sin(\theta_3 + \gamma_6) A_1) + F_y (z_2 \cos \theta_2 + z_6 \cos(\theta_3 + \gamma_6) A_1) + \mathbf{M} A_1 - k_2 \sigma_2 \frac{\partial \sigma_2}{\partial \alpha_2} - k_3 \sigma_3 \frac{\partial \sigma_3}{\partial \alpha_2} - k_4 \sigma_4 \frac{\partial \sigma_4}{\partial \alpha_2} - k_5 \sigma_5 \frac{\partial \sigma_5}{\partial \alpha_2} \right) \partial \alpha_2 = 0 \\
& \left[\begin{array}{l} \sigma_2 = \theta_{2,initial} + \alpha_2 - \Omega_2 \quad \frac{\partial \sigma_2}{\partial \alpha_2} = 1 \\ \sigma_3 = (\theta_{3,initial} + \beta - \Omega_3) - (\theta_{2,initial} + \alpha_2 - \Omega_2) \quad \frac{\partial \sigma_3}{\partial \alpha_2} = A_1 - 1 \\ \sigma_4 = \theta_{4,initial} + \alpha_4 - \Omega_4 \quad \frac{\partial \sigma_4}{\partial \alpha_2} = A_2 \\ \sigma_5 = (\theta_{5,initial} + \beta - \Omega_5) - (\theta_{4,initial} + \alpha_4 - \Omega_4) \quad \frac{\partial \sigma_5}{\partial \alpha_2} = A_1 - A_2 \end{array} \right] \quad (5.21)
\end{aligned}$$

The sum of virtual work done by the external forces, reaction torque at joint and spring forces is equal to zero. Thus reaction torque at driving joint $T_{reaction}$ is

$$\begin{aligned}
T_{reaction} + T_{Ext} + T_{Spring} &= -T_{Joint} + T_{Ext} + T_{Spring} = 0 \\
T_{reaction} + F_x (-z_2 \sin \theta_2 - z_6 \sin(\theta_3 + \gamma_6) A_1) + F_y (z_2 \cos \theta_2 + z_6 \cos(\theta_3 + \gamma_6) A_1) + M A_1 + T_{Spring} &= 0 \quad (5.22) \\
(T_{Ext} &= -F_x (z_2 \sin \theta_2 + z_6 \sin(\theta_3 + \gamma_6) A_1) + F_y (z_2 \cos \theta_2 + z_6 \cos(\theta_3 + \gamma_6) A_1) + M A_1)
\end{aligned}$$

The additional spring torque determined by spring constant and preload angle is

$$\begin{aligned}
T_{Spring} &= -k_2 (\theta_{2,initial} + \alpha_2 - \Omega_2) - k_3 (A_1 - 1) ((\theta_{3,initial} + \beta - \Omega_3) - (\theta_{2,initial} + \alpha_2 - \Omega_2)) \\
&\quad - k_4 A_2 (\theta_{4,initial} + \alpha_4 - \Omega_4) - k_5 (A_1 - A_2) ((\theta_{5,initial} + \beta - \Omega_5) - (\theta_{4,initial} + \alpha_4 - \Omega_4)) \\
&= (-k_2 + k_3 (A_1 - 1)) \alpha_2 + (-k_4 A_2 + k_5 (A_1 - A_2)) \alpha_4 + (-k_3 (A_1 - 1) - k_5 (A_1 - A_2)) \beta \\
&\quad + (-k_2 (\theta_{2,initial} - \Omega_2) - k_3 (A_1 - 1) ((\theta_{3,initial} - \Omega_3) - (\theta_{2,initial} - \Omega_2)) - k_4 A_2 (\theta_{4,initial} - \Omega_4) - k_5 (A_1 - A_2) ((\theta_{5,initial} - \Omega_5) - (\theta_{4,initial} - \Omega_4))) \\
&= a \alpha_2 + b \alpha_4 + c \beta + d \quad (5.23)
\end{aligned}$$

The spring equation can also be rewritten in terms of the relative angular motion of the three joints as a linear equation. α_4 and β are nonlinear function of α_2 but we can write spring torque in the form of linear equation with constant a, b, c and d. This demonstrates the fact that all linear torsional springs of fourbar mechanism can in fact be replaced by a single linear equation.

To check the relationship between reaction torque at the driving joint (T_{Joint}) and eight constants related with spring load $k_2, k_3, k_4, k_5, \Omega_2, \Omega_3, \Omega_4$ and Ω_5 , we plot torque profile with respect to possible kinematic configurations shown in the previous chapter. The range of spring constants and spring preload are decided by commercial availability such as $0.1 \sim 40 \text{ in} \cdot \text{lb}$ for spring constant and $0 \sim 180$ degree for spring preload.

The desired torque curve is assumed to be given as a function of $\alpha_2, \alpha_4(\alpha_2)$ and $\beta(\alpha_2)$ to be decided by kinematic configuration. Noting from Eq. (5.23), we only have four design variables (a, b, c, d) for use in the static synthesis process of fourbar mechanism. These can be used in the following ways:

- Four static precision points and no free choices (as seen in Section 5.4.1).
- No static precision points and using four variables as free-choices (as seen in Section 5.4.2).

5.4.1 Four static precision points and no free choices.

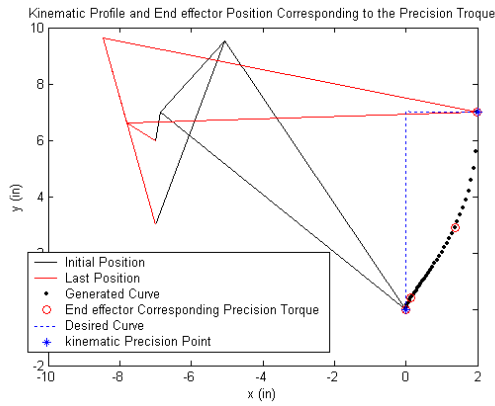
For a four static precision position problem, the spring constants and spring preloads are calculated by substituting precision torques – the specified torques ($T_i(\phi_i)$) at the precision points (α_2) – into equation (5.22) and (5.23).

$$\begin{bmatrix} a \\ b \\ c \\ d \end{bmatrix} = \begin{bmatrix} \alpha_{2,1} & \alpha_4(\alpha_{2,1}) & \beta(\alpha_{2,1}) & 1 \\ \alpha_{2,2} & \alpha_4(\alpha_{2,2}) & \beta(\alpha_{2,2}) & 1 \\ \alpha_{2,3} & \alpha_4(\alpha_{2,3}) & \beta(\alpha_{2,3}) & 1 \\ \alpha_{2,4} & \alpha_4(\alpha_{2,4}) & \beta(\alpha_{2,4}) & 1 \end{bmatrix}^{-1} \begin{bmatrix} T_{Jo\,int,1} - T_{Ext}(\alpha_{2,1}) \\ T_{Jo\,int,2} - T_{Ext}(\alpha_{2,2}) \\ T_{Jo\,int,3} - T_{Ext}(\alpha_{2,3}) \\ T_{Jo\,int,4} - T_{Ext}(\alpha_{2,4}) \end{bmatrix} \quad (5.24)$$

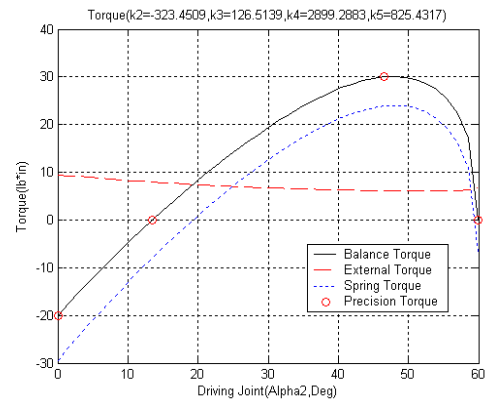
The desired k_i and corresponding Ω_i can be decided by solving:

$$\begin{bmatrix} k_2 \\ k_3 \\ k_4 \\ k_5 \end{bmatrix} = \begin{bmatrix} -1 & (A_1 - 1) & 0 & 0 \\ 0 & 0 & -A_2 & (A_1 - A_2) \\ 0 & -(A_1 - 1) & 0 & -(A_1 - A_2) \\ -(\theta_{2,initial} - \Omega_2) & -(A_1 - 1)((\theta_{3,initial} - \Omega_3) - (\theta_{2,initial} - \Omega_2)) & -A_2(\theta_{4,initial} - \Omega_4) & -(A_1 - A_2)((\theta_{5,initial} - \Omega_5) - (\theta_{4,initial} - \Omega_4)) \end{bmatrix}^{-1} \begin{bmatrix} a \\ b \\ c \\ d \end{bmatrix} \quad (5.25)$$

In equation (5.25) it gives us freedom for selection of a spring constants. There are limit for commercially available values of spring constant so we can minimize them by setting spring preloads as design variables.

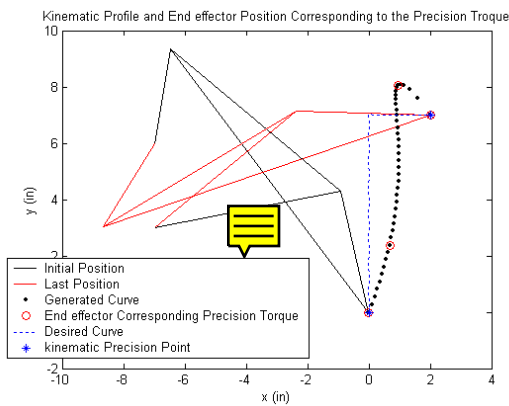


(a)

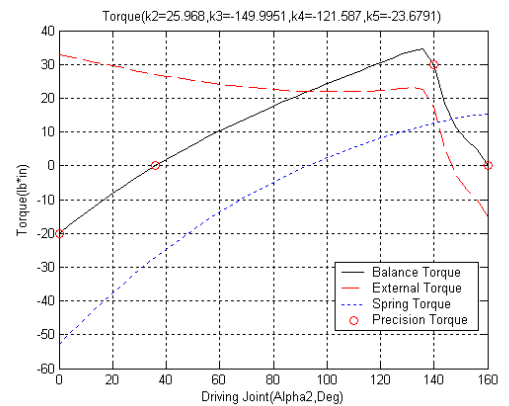


(b)

Figure 5.7 (a) Kinematic Configuration I of Fourbar for open desired trajectory and (b) Torque at driving joint

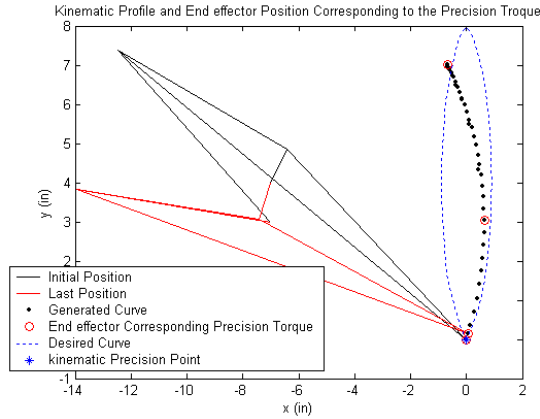


(a)

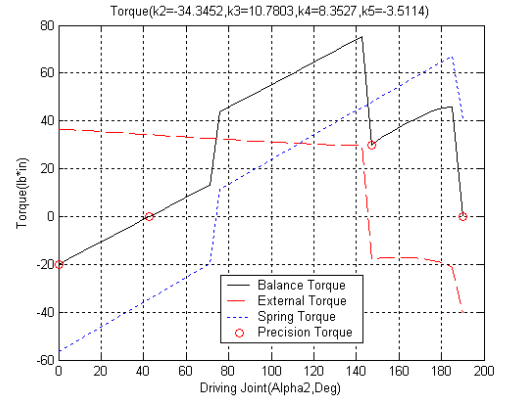


(b)

Figure 5.8 (a) Kinematic Configuration II of Fourbar for open desired trajectory and (b) Torque at driving joint

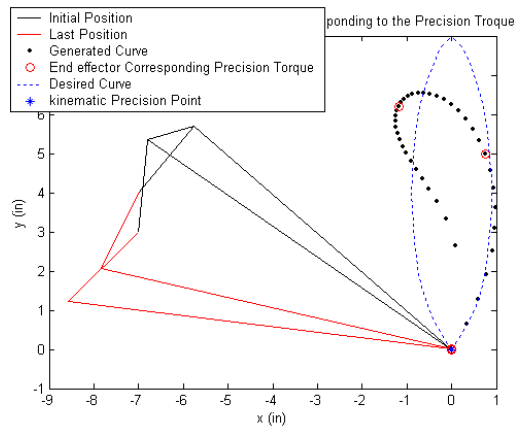


(a)

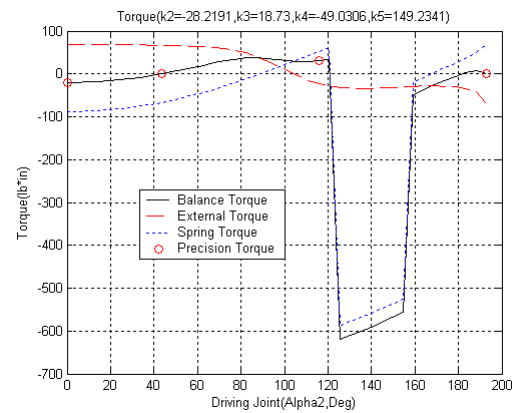


(b)

Figure 5.9 (a) Kinematic Configuration I of Fourbar for closed desired trajectory and (b) Torque at driving joint



(a)



(b)

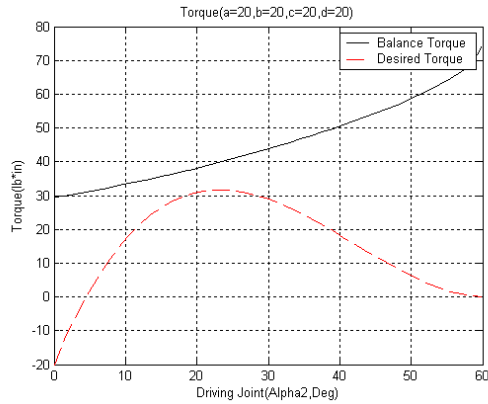
Figure 5.10 (a) Kinematic Configuration II of Fourbar for closed desired trajectory and (b) Torque at driving joint

Similar to the case of SDCSC, Part (a) of, Figure 5.7, Figure 5.8, Figure 5.9 and Figure 5.10 show the kinematic configurations at each precision point and the position to the precision torque. To design precision torque we should consider the position on the kinematic profile (a) and torque profile (b). In part (b) of, Figure 5.7, Figure 5.8, Figure 5.9 and Figure 5.10, we set first precision torque as negative to increase system's stiffness to the disturbance and determine second torque as zero to demonstrate the capability of designing stable/unstable equilibrium position. To make it ease to move system's configuration to second configuration we set third torque as positive value. The issues of pertaining to selection of precision points and corresponding torques will be discussed further in the equilibrium analysis chapter 6.

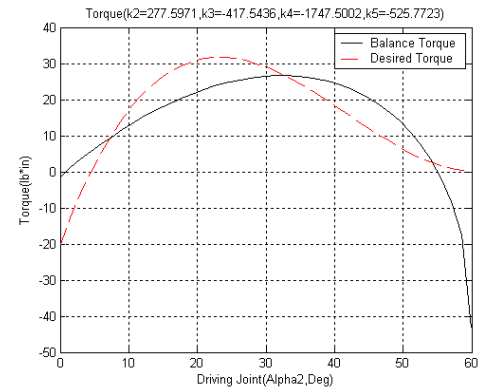
5.4.2 No static precision points and using four variables as free-choices

Similar to the case of SDCSC, we minimize discrepancy between desired and generated curve of end-effector over the entire range of motion. The optimization is carried out over the many candidate solution to obtain best specification. Now we

introduce possible sets of minimizations including force consideration in their objective and using a , b , c and d (Eq. (5.23)) as the design variables.

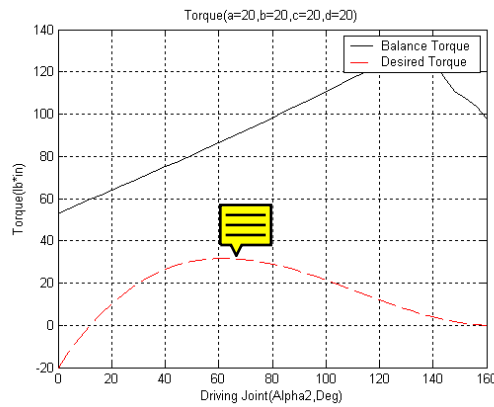


(a)

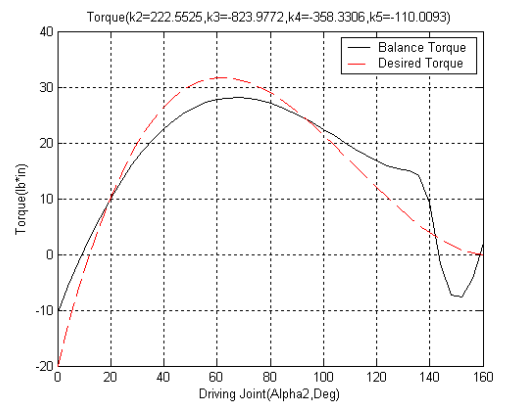


(b)

Figure 5.11 Trajectory Optimization of Fourbar for Open Desired Curve Configuration I (a) At First Iteration of Optimization and (b) Final Result of Optimization

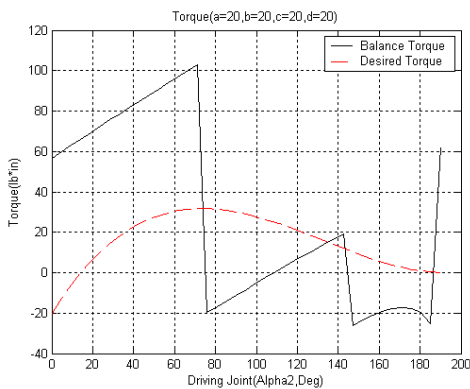


(a)

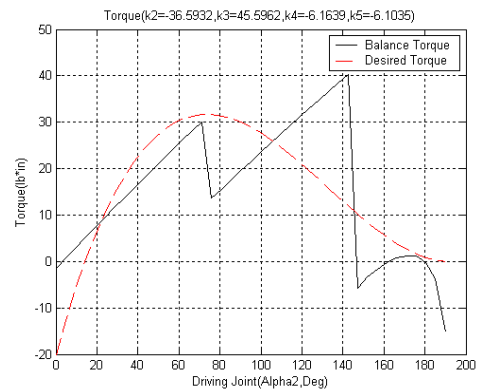


(b)

Figure 5.12 Trajectory Optimization of Fourbar for Open Desired Curve Configuration II (a) At First Iteration of Optimization and (b) Final Result of Optimization

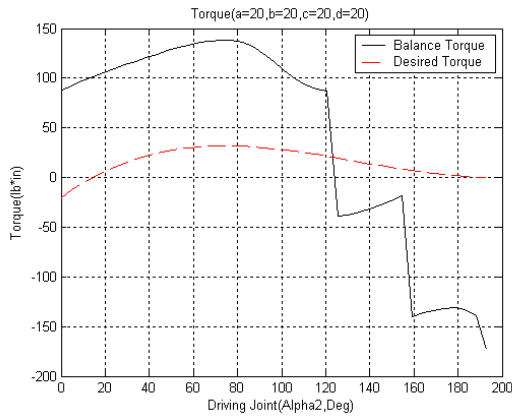


(a)

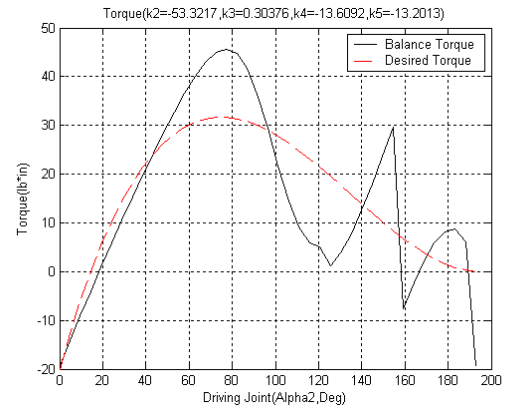


(b)

Figure 5.13 Trajectory Optimization of Fourbar for Closed Desired Curve Configuration I (a) At First Iteration of Optimization and (b) Final Result of Optimization



(a)



(b)

Figure 5.14 Trajectory Optimization of Fourbar for Closed Desired Curve Configuration II
(a) At First Iteration of Optimization and (b) Final Result of Optimization

6 Static Equilibrium Analysis

In the articulated systems under consideration, we have external forces applied typically to the end-effector and internal actuation forces applied actively due to motors or passively by springs and dampers in the system. The entire system comes to equilibrium when these forces are balanced and our interest is in locating these positions of equilibrium. These equilibrium locations depend critically upon various mechanism parameters including the physical parameters such as link-lengths and spring constants as well as the current, initial and unloaded configurations of the entire system. The designer has considerable control over selection of these parameters and one of the goals of this chapter is to explore the influence of these parameters on the system equilibria. In particular, we wish to examine not only the locations of the system equilibria but also other affiliated properties such as regions of stability and basins of attraction among other. Specific attention will be paid on the ability of the designer to customize/tailor these by both the initial/offline selection of the mechanical parameters as well as online selection of the configuration/reconfiguration of select system parameters.

These will be initially explored in the context of a case-study of a massless planar one-link revolute-jointed mechanism that supports an external end-effector load primarily by the use of a torsional spring mounted at the base revolute joint. Subsequently some preliminary results obtained for equilibrium analyses of an SDCSC-based and fourbar-based articulated leg-wheel design will be presented.

6.1 Background

6.1.1 Structures and mechanisms

Thus far we have been considering the articulated leg-wheel subsystem as a mechanism, i.e. as a set of rigid bodies attached to each other through sets of joints that are intended to transmit or constrain relative movements. In this chapter, we will make the transition to an alternative view of these articulated leg-wheel subsystems as structures. i.e. as a set of rigid bodies attached to each other through sets of joints and expected to support/carry specified loads without incurring significant displacement.

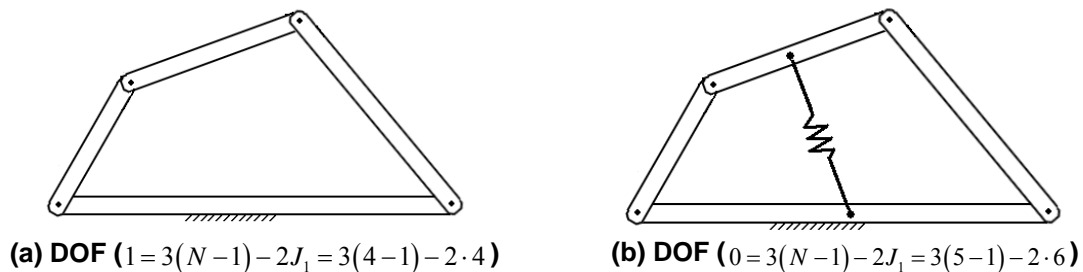


Figure 6.1 (a) Fourbar and (b) Fourbar with a constraint

We note that the single degree-of-freedom mechanisms, such as the fourbar or SDCSC mechanisms, can become structures by the simple process of addition of springs. The system together with the spring forms a structure which reaches various equilibrium configurations. When adequate external force is applied to overcome these spring forces the structure converts back into a mechanism which undergoes a specific motion

prescribed by its geometric-compatibility/loop closure constraints. By applying enough of a preload (adequate to overcome the preload of the spring) we control the structure into a mechanism. In structural analysis, people have used this idea of equilibrium paths.

We note, however, that the designer has some freedom in terms of altering these geometric compatibility constraints. Together with changes to other structural parameters, this can alter the internal distribution of energy and thereby affects the equilibrium configuration (as we will pursue in the rest of this chapter)

6.1.2 Equilibrium Analysis

6.1.2.1 Equilibrium path and response diagram

The gross or overall static behavior of many structures can be characterized by a load-deflection or force-displacement response which is usually drawn in two dimensions as a x-y plot as illustrated in Figure 6.2. In this figure a “representative” force quantity is plotted against a “representative” displacement quantity and can be used to depict a variety of linear and nonlinear behaviors.

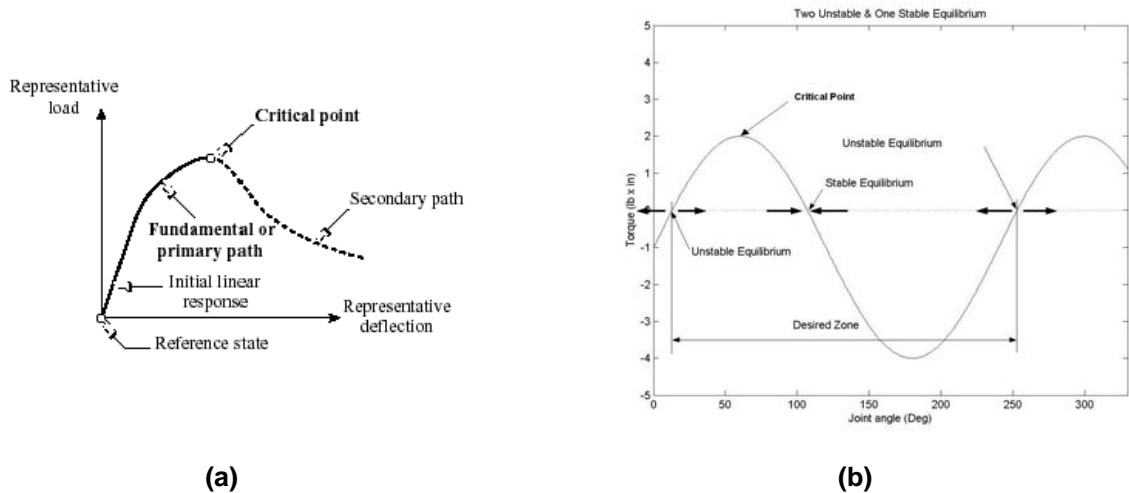


Figure 6.2 (a) Equilibrium Paths for Load Vs Deflection [24] and (b) Equilibrium Paths for Joint angle Vs Torque for a single-degree-of-freedom systems under consideration.

A smooth curve shown in a load-deflection Figure 6.2 (a) and joint angle-torque Figure 6.2 (b) diagram are called a path. Each point in the path represents a possible configuration or state of the structure and one link mechanism. If the path represents configurations of static equilibrium it is called an equilibrium path (and each point is called an equilibrium point). Certain points of an equilibrium path have special significance in the applications and named as critical, turning and failure points. Critical point notes two types such as limit point which the tangent to the equilibrium path is horizontal and bifurcation points which two or more equilibrium paths cross at critical points so the relation is not unique. Turning point is at the tangent to the equilibrium path is vertical and Failure points are points at which a path suddenly stops or breaks because of physical failure [24].

6.1.2.2 Tangent stiffness and stability

The condition for static equilibrium is that an object is in when there are forces acting on it, but it is not moving and the sum of the forces must equal to zero, and the sum of the torques must equal zero. An equilibrium is considered stable if the system always returns to it after small disturbances. If the system moves away from the equilibrium after small disturbances, then the equilibrium is unstable.

Much of stability theory for structural analysis focuses on the study of critical points of these paths. The tangent to an equilibrium path may be informally viewed as the limit of the ratio of the force increment to a displacement increment and hence by definition represents a stiffness or, more precisely, the tangent stiffness associated with the representative force/torque and displacement/joint angle.

The sign of the tangent stiffness is closely associated with the question of stability of an equilibrium state. A positive stiffness is necessarily associated with unstable equilibrium. A negative stiffness is necessary but not sufficient for stability. Since the load and deflection quantities are conjugate in the virtual work sense, the area under a load-deflection diagram may be interpreted as work performed by the system.

Restricting our attention to the special case of structures subject to conservative forces and systems that can be described with a single (or finite number of) generalized coordinates (q), we note that the total potential energy is written in terms of work done by the external forces on corresponding displacements $E = \int F.dq$. Hence by considering this total potential energy to be expressed in terms of finite number of generalized coordinate and the stationary (equilibrium) configurations can be found using $\frac{\partial E}{\partial q} = 0$ and their stability analyzed by considering the definition of the corresponding Hessian $\frac{\partial^2 E}{\partial q^2}$ [24],[25].

6.2 Static Equilibration (in a mechanism context)

6.2.1 Static Balance and Gravity Compensation

6.2.1.1 Statically Balanced Mechanism

A statically balanced mechanism is in static equilibrium in all possible configurations. A mechanism with perfect static balance has constant potential energy throughout its range of motion. To achieve static balance, a balancing mechanism providing some connection between the moving platform and earth need to be added to keep potential energy as a constant value by including energy storage devices. The requiring design factors for energy storage device should be active/passive, type and numbers of it. Such a static balance is a subset of dynamic balance. To achieve complete balance, dynamic balancing be done. In some cases, static balancing can be an acceptable substitute for dynamic balancing and it is generally easier to do. The requirement for static balance is simply that the sum of all forces on the moving system must be zero [26].

$$\sum \mathbf{F} - m\mathbf{a} = 0$$

6.2.1.2 Gravity Compensated Mechanism

A well-known application of static balancing is the compensation of gravity forces. Gravity compensation yields many advantages, including reduced energy consumption, smaller actuators, improved performance and inherent safety in case of power failure. Most gravity balancers designed to date have revolute joints. This is due to the fact that both a mass-lever element and a spring-lever element incorporating a zero-free-length spring are constant force generators.

6.2.2 Methods for Equilibration

A number of solutions for gravity compensation have been proposed for *active balancing* using active actuation of various joints or *passive balancing* by adding counterweights or using springs. We will focus our attention on some of the passive balancing methods in this chapter. Before a discussion of these methods, we would also draw the reader's attention to the fact that as a subset of static balancing problems, gravity compensation in mechanisms can be a far simpler problem. However, it is important to note that many of these solutions tend to depend critically upon the direction and magnitude of the gravitational field [25],[26].

6.2.2.1 Counterweight

Passive counterbalancing has been done by adding masses, off-setting a system mass with another mass creating an opposite moment. Adding a counterweight so that the mass center is coincident with the pivot point. Statically, mass counterbalancing is an acceptable solution. However, there are dynamic penalties for the added inertia. While adding a counterbalance mass is an excellent solution for static and slow speed systems. This approach does provide a system that is balanced for all positions, however, this is achieved at the expense of weight and inertia. A mechanism that is gravity balanced using counterweight has the advantage that it has become insensitive for its orientation with respect to the gravity acceleration vector [19].

6.2.2.2 Spring-equilibrium System

Alternatively, a counterbalancing system is using the stored energy in springs to counter the effects of gravity and should offer improved dynamic performance. The benefits using spring-equilibrated system is the reduced inertia added to the equilibrated system. The spring approach appears to be more attractive since no undue energy is added to the system. Since the moment due to gravity is configuration dependent, it is non-linear. Advantages of the use of spring are that the additional mass and inertia associated with counterweight is avoided, which result in increased accelerations [26].

6.3 Case Study of One-Link Mechanism

6.3.1 Examples of perfect static equilibration (using counterweight system)

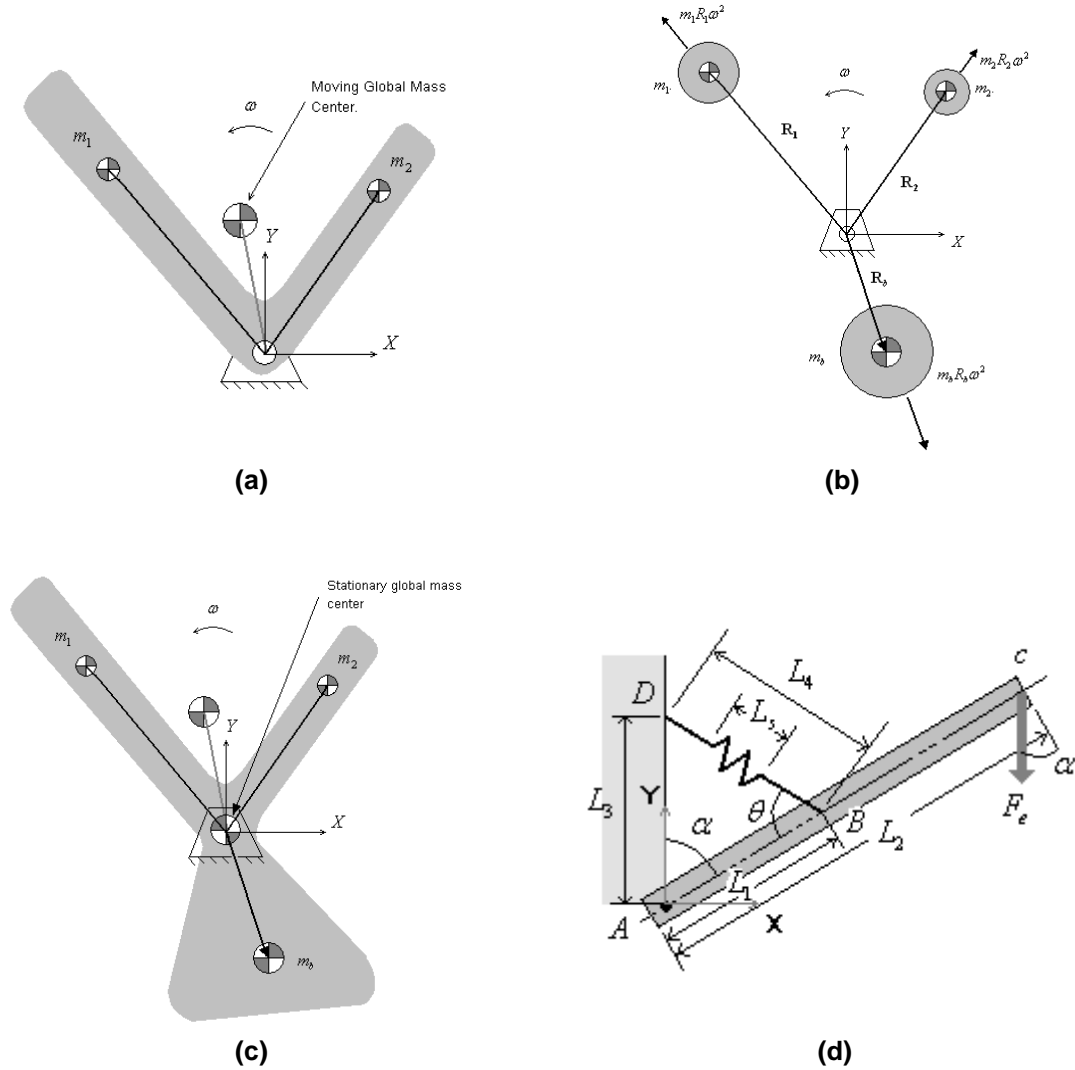


Figure 6.3 (a) Unbalanced, (b) Dynamic Model, (c) Statically Balanced Link and (d) One link and Tension Spring [16],[23].

Figure 6.3 (a),(b) and (c) show a link in the shape of a vee which is part of a linkage. We want to statically balance it. We can model this link dynamically as two point masses m_1 and m_2 concentrated at the local CGs of each leg of the link as shown in Figure 6.3 (b).

Writing vector equation,

$$-m_1 \mathbf{R}_1 \omega^2 - m_2 \mathbf{R}_2 \omega^2 - m_b \mathbf{R}_b \omega^2 = 0 \quad (6.1)$$

$$m_b \mathbf{R}_b = -m_1 \mathbf{R}_1 - m_2 \mathbf{R}_2$$

$$\mathbf{R}_b = \frac{-m_1 \mathbf{R}_1 - m_2 \mathbf{R}_2}{m_b} \quad (6.2)$$

Once a combination of m_b and \mathbf{R}_b is chosen, it remains to design the physical counterweight. The \mathbf{R}_b is vector from the pivot to the CG of the counterweight mass as shown in Figure 6.3 (b) and (c).

6.3.2 Example of perfect gravity balancing (using Linear Springs)

A simple method to counter the effects of gravity in articulated mechanism is using spring-equilibrium system. The scheme uses kinematics and linear springs to produce a non-linear restoring force to oppose the gravitational moment. The method equilibrates a rotational mechanism for all postures.

Taking the moment about point A yield equation,

$$F_e L_2 \sin \alpha - F_s L_1 \sin \theta = 0 \quad (6.3)$$

$$F_e L_2 \sin \alpha - k \Delta L_1 \sin \theta = 0 \quad (6.4)$$

by using sine law, we obtain

$$\frac{L_4}{\sin \alpha} = \frac{L_3}{\sin \theta} \quad (6.5)$$

$$L_4 = \frac{\sin \alpha L_3}{\sin \theta}$$

Suppose the unstretched length of the spring as zero then $\Delta = L_4$

$$F_e L_2 \sin \alpha - k \frac{\sin \alpha L_3}{\sin \theta} L_1 \sin \theta = 0 \quad (6.6)$$

$$F_e L_2 \sin \alpha - k L_1 L_3 \sin \alpha = 0$$

$$(F_e L_2 - k L_1 L_3) \sin \alpha = 0$$

Thus

$$F_e L_2 - k L_1 L_3 = 0 \quad (6.7)$$

$$k = \frac{F_e L_2}{L_1 L_3}$$

The spring constant which from above equation, $k = \frac{F_e L_2}{L_1 L_3}$, makes system counter the effect of gravity.

6.3.3 Examples for selective equilibria (using Hookian torsional springs)

The problem being considered is a relatively general problem and the set of tools that we will be developing can address a wide variety of scenarios, including specification of the magnitudes of the external loads, locations of the equilibrium positions, selection of the initial unloaded configurations etc.

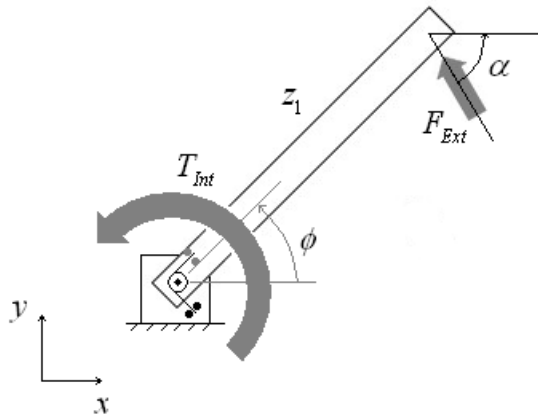


Figure 6.4 One link with revolute joint and Hookian torsion spring

Consider the example of a planar massless one-link system which has an external force F_E applied to the end-effector and torsional spring obeying Hooke's law attached to the revolute joint. As shown on Figure 6.3, the external force applied at the end of link with angle α can be expressed as:

$$\mathbf{F}_E = F(-\cos \alpha \mathbf{i} + \sin \alpha \mathbf{j}) \quad (6.8)$$

and torque caused by this external force at the revolute joint is

$$\begin{aligned} T_{Ext} &= \mathbf{Z}_1 \times \mathbf{F}_E \\ &= z_1 (\cos \phi \mathbf{i} + \sin \phi \mathbf{j}) \times F(-\cos \alpha \mathbf{i} + \sin \alpha \mathbf{j}) \\ &= z_1 F (\cos \phi \sin \alpha \mathbf{k} + \sin \phi \cos \alpha \mathbf{k}) \\ &= z_1 F \sin(\phi + \alpha) \mathbf{k} \end{aligned} \quad (6.9)$$

We assume that under the action of this force the link is displaced from its initial absolute configuration, θ , to its current configuration $\theta + \phi$. We also assume that the configuration of system when the spring is assembled is described by Ω . Thus $\beta = \theta + \phi - \Omega$ is the angular extension of the spring at the current configuration and the spring torque (T_{Spring}) acting on revolute joint can be calculated as:

$$T_{Spring} = -k_{Torsion} \beta = -k_{Torsion} (\theta + \phi - \Omega) \quad (6.10)$$

Hence the net torque at the revolute joint can be calculated as:

$$T_{Balance} = T_{Ext} + T_{Spring} \quad (6.11)$$

In order to visualize this better, we plot the various torques, T_{Ext} , T_{Spring} and $T_{Balance}$ in Figure 6.5.



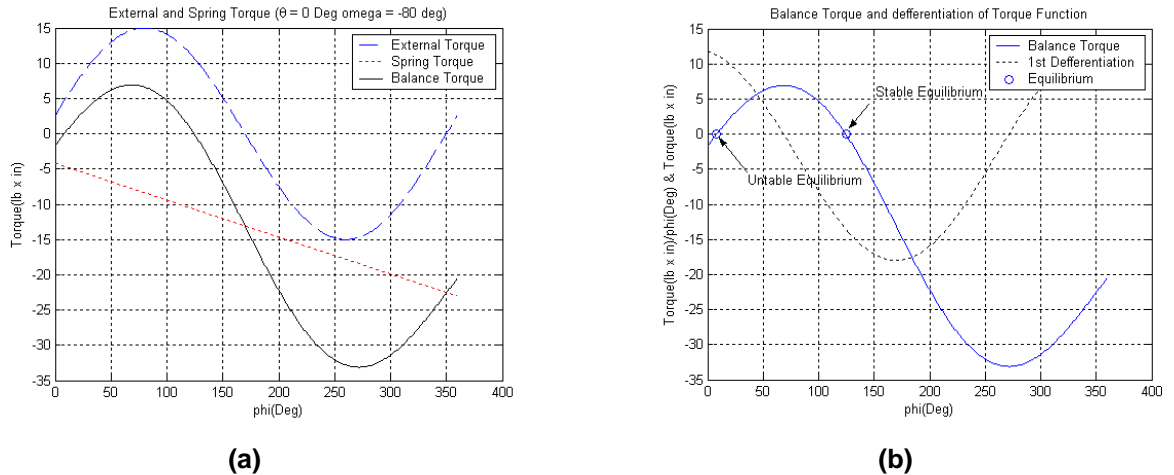


Figure 6.5 (a) Spring/External/Balance Torque at Joint and (b) Unstable Equilibria

We will also restrict our attention to specific ranges of configurations and look for locations of equilibria within these ranges. Within the range of the input crank angle between 0 and 360 degrees it may be possible that the internal and external torques do not ever reach a common value with the implication that no equilibria exist. However, it is important to note that this is true only for this limited range of configurations – since these are physical systems, the equilibrium must exist but may lie outside the range of interest.

In the next few subsections we will discuss the types of equilibria, their *basins of attraction* and the relationship to the mechanism parameters.

6.4 Analysis of Equilibria

6.4.1 Equilibrium Analysis for Spring equilibria

The condition for static equilibrium is that an object is in when there are forces acting on it, but it is not moving and the sum of the forces must equal to zero, and the sum of the torques must equal zero. An equilibrium is considered stable if the system always returns to it after small disturbances. If the system moves away from the equilibrium after small disturbances, then the equilibrium is unstable.

Let us consider the stability of 2 equilibrium points for the example first discussed in Section 6.3.3 which is reproduced below in Figure 6.6. In this figures when the external torque is larger than spring torque the links move in the counter-clock wise direction and when spring torque is larger than external torque the link will turn in the clockwise direction. Equilibrium is reached when $T_{Ext} = T_{Spring}$.

The same phenomenon can alternatively be demonstrated by considering only the balance torque in Figure 6.6(b) where the balancing torque ($T_{balance}$) is plotted versus joint angle. If $a < \phi < b$, then $T_{Balance}$ is positive, link turns counter-clockwise direction. If $\phi < a$ or $\phi > b$, then overall torque is negative, link rotates clockwise direction. Examining the nature of the balance torques around each equilibrium point arrow in the figure shows that the equilibrium $\phi = a$ is unstable, whereas the equilibrium $\phi = b$ is stable. This means that given a small disturbance/change of angle ϕ , the link cannot

return back to unstable equilibrium ($\phi = a$). Instead, the link rotates until it reaches the stable equilibrium ($\phi = b$). In the case of small disturbance/deviation from $\phi = b$, the link always turns back to this equilibrium.

Visually we notice that the characteristic feature of stable and unstable equilibria is in the slope of the tangent to the curve. Stable equilibria are characterized by a negative slope whereas unstable equilibria are characterized by a positive slope. These equilibria are dependent upon the mechanism parameters as will be discussed in the next section.

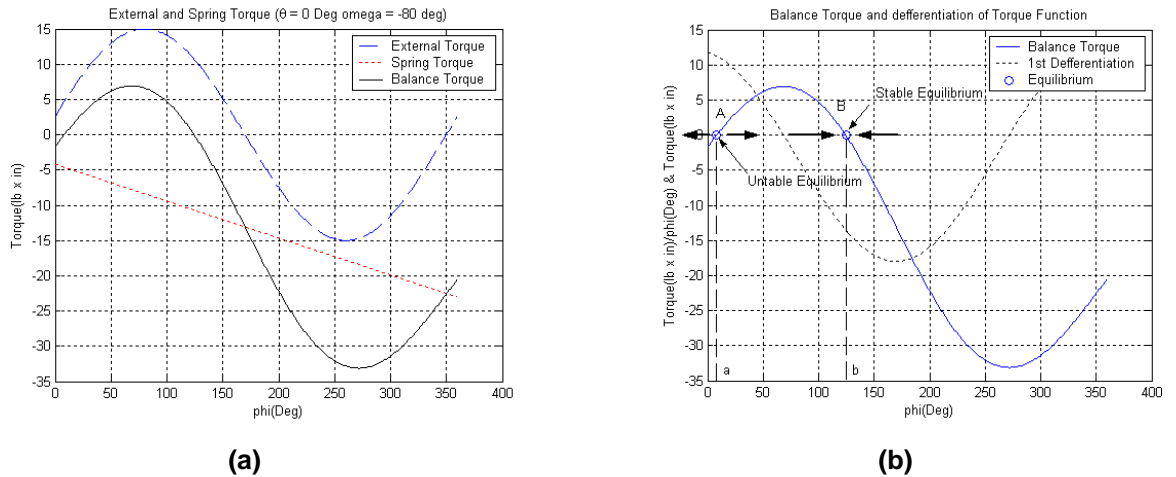


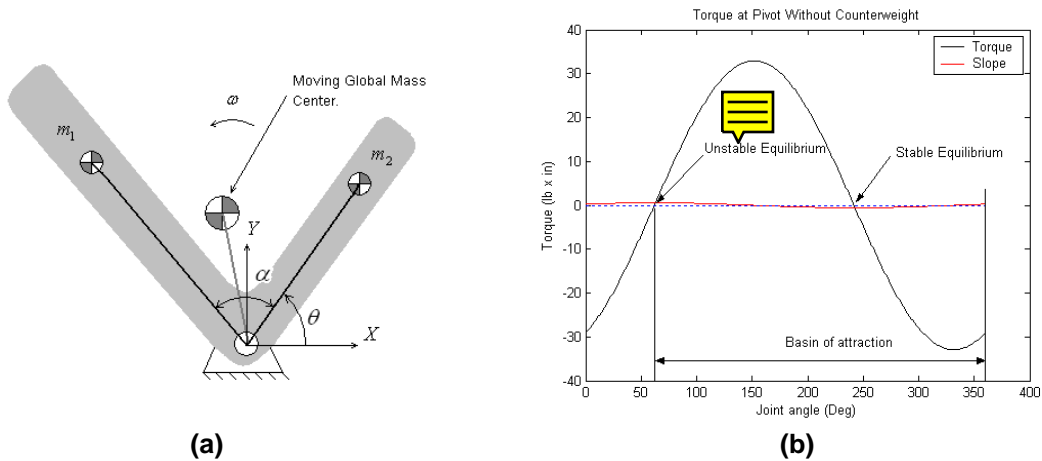
Figure 6.6 (a) Internal/Spring/Overall Torque at Joint and (b) Stable/Unstable Equilibria

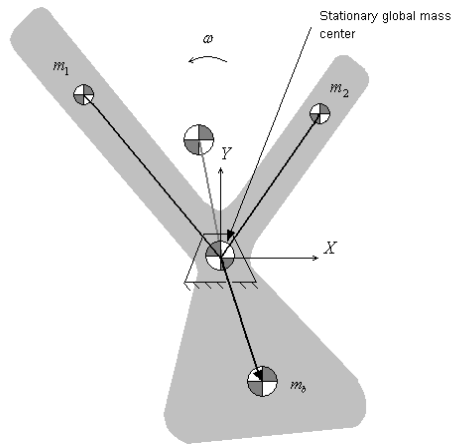
6.4.2 Equilibrium Analysis for Counterweight

The torque at the pivot joint of the unbalanced system in Figure 6.7 (a) is

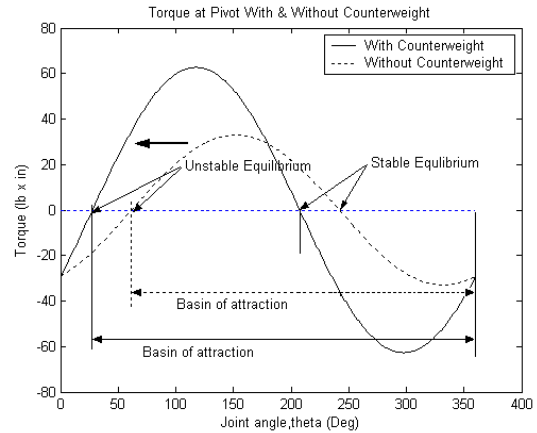
$$T_{Pivot} = -m_1 r_1 \cos(\alpha + \theta) - m_2 r_2 \cos \theta \tag{6.12}$$

and when we increase θ from 0 to 360 degree the torque at the pivot joint profile has one stable and one unstable equilibrium and desired zone can be defined from unstable pivot joint to end of θ range (360 degree).

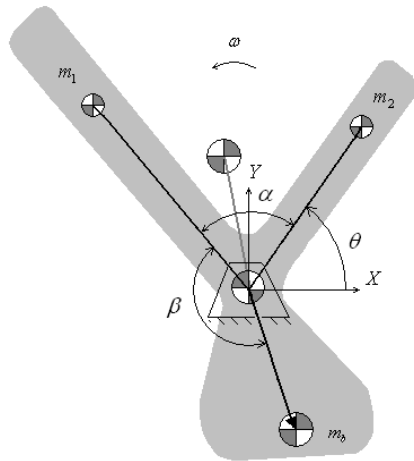




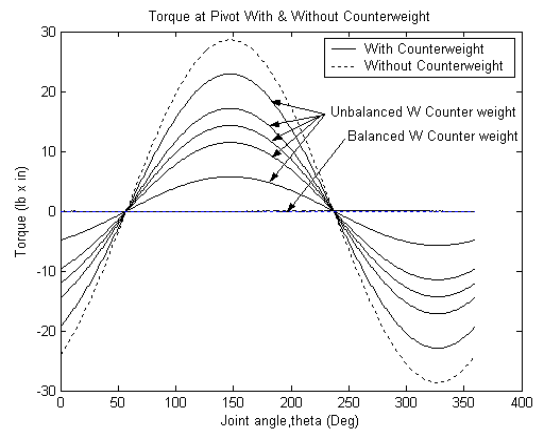
(c)



(d)



(e)



(f)

Figure 6.7 (a-b) Unbalanced System (c-d) Partially balanced and (e-f) Perfectly balanced

As shown in Figure 6.7 (b), negative slope is related with stable equilibrium and positive slope is related with stable equilibrium. Once balanced by offset counterweight, the torque caused by the counterweight should cancel out the torque by m_1 and m_2 . Instead offsetting the torque, we can move equilibrium positions to design retroactive system by using counterweight. By changing weight we can change amplitude of curve (Figure 6.7 (f)) and shift curve by changing vector from pivot to center of counter weight (Figure 6.7 (d)).



6.5 Quantitative Measures for Evaluation of Equilibria

6.5.1 Location of the equilibrium

In situations where the external force direction and magnitude are well-known a priori, we can design a compensatory system easily. However, in general we do not have much of control over the external forces but can exercise considerable control over the spring constant and preload. As shown in Figure 6.8, by changing preload angle, we can alter

the spring torque curve up and down and thereby design the locations and type of equilibrium.

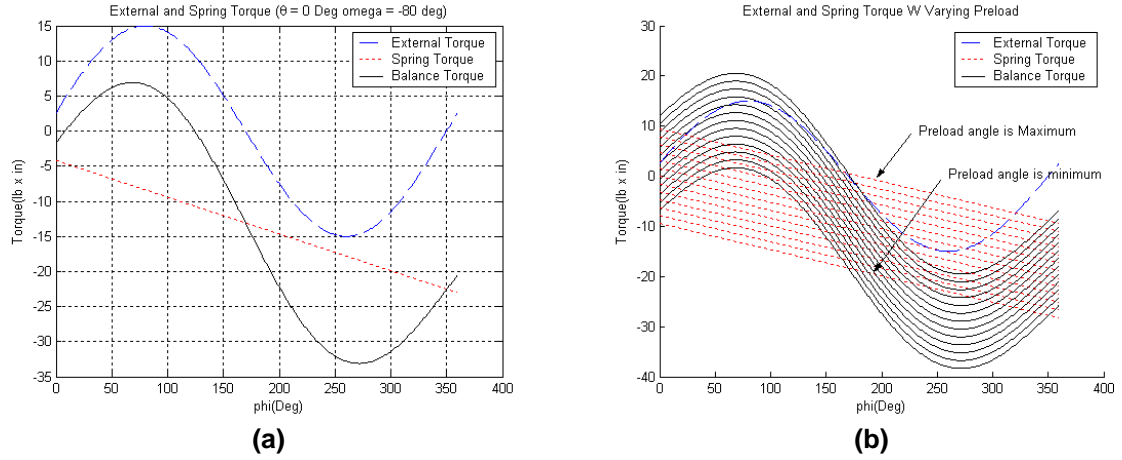


Figure 6.8 (a) External/Spring Torque (Without preload) and (b) External/Spring Torque (Varying Preload Angle)

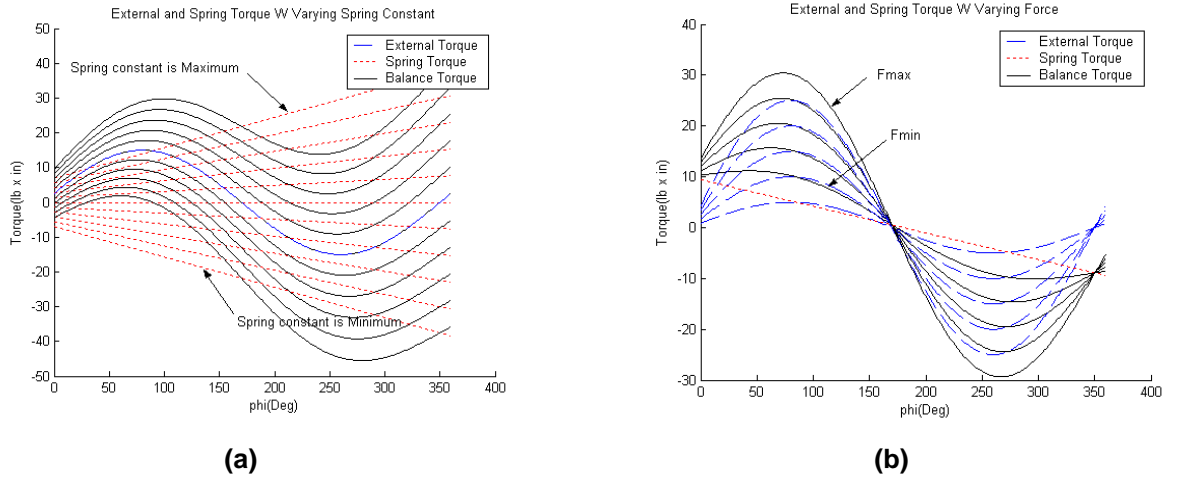


Figure 6.9 (a) Torque (Varying Spring Constant) and (b) Torque (Varying External Force)

6.5.2 Sensitivity of the equilibrium

The magnitude of the slope can also serve as a measure of the sensitivity and serve to characterize the equilibrium point in terms of the robustness of the configuration to errors in the external applied loads or to parameter variations.

Sensitivity is expressed as:

$$\frac{\Delta T}{T} = S_{\phi}^T \frac{\Delta \phi}{\phi} \quad \left(S_{\phi}^T = \frac{\phi}{T} \frac{\Delta T}{\Delta \phi} \right) \quad (6.13)$$

and S_{ϕ}^T is called the sensitivity of T with respect to change in ϕ . Assuming S_{ϕ}^T as 2, then a 1% change of ϕ will produce 2% change in T , approximately. Thus sensitivity at the stable equation is the one of objective function for optimization [29].

The tangent to an equilibrium path may be informally viewed as the limit of the ratio

$$\text{Tangent Stiffness} = \frac{\text{force increment}}{\text{displacement increment}} \cdot \frac{\text{Torque}}{\text{Joint angle}}$$

This is by definition a stiffness or, more precisely, the tangent stiffness associated with the representative force/torque and displacement/joint angle. The reciprocal ratio is called flexibility or compliance. The sign of the tangent stiffness is closely associated with the question of stability of an equilibrium state. A positive stiffness is necessarily associated with unstable equilibrium. A negative stiffness is necessary but not sufficient for stability. Since the load and deflection quantities are conjugate in the virtual work sense, the area under a load-deflection diagram may be interpreted as work performed by the system [25].

6.5.3 Basin of Attraction – magnitude and range

Another objective is maximum and minimum torque described in figure. These are related with allowable external loads which can return link to the stable equilibrium.

$$\begin{aligned} T_{Ext}(\phi) &\leq T_{Joint}(\phi) \\ T_{Ext}(\phi) - T_{Joint}(\phi) &\leq 0 \end{aligned} \quad (6.14)$$

where T_{Ext} is additional external load to the equilibrium system with respect to joint angle ϕ and T_{Joint} is torque at joint calculated by subtracting torque caused by external force from the torque caused by internal force.

The other objective is the basin of attraction. Any configuration of system, in this system joint angle ϕ , in the basin of attraction will try to go to corresponding stable equilibrium. In Figure 6.10 to Figure 6.11 show four equilibria cases. In the view of leg-wheel system design we use the basin of attraction as objective for optimization. It can be just maximized or minimized and discrepancy between certain range and the basin of attraction.

$$\min_{k, \Omega} D_{\text{The basin of attraction}} \quad \max_{k, \Omega} D_{\text{The basin of attraction}} \quad (6.15)$$

or

$$\min_{k, \Omega} \left(D'_{\text{The basin of attraction}} - D_{\text{The basin of attraction}} \right)^2 \quad (6.16)$$

6.6 Possible Equilibrium Configurations for a One-Link Mechanism

Considering a candidate one link system with joint angle range as 0 to 360 degree and external load condition is such that force is 3 lb, force angle is 10 degree and link length is 5in. The one-link system can be classified into 4 cases based on the type and number of equilibria that can be realized within a given range.

A. One unstable equilibrium

In this case, there is a single unstable equilibrium and the system will always move away from this unstable configuration to the corresponding end of the range Figure 6.10 (a).

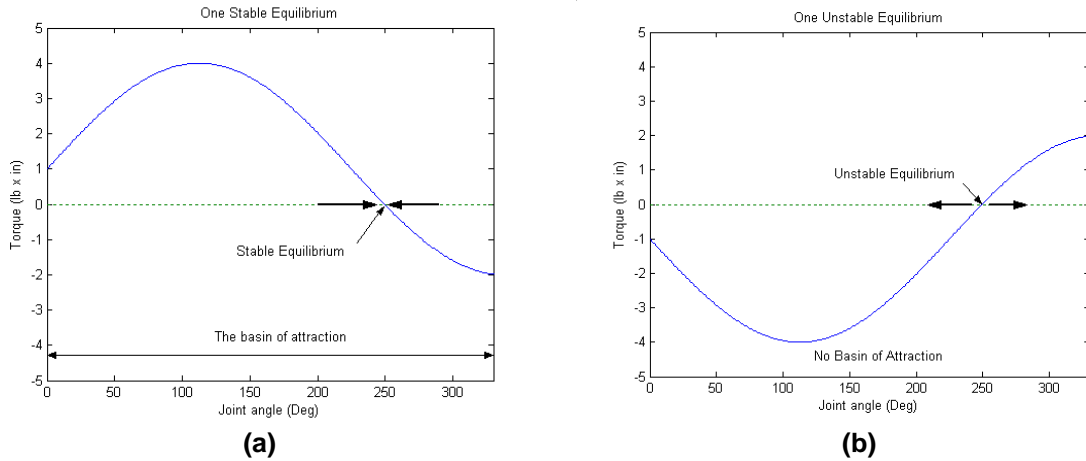


Figure 6.10 (a) One Stable Equilibrium and (b) One Unstable Equilibrium

B. One Stable equilibrium

In this case the basin of attraction is the entire range of configurations and the balancing torque always restores the system to the stable equilibrium configuration Figure 6.10 (b).

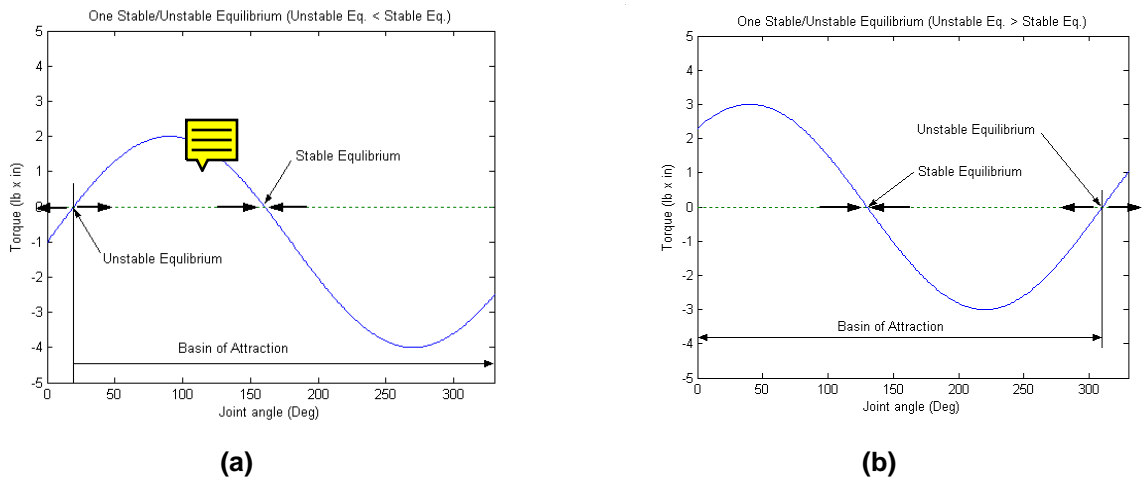


Figure 6.11 (a) . Unstable Equilibrium < Stable Equilibrium and (b) . Unstable Equilibrium > Stable Equilibrium

C. One unstable and one stable equilibrium

As shown in the Figure 6.11 (a), when unstable equilibrium is closer to origin than stable equilibrium, the basin of attraction starts from unstable equilibrium to the upper-end of configuration range.

D. One stable and one unstable equilibrium

In the other case, when stable equilibrium is closer to origin than unstable equilibrium then the range from origin to unstable equilibrium is basin of attraction Figure 6.11 (b).

E-F. Multiple Stable/Unstable Equilibria

When system has multiple stable/unstable equilibrium, many basins of attraction can result and these can be determined as either: (i) the range between two unstable equilibria

(which must by necessity include a stable equilibrium) Figure 6.12 (a); or (ii) as multiple ranges between unstable equilibria and the upper/lower ends of the permissible configuration ranges Figure 6.12 (b).

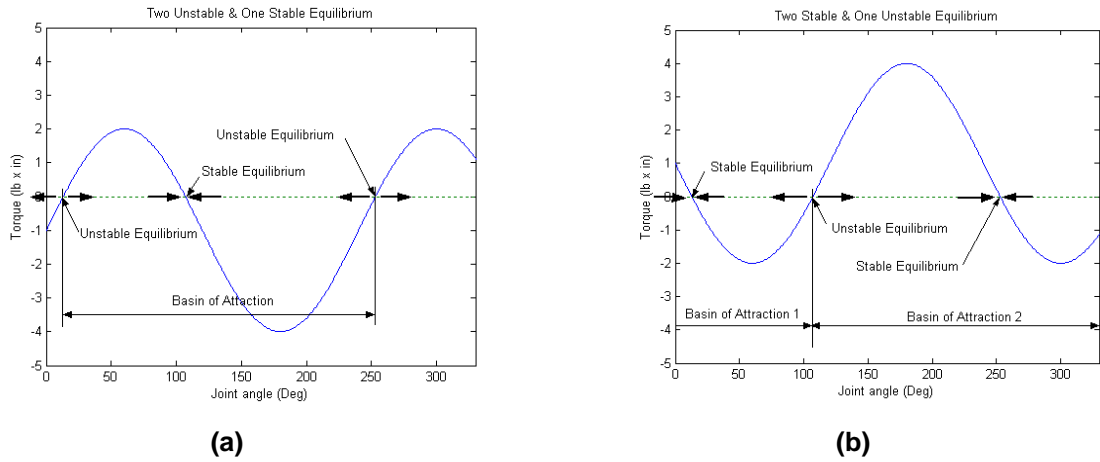


Figure 6.12 (a) Two Unstable & One Stable Equilibrium and (b) One Unstable & Two Stable Equilibrium

6.7 Most Useful Equilibrium Case of a One Link System

Among all possible configurations, the most useful scenario arises when we consider the situation with two unstable equilibria on either side of a stable equilibrium (Figure 6.16)– Case E in Section 6.6

In this section we will examine the dependence of the sensitivity and basins of attraction of this case upon the mechanism parameters – in particular the preload angle and the spring constant.

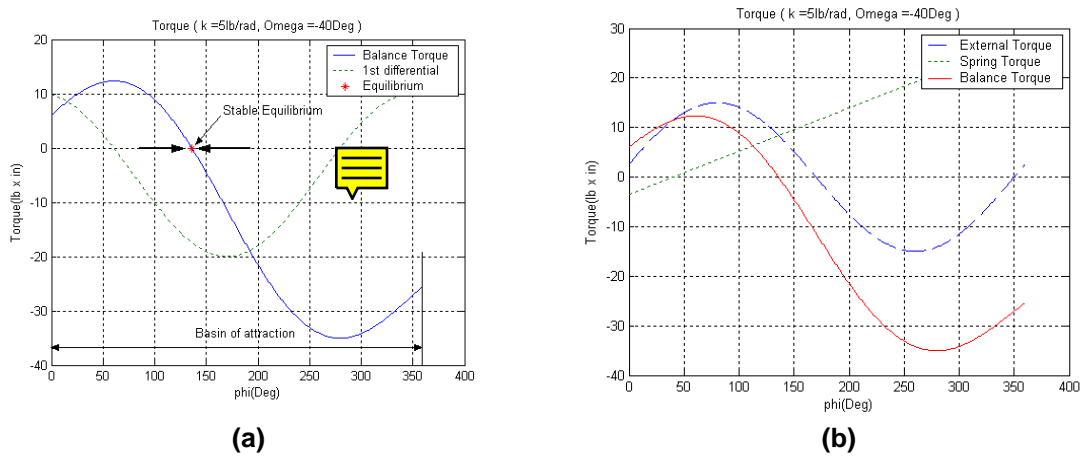
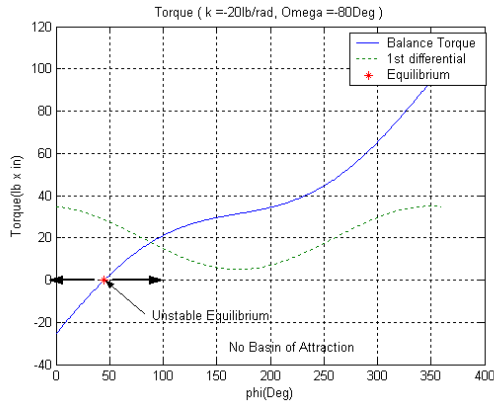
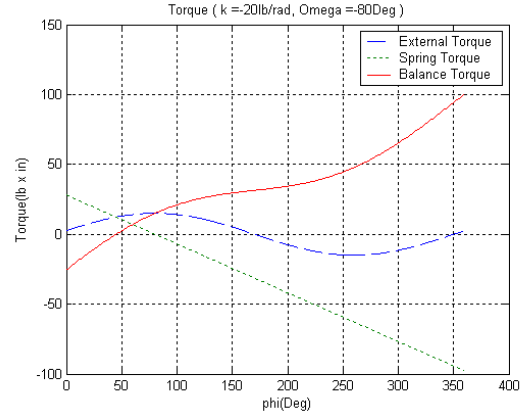


Figure 6.13 (a) Basin of Attraction for One Stable Equilibrium Case ($k = 5\text{lb/Rad}$, $\Omega = 40\text{ Deg}$) and (b) Torque at the End-effector



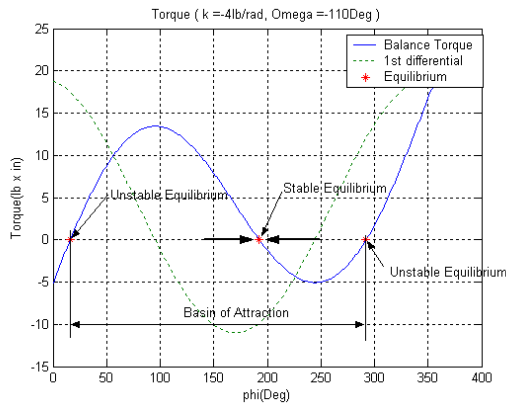


(a)

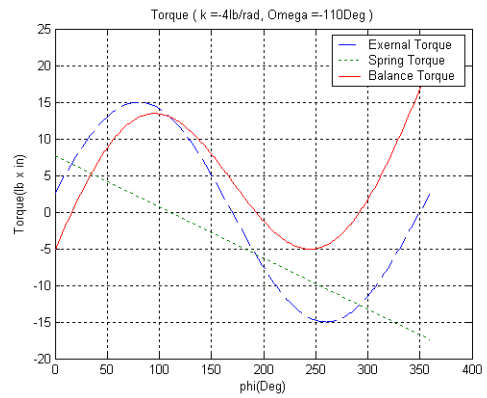


(b)

Figure 6.14 (a) Basin of Attraction for One Unstable Equilibrium Case ($k = 20\text{lb/Rad}$, $\Omega = -80\text{ Deg}$) and (b) Torque at the End-effector.

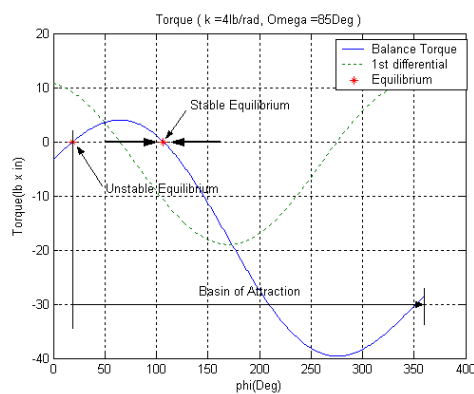


(a)

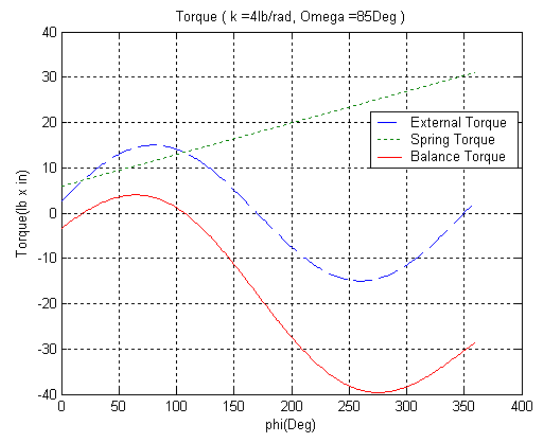


(b)

Figure 6.15 (a) Basin of attraction for Two Unstable Equilibrium Case ($k = -4\text{lb/Rad}$, $\Omega = -110\text{ Deg}$) and (b) Torque at the End-effector.



(a)



(b)

Figure 6.16 (a) Basin of attraction for One Unstable Equilibrium Case ($k = 4\text{lb/Rad}$, $\Omega = 85\text{ Deg}$) and (b) Torque at the End-effector.

6.8 Basin of Attraction Optimization

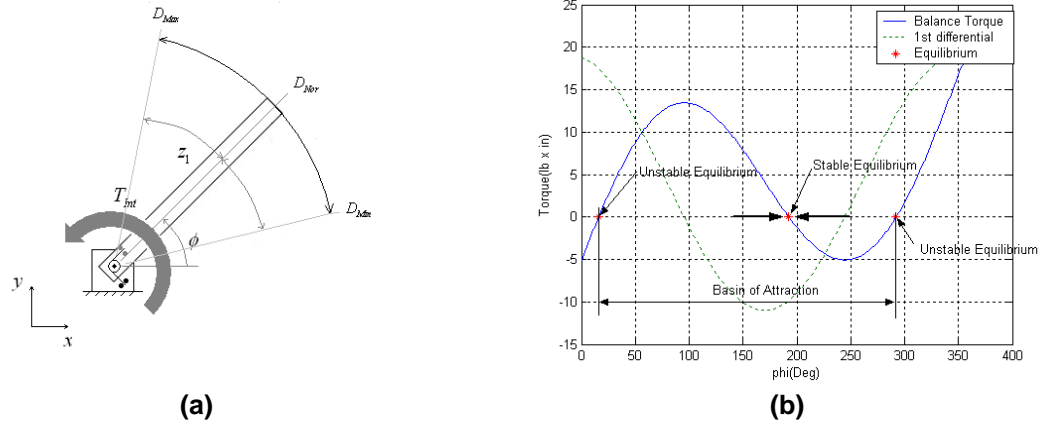


Figure 6.17 (a) Desired Zone for One Link System and (b) Two Unstable & One Stable Equilibrium

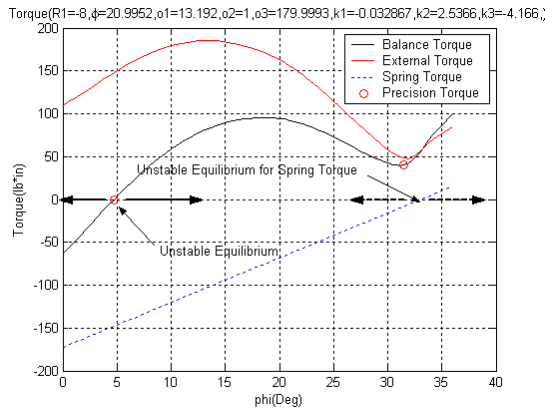
As shown on figure, multiple stable/unstable equilibrium case is good our design purpose because we can design position of equilibriums ($D_{1,Us}$, $D_{2,St}$, $D_{3,Us}$) by changing design variables. Objective function of the problem is:

$$\min_{k, \Omega} \left(K_1 (D'_{1,Us} - D_{1,Us})^2 + K_2 (D'_{2,St} - D_{2,St})^2 + K_3 (D'_{3,Us} - D_{3,Us})^2 \right) \quad (6.17)$$

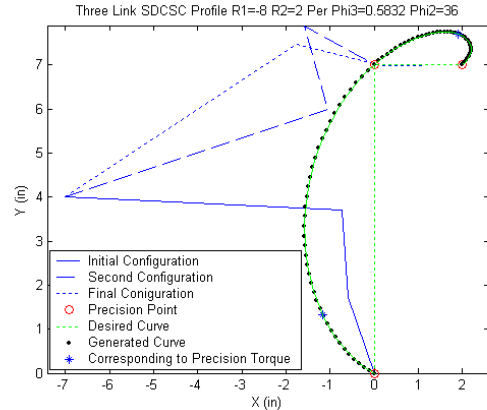
where $D_{1,Us}$, $D_{2,St}$, $D_{3,Us}$ are for desired design and $D'_{1,Us}$, $D'_{2,St}$, $D'_{3,Us}$ are for generated design and K_1 , K_2 & K_3 are weighting variables.

6.9 Equilibrium Analysis for an SDCSC-based Articulated Leg-Wheel Design

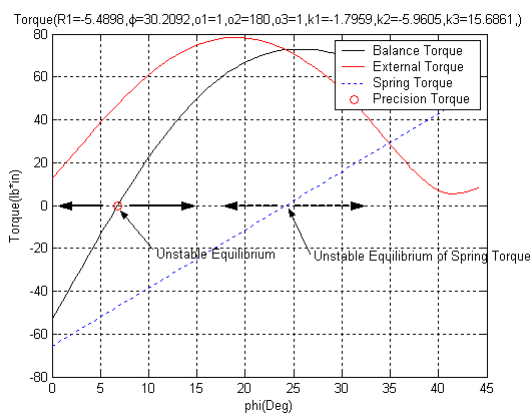
As described in Chapter 3, one of disadvantage of leg-wheel system is that it consumes a lot of power just supporting its configuration. By this reason, we are emphasizing on static balancing of legged system when wheel is on flat surface. It can be realized by optimizing variables such as spring constants and preloads to optimize torque at first joint when slant is 0° . We set first precision torque to enhance stiffness of system to the disturbance from ground. That is to say, when the end-effector is in between initial configuration and the first precision position, system torque will try to move system back to the initial configuration. Once end-effector passes by first precision position then system torque will turn system to the last configuration. One of a failure case, the end-effector is losing contact with ground then external torque will be zero and the direction of spring torque is determined by kinematic configuration of SDCSC. When SDCSC's end-effector is located in the range of initial position to unstable equilibrium of spring torque, spring torque will try to move system to initial configuration. Otherwise spring torque will turn system to final configuration.



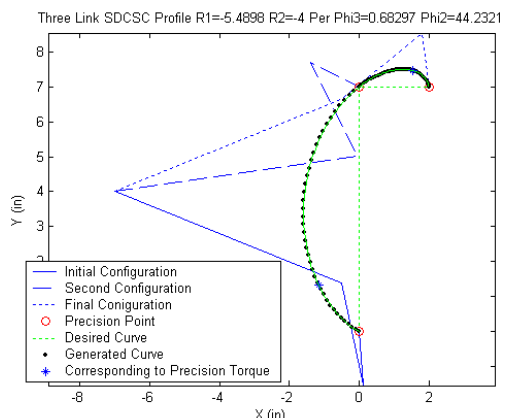
(a)



(b)

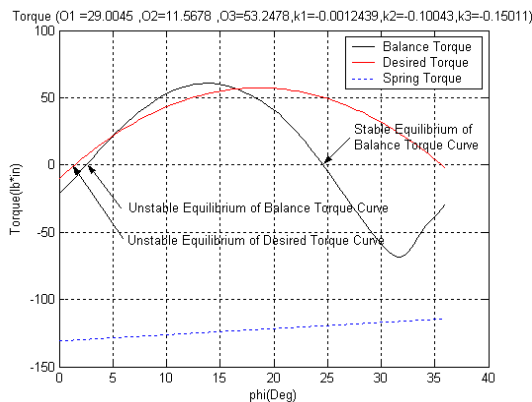


(c)

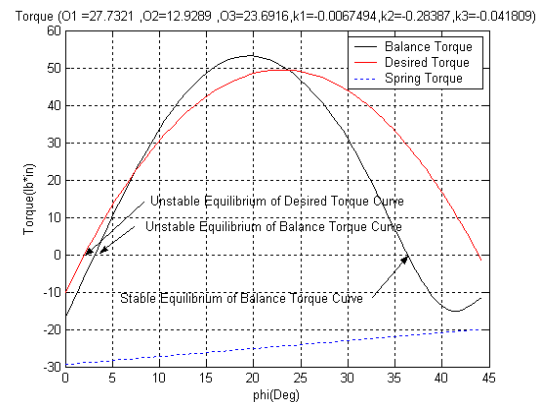


(d)

Figure 6.18 Equilibrium Position and corresponding position in the kinematic configuration of (a) Three Link SDCSC Configuration I and (b) Three Link SDCSC Configuration II



(a)



(b)

Figure 6.19 Stable and unstable equilibrium of (a) Three Link SDCSC Configuration I and (b) Three Link SDCSC Configuration II

We designed desired torque curve has one unstable equilibrium close to the initial configuration. In Figure 6.19, spring torque of system is negative overall configuration,

thus spring torque of the system will try to move itself to initial configuration when end-effector loses ground contact.

6.10 Equilibrium Analysis for a Fourbar based Articulated Leg-Wheel Design

In the fourbar case we can choose four precision torques for precision torque synthesis problem. As shown in Figure 6.20 (a), we design one unstable equilibrium overall range of operation of mechanism by determining the values and positions of four precision torques. In the failure case, such as losing contact of end-effector, spring torque will try to return system to initial configuration when mechanism is in the configuration between initial an unstable equilibrium of spring torque. Otherwise spring torque will move system to final kinematic configuration. Figure 6.21 shows one of example that demonstrates capability of designing position and number of equilibrium to satisfy static requirement by modifying shape of desired torque curve.

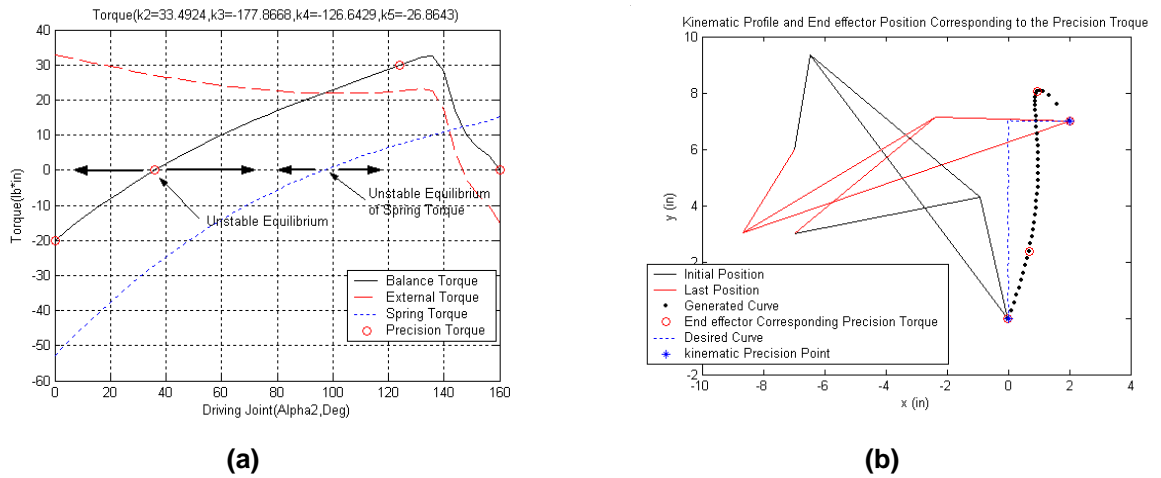


Figure 6.20 (a) Equilibrium Position and (b) corresponding position in the kinematic configuration of Fourbar Open Desired Curve Configuration II

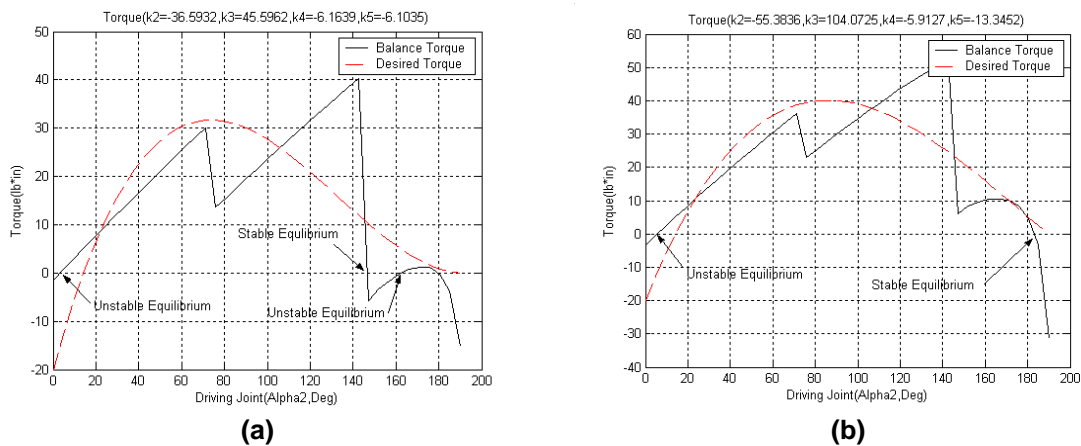


Figure 6.21 End-effector Torque of Closed Desired Curve Configuration I which has (a) Two Unstable Equilibriums and One Stable Equilibrium and (b) One Stable Equilibrium and One Unstable Equilibrium.

7 Conclusion and Future Work

In this thesis, we considered the creation of articulated leg-wheel subsystems to enable vehicle systems to locomote in difficult environments and rough terrain. The primary role envisaged for the leg-wheel subsystems is to provide vehicle with the ability to modulate the motion and force interactions between the ground and the chassis, while retaining selective transmission of kinesthetic and tactile information, reduced degree of freedom actuation and control, passivity in the form of a mechanical coupling and overall ease of operation. The long-term goal of this effort is to create an uneven terrain locomotion system, having capabilities of traversing obstacles, customizing wheel axle trajectory, providing semi-active support and possessing reconfigurability.

Numerous variants of articulated leg-wheel designs could be created using lower pair joints (revolute/prismatic) between the wheel and the chassis depending upon the type, number, sequencing and nature of actuation (active/passive) of the joint. We focused our attention on single degree-of-freedom Articulated Leg-Wheel designs that permits the greatest motion capability between the chassis and wheel while maintaining the smallest degree of freedom within the articulated system.

We focused our attention on passive mechanical implementation of such single-degree-of-freedom intermediate articulation using two configurations: a fourbar-based design and an SDCSC-based design. The issues pertaining to creation, analysis and realization leading to the development of the full potential of these two candidate single-degree-of-freedom designs for the articulated leg-wheel system motivated the research. We emphasized the design-customization and adaptation of these two single degree-of-freedom mechanisms for use on rough terrain. We examined the application of kinematic and kinetostatic design optimization methods to select design parameters of the leg-wheel subsystems to allow them to tackle increasing terrain roughness, achieve better chassis-terrain decoupling and reduce actuation requirements. We also examined the influence of the mechanical parameters on the static equilibrium curves of the articulated leg-wheel subsystem from the viewpoint of developing future capabilities to customize/tailor these mechanical system responses (preflexes) to desired behaviors in an offline/online manner.

7.1 Research Contributions

- Systematic evaluation of the nature of the articulations and affiliated hardware constraints in achieving the desired workspace and the desired suspension characteristics.
- Adaptation of the kinematic and kinetostatic design procedure developed for dimensional synthesis of mechanisms for designing articulated leg-wheel system.
- Application of this modified dimensional synthesis process to assist in the selection of the optimal design of fourbar and SDCSC-based articulated leg-wheel systems to guide the wheel axle through several positions while supporting *external loads*.
- Careful examination of the role of structural- and spring-assisted equilibration for minimization of the actuation requirements to support the external loads for both fourbar and SDCSC based designs.

- Analysis of the role of various mechanism parameters on locations, stability and basins of attraction of the static system equilibria in the articulated leg-wheel designs.
- Particular attention is paid to developing the ability to customize/tailor these by both the offline selection of the mechanical parameters as well as online selection of the configuration/reconfiguration of select system parameters.

7.2 Future Work

7.2.1 Immediate Extensions

- All that has been done is to demonstrate the kinetostatic design process for selection of mechanical parameters of articulated leg-wheel subsystem. The result of this research need to be validated – using virtual and physical prototypes – to verify the validity/applicability/usefulness of this approach to selection of mechanical parameters.
- Nonlinear spring torque profiles, potentially obtained by combining linear springs with linkages or cams, would allow exact/perfect equilibration of more complex desired torque-profiles than currently possible using just the linear torsional springs.
- Similar to the Hookian/linear spring considered in this work, counterweights can also be used to modify torque profile by amplifying minimum/maximum torque and moving equilibriums.
- Consideration of weight of links and friction are required for practical design solution of mechanism and need to be considered for future extensions.
- In this thesis we considered planar motions in the sagittal plane alone – the extension of these methods to the spatial case would be critical to developing some of these articulated leg-wheel applications.

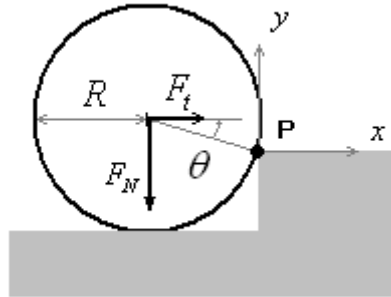
7.2.2 Longer-Term Extensions

- Currently, these devices have been *designed* to satisfy a given set of *kinematic and static design specifications*. Future plans include prescription and satisfaction of design specifications on *dynamic behavior* of such devices.
- Once designed, the end-effector motion paths and supported forces remain fixed for the range of the motion. The sensitivity of these obtained mechanism performance to variations in the mechanism parameters creates possibilities for designing devices to realize ranges of desired specifications by varying over ranges of mechanism parameters. A three stage extension of the capabilities will be pursued :
 - The first stage is to enhance the reconfigurability of the device by a discrete variation of the parameters of the mechanism. Adjustable link lengths (for both fourbar and SDCSC designs) and adjacent sets of pulley ratios (for the SDCSC design) hold considerable promise to permit matching of *multiple sets* of design specifications. An optimized design process is to determine the initial configuration; range of variation of the parameters; and minimal transitions of the parameters to achieve reconfiguration to the new task.
 - In the second stage we will consider the computer control of the parameters of the device during operation to enhance the performance. The opposed conical

continuously variable transmissions (CVT) and telescoping links enable us to vary the primary mechanism parameters under computer control. These parameters can be varied continuously under servo control or discretely using stepper motors. Other adjustable parameters include tunable springs, adjustable dampers and brakes offer considerable potential for enhancement of the kinematic and dynamic performance of the device.

- In the final stage we will explore the use of active elements to provide a power assist to augment the strength in addition to aiding the manipulation needs of people. Such devices can stabilize the motions (natural and unnatural vibrations) and additionally amplify complex constrained motions. The principally passive mechanical nature of the articulated leg-wheel system can guarantee stability even in the presence of augmentation.

APPENDIX A : CALCULATION OF HIGHEST OBSTACLE



In general, the highest obstacle which wheel can go over can be $0.38 \cdot R$ as derived below. Let traction force is same as static friction force and normal force is same as wheel weight then,

$$F_t = \mu F_N$$

Torque at the point P is

$$T = F_N R \cos \theta - \mu F_N \sin \theta \cdot R \sin \theta$$

To get critical value of θ which wheel can get over obstacle can be calculated by

$$F_N R \cos \theta = \mu F_N \sin \theta \cdot R \sin \theta$$

$$\cos \theta = \frac{-1 \pm \sqrt{1 + 4\mu^2}}{2\mu}$$

In ideal case, $\mu = 1$, we can get

$$\theta = 51.8^\circ$$

so the highest obstacle which wheel can go over is:

$$R - R \cos \theta = R(1 - \cos \theta) = 0.38 \cdot R$$

References

- [1] H. Hacot, Dubowsky, S., and Bidaud, P. "Modeling and Analysis of a Rocker-Bogie Planetary Exploration Rover." Proceedings of the Twelfth CISM-IFTOMM Symposium (RoManSy 98), Paris, France, July 1998.
- [2] H. Hacot, "Analysis and Traction Control of a Rocker-Bogie Planetary Rover," Master's Thesis, Department of Mechanical Engineering, MIT, 1998.
- [3] B. Merminod, M. Lauria, R. Piguet, R. Siegwart, "An innovative space rover with extended climbing abilities," Proceedings of the Space and Robotics 2000.
- [4] M.Bualat et al., "Operating Nomad during the Atacama Desert Trek", Proceedings of Field and Service Robotics Conference, Canberra, Australia, December 1997.
- [5] A. Halme, I. Leppänen and S. Salmi, "Development of WorkPartner-robot – design of actuating and motion control system," CLAWAR'99, Portsmouth 1999.
- [6] A. Halme, I. Leppänen, M. Montonen, S. Ylönen. "Robot motion by simultaneous wheel and leg propulsion," 4th International Conference on Climbing and Walking Robots Karlsruhe Germany, Professional Engineering Publishing Ltd, s. 1013-1020, 2001.
- [7] S. Hirose. "Super Mechano-System," International Symposium on Experimental Robotics (ISER2000), Honolulu, December 2000.
- [8] S-M. Song and K. Waldron, "The Adaptive Suspension Vehicle", MIT Press, Cambridge, MA, 1988.
- [9] K. Berns, "Walking Machine Catalogue" [URL:http://www.walking-machines.org/](http://www.walking-machines.org/), 2002.
- [10] M. Bekker, "Theory of Land Locomotion: The Mechanics of Vehicle Locomotion: The mechanics of Vehicle Mobility," The university of Michigan Press, Ann Arbor, 1956.
- [11] M. Bekker, "Introduction to terrain vehicle systems," The university of Michigan Press, Ann Arbor, 1956.
- [12] J. Wong, "Terramechanics and off-road Vehicles," Elsevier Health Sciences, 1989.
- [13] M.Hiller and D. German, "Manoeuvrability of the Legged and Wheeled Vehicle ALDURO in Uneven Terrain with Consideration of Nonholonomic Constraints" Proceeding of ISOM 2002, Chemnitz, Germany, March 21-22, 2002.
- [14] K.Iagnemma, A.Rzepniewskia, S.Dubowsky, P.Pirjaniab, T.Huntsbergerb, and P.Schenker, "Mobile robot kinematic reconfigurability for rough-terrain," in Proceedings SPIE's International Symposium on Intelligent Systems and Advanced Manufacturing, August 2000.

- [15] V. Krovi, "Design and Virtual Prototyping of User-Customized Assistive Devices," Ph.D. Thesis, Dept. Of Mechanical Engineering and Applied Mechanics, University of Pennsylvania, Philadelphia PA, September 1998.
- [16] V. Krovi, "Modeling and Control of a Hybrid Locomotion System," Masters Thesis, Dept. Of Mechanical Engineering and Applied Mechanics, University of Pennsylvania, Philadelphia PA, December 1995
- [17] V. Krovi, G. Ananthasuresh and V. Kumar, "Kinematic Synthesis of Coupled Serial Chains" Proceeding to Design Engineering Technical Conferences September 13-16, 1998, Atlanta, Georgia, USA.
- [18] G. Sandor and A. Erdman, 1984, Advanced Mechanism Design: Analysis and synthesis. Vol. 2. Englewood Cliffs, NJ: Prentice Hall International.
- [19] R. Norton, "Design of Machinery," Second Edition. Americas, New York, NY, McGraw-Hill.
- [20] D. Greenwood, "Principle of Dynamics," Second Edition. Englewood Cliffs, NJ: Prentice Hall Inc.
- [21] C. Huang and B. Roth, "Dimensional Synthesis of Closed-Loop Linkages to Match Force and Position Specifications," ASME Journal of Applied Mechanics Vol. 115, June 1993, pp. 194-198.
- [22] C. Gosselin and T. Laliberté, "Static Balancing of spatial Parallel Platform Mechanisms – Revisited," ASME Journal of Mechanical Design Vol. 122, March 2000, pp 43-51.
- [23] T. Laliberté and C. Gosselin and, "Static Balancing of 3_DOF Planar Parallel Mechanism," IEEE/ASME Transaction on Mechatronics, Vol. 4, No. 4, Dec., 1999.
- [24] C. Felippa, "Nonlinear Finite Element Method," Department of Aerospace Engineering Science and Center for Space Structures and Controls, University of Colorado, Boulder, Colorado, Aug, 2001.
- [25] A. Carr. "Position Control Comparison of Equilibrate and Mass Counterweight Systems," Master's Thesis, Department of Mechanical Engineering, Virginia Polytechnic Institute and State University.
- [26] T.Rahman et al, "A Simple Technique to Passively Gravity –Balance Articulated Mechanisms," Transactions of the ASME, Journal of Mechanisms Design, Vol 117(4), pp 655-658, December 1995.
- [27] L. Sciavicco and B. Siciliano, "Modeling and Control of Robot Manipulator," New York, NY, McGraw-Hill.

- [28] Y. Nakamura, "Advanced Robotics Redundancy and Optimization," Boston, MA, Addison-Wesley Publishing Company, Inc.1991
- [29] W. Palm III, "Modeling, Analysis and control of Dynamic System" Second edition, John Wiley & Sons, Inc. New York, NY 2000.